

# Water vapor and lapse rate feedbacks in the climate system

Robert Colman<sup>\*,†</sup>

*Australian Bureau of Meteorology, GPO Box 1289, Melbourne, Victoria 3001, Australia*

Brian J. Soden<sup>‡</sup>

*Rosenstiel School of Marine and Atmospheric Science, University of Miami, Miami, Florida 33149, USA*

 (published 30 November 2021)

Water vapor is a greenhouse gas that dominates Earth’s terrestrial radiation absorption. As the planetary temperature warms, forced by increasing CO<sub>2</sub> and other greenhouse gases, water vapor content of the atmosphere increases, thereby producing the strongest positive feedback in the climate system. At the same time, the rate at which atmospheric temperature drops with height (the “lapse rate”) is expected to decrease with warming. This represents a smaller, but significant, negative feedback since it enables the planet to radiate more effectively to space. The two feedbacks are closely coupled to each other, and the combined result represents the foundational net positive feedback in the climate system, mandating substantial global warming in response to increased greenhouse gases. This review summarizes the published work that has provided an ever deepening understanding of these critical feedbacks. The historical context, beginning with the 19th century awakening to the importance of water vapor in the climate, is outlined before the review’s focus shifts to the theoretical, observational, and modeling work in recent decades that has transformed our understanding of the feedbacks’ role in climate change. It is shown that the evidence is now overwhelming that combined water vapor and lapse rate processes indeed provide the strongest positive feedback in the climate system. However, important challenges remain. This review provides physicists with a deeper understanding of these feedbacks and stimulates engagement with the climate research community. Together the scientific community can facilitate further rigor, understanding, and confidence in these most fundamental Earth system processes.

DOI: [10.1103/RevModPhys.93.045002](https://doi.org/10.1103/RevModPhys.93.045002)

## CONTENTS

I. Introduction	2	3. Challenges to water vapor feedback “orthodoxy”:	
II. Water Vapor, Lapse Rate, and the Greenhouse Effect	3	Convective drying and the role of microphysics	12
A. A historical perspective	3	4. The role of model parametrizations in humidity distributions	14
B. Radiative forcing and the “enhanced” greenhouse effect	4	5. Simple models of water vapor distribution	15
III. Global Radiative Feedbacks and Climate Sensitivity	5	6. Deviations from unchanged relative humidity	16
A. A global feedback paradigm	5	7. Water vapor feedback and convective aggregation	17
B. Alternate feedback formulations	6	8. Impact of water vapor or lapse rate changes on radiative forcing	17
C. Feedbacks at Earth’s surface	7	E. Relationship between water vapor and lapse rate feedbacks	18
IV. Physical Processes	7	1. What causes the (anti)correlation between water vapor and lapse rate feedbacks?	18
A. Radiative properties of water vapor	7	2. What causes the spread in combined water vapor + lapse rate feedbacks in models?	19
B. Fundamentals of temperature and water vapor distributions in the atmosphere	8	F. Stratospheric water vapor feedback	20
1. Lapse rate	8	G. State and forcing dependence of water vapor and lapse rate feedbacks	21
2. Water vapor	9	H. A surface perspective on feedbacks	23
3. Relative humidity distribution	9	I. The role of lapse rate and water vapor feedbacks in regional climate variability and change	24
C. Spectrally dependent response to warming	10	1. Polar amplification of warming	24
D. Changes in temperature and water vapor under global warming and their radiative impact	11	2. Climate features and regional variability	27
1. The importance of different regions for water vapor and lapse rate feedback	11	V. Observational Evidence for Water Vapor and Lapse Rate Feedback	28
2. Factors controlling relative humidity in a warming world	12	A. Moisture trends and variability in the lower atmosphere	28
		B. Upper tropospheric moisture	28

<sup>\*</sup>Visiting scientist.  
<sup>†</sup>Corresponding author.  
 robert.colman@bom.gov.au

1. Methods of measuring upper tropospheric humidity	28
2. Trends in upper tropospheric humidity	29
C. Use of variability analogues for evaluating water vapor feedback	30
D. Volcanoes and water vapor feedback	33
E. Paleo evidence	34
F. Observed lapse rate changes and variability	34
VI. Model Representation of Feedbacks and Feedback Processes	35
A. Quantification of feedbacks in models	35
B. Model representation of water vapor distribution, variability, and trends and their radiative impact	35
C. Conclusions on feedback impacts on global variability	36
VII. Evaluation and Assessment of Water Vapor and Lapse Rate Feedbacks	37
A. IPCC assessment of water vapor and lapse rate feedbacks	37
B. Summary “best” estimate of feedback strengths and uncertainty ranges	38
VIII. Conclusions	39
A. On the strength and consistency of evidence for water vapor and lapse rate feedbacks	39
B. A look to the future: Current research gaps	41
List of Symbols and Abbreviations	42
Acknowledgments	42
Appendix A: Quantifying Water Vapor and Lapse Rate Feedbacks in Models and Observations	42
1. TOA clear-sky radiation changes	42
2. Partial radiative perturbation	43
3. Radiative kernels	43
4. Cutting feedback loops	44
Appendix B: Evaluations of Water Vapor and Lapse Rate Feedbacks	44
References	45

## I. INTRODUCTION

Understanding and quantifying climate change is one of the outstanding scientific challenges of our era. The world is already seeing the impact of a changing climate, with just over 1.0°C warming worldwide since preindustrial times causing major impacts. These include the loss of Arctic sea ice, rising sea levels, erosion of continental glaciers, melting permafrost, and the increased incidence of extreme weather and climate such as heat waves, drought, fires, heavy rainfall, and coastal flooding, among many other changes (Intergovernmental Panel on Climate Change, 2013, 2014, 2019, 2021). Projections of warming over the rest of this century depend on the future emissions of carbon dioxide, methane, nitrous oxide, and other greenhouse gases (GHGs), but under a moderate emissions mitigation scenario they are in the range 1–3°C, with a potential further warming of 1–2°C for “business as usual” emissions (Collins *et al.*, 2013; Intergovernmental Panel on Climate Change, 2021).

Water vapor and lapse rate feedbacks play key roles in determining the magnitude of that warming. Water vapor feedback results from the increasing moisture holding capacity of the atmosphere with temperature, diminishing the escape of outgoing terrestrial radiation. This dictates further warming to restore radiative equilibrium. At the same time, in

latitudes spanning the tropics through to the midlatitudes, the upper troposphere warms faster than the surface, a change in the vertical “lapse rate” with temperature, enabling Earth to radiate to space more effectively. This process offsets some, but notably not all, of the effects of increasing water vapor. Other feedbacks also operate, involving changes in clouds, snow, and sea ice, but the combined water vapor and lapse rate feedbacks can be considered to provide a fundamental amplification of climate warming, further enhancing the effects of other positive feedbacks.

Given their key importance to climate change, water vapor and lapse rate feedbacks have been the subject of intense research over the past four decades, and before that of studies stretching back to the early 19th century. This research spans theoretical understanding of radiative impacts of humidity as the climate warms, along with extensive modeling and observational studies. This review summarizes this research and assesses the current state of knowledge. It also highlights areas where further rigor and understanding would provide even more confidence in these critical Earth system processes.

The layout of this review is as follows. Section II provides a historical background of the understanding of the importance of water vapor in the climate system, and amplification of warming by water vapor feedback. Section III describes a formalism linking changes in “forcing” from GHGs to climate feedbacks and the response of the climate system.

Section IV describes the radiative properties of water vapor that make it so important, as well as the fundamental distributions of temperature and water vapor in the atmosphere. It describes the understanding of the manner in which spectral absorption by water vapor is related to changes in the surface temperature, and what this implies for water vapor feedback. It also describes the unfolding of the understanding of the importance of different regions in the atmosphere in setting the magnitude of both water vapor and lapse rate feedbacks. It further addresses debates and research that have led to a much deeper understanding of the processes controlling water vapor distribution in the current climate and the response in a warmer climate.

Section V lays out the observational evidence for strong positive water vapor and negative lapse rate feedbacks, including evidence from climate variability, from climate change to date, from paleo climates, and from responses to volcanic eruptions.

Section VI provides an assessment of global climate model (GCM) representation of key physical processes, as well as a comparison with observed changes and variability to evaluate confidence in model water vapor and lapse rate feedbacks. Appendix A summarizes methodologies for quantifying feedbacks, as these techniques have played an important part in the development of understanding and assessment.

Section VII gives a perspective on the climate community understanding and consensus on these feedbacks, as expounded by evaluations carried out by the Intergovernmental Panel on Climate Change (IPCC) since the first report in 1990. Section VII also describes and evaluates quantitative estimates of feedback strength, with details listed in Appendix B.

Section VIII provides a summary on the strength and consistency of evidence of the nature and magnitude of water vapor and lapse rate feedbacks. Finally, we look to the future to highlight the remaining knowledge gaps and identify outstanding areas of further research.

## II. WATER VAPOR, LAPSE RATE, AND THE GREENHOUSE EFFECT

### A. A historical perspective

Our understanding of the importance of the atmosphere in maintaining Earth's temperature through greenhouse trapping goes back nearly 200 years to Joseph Fourier, and his insight that, although the atmosphere is relatively transparent to incoming solar radiation, it strongly absorbs outgoing terrestrial radiation (Fourier, 1827). Laboratory measurements by John Tyndall (pictured in Fig. 1) later in the 19th century established that the trace gases, water vapor and  $\text{CO}_2$ , were primarily responsible for the absorption of terrestrial radiation, rather than the primary atmospheric constituent gases of nitrogen and oxygen (Tyndall, 1861, 1872). Tyndall concluded that water vapor provided “a blanket, more necessary to the vegetable life of England than clothing is to man” (Fleming, 1998).

Svante Arrhenius (pictured in Fig. 1) wrote in 1896: “The selective absorption of the atmosphere ... is not exerted by the chief mass of air, but in a high degree by aqueous water vapour and carbonic acid ( $\text{CO}_2$ ).... The influence of this absorption is comparatively small on the heat of the Sun, but must be of great importance in the transmission of rays from the Earth.”

By the end of the 19th century there was an appreciation that water vapor could act as an amplifying “feedback” to other trace gas forcing (Arrhenius, 1896; Chamberlin, 1899). A statement essentially articulating the modern concept of

water vapor feedback was made by Chamberlin (Fig. 1) in a letter to G. C. Abbott in 1905:

“[W]ater vapor, confessedly the greatest thermal absorbent in the atmosphere, is dependent on temperature for its amount, and if another agent, as  $\text{CO}_2$ , not so dependent, raises the temperature of the surface, it calls into function a certain amount of water vapor which further absorbs heat, raises the temperature and calls forth more vapor....”

Twentieth century quantum theory has since provided theoretical understanding of the water vapor absorption spectrum, including the myriad of absorption lines due to rotational and vibrational absorption of infrared photons; see Sec. IV.A. An additional “continuum” absorption, noted in the early 20th century (Brunt, 1932), is an important source of absorption between bands but remains the least well understood component of the water vapor absorption spectrum (Shine, Ptashnik, and Rädcl, 2012); see Sec. IV.A.

Through the early to mid-20th century, further studies considered the quantitative role of water vapor feedback in determining response to  $\text{CO}_2$  changes in the atmosphere; see Held and Soden (2000) for an overview. Major advances occurred in the 1960s, with the development of one-dimensional models consisting of global mean profiles of temperature and moisture, with the temperature profile constrained not to exceed a specified lapse rate, i.e., a decrease in temperature with height. This lapse rate was considered to be set primarily by tropospheric convective processes; see Sec. IV.B. These so-called radiative-convective models (RCMs) (Manabe and Strickler, 1964; Manabe and Wetherald, 1967) were able to provide a first-order representation of the troposphere,<sup>1</sup> with the tropopause height determined by a combination of radiative and convective processes, and topped by a stratosphere in pure radiative equilibrium. These models were then used to estimate climate change induced by the addition of radiative absorbers such as anthropogenic  $\text{CO}_2$  (Manabe and Wetherald, 1967; Ramanathan and Coakley, 1978).

A key advance for understanding the global response to  $\text{CO}_2$  (and other GHG) increases, was the realization that top of atmosphere (TOA) radiative balance, rather than surface radiation-evaporation balance dictated climate sensitivity (Manabe and Strickler, 1964; Manabe and Wetherald, 1967). An important additional step was the hypothesis that nearly unchanged relative humidity, rather than specific humidity, is more appropriate for climate change simulations (Manabe and Wetherald, 1967). Three-dimensional GCMs (latitude, longitude, height) replaced 1D models for climate change experiments from the 1970s, although the early RCMs shed crucial light on the role of water vapor feedback and lapse rate in climate sensitivity; see Kluff *et al.* (2019) for a recent analysis.

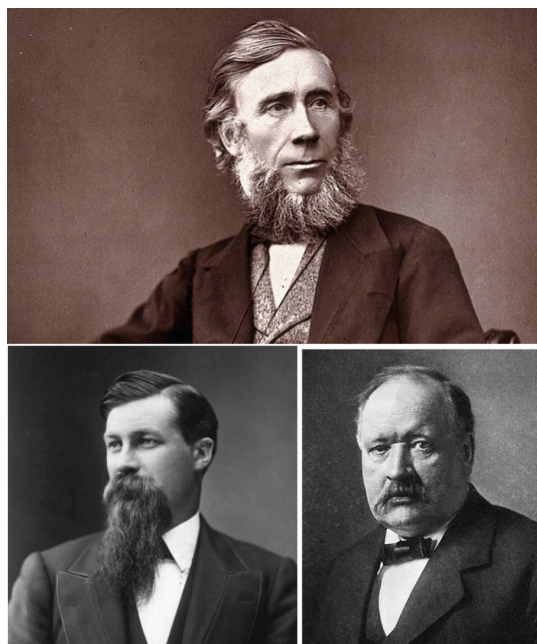


FIG. 1. John Tyndall (top), Thomas Chamberlin (bottom left), and Svante Arrhenius (bottom right). Tyndall performed laboratory measurements of the absorption spectrum of water vapor in the mid-19th century. Thomas Chamberlin articulated the fundamental process controlling water vapor feedback. Arrhenius in the late 19th century laid out a coherent framework of  $\text{CO}_2$ -induced climate change, as amplified by water vapor feedback.

<sup>1</sup>The troposphere is the bottom roughly 6–10 km of the atmosphere, and of generally decreasing temperature with height. Weather events are confined to this zone. It is separated from the overlying stratosphere by the tropopause.

## B. Radiative forcing and the “enhanced” greenhouse effect

We now consider what a simplified RCM implies about global response to additional terrestrial wavelength absorbers [hereafter called longwave (LW) absorbers]. The incident TOA average annual solar radiation flux (vertical to the equatorial horizontal)  $S_0$  is around  $1360 \text{ W m}^{-2}$  (Lacis *et al.*, 2013). Since the atmosphere is largely transparent to incident solar radiation (see Sec. IV.A), most absorption takes place at the surface, modulated by the albedo (reflectivity) of clouds and Earth surface, including high albedo surfaces such as snow and sea ice. The observed global mean planetary albedo  $\alpha$  is around 30% (Ramanathan, 2014). A straightforward calculation gives net absorbed solar [hereafter called short-wave (SW)] radiation of  $(S_0/4)(1 - \alpha)$ , or approximately  $240 \text{ W m}^{-2}$ .

Most LW radiation from the surface cannot escape directly to space due to the opacity of the atmosphere (see Sec. IV.A), and multiple absorptions and emissions culminate in an effective radiating height  $Z_e$  of around 500 hPa (or approximately 5 km) at a global mean effective radiating temperature  $T_e$  of around 255 K. Assumption of a fixed lapse rate  $\Gamma$ , corresponding to the observed global mean value of  $\sim 6.5 \text{ K/km}$ , gives a surface temperature of  $T_s = T_e + \Gamma Z_e$ , or approximately 288 K in the preindustrial era. This simple calculation describes a “natural greenhouse effect” of the atmosphere, resulting in a planetary surface temperature that is around 33 K warmer than that with no atmosphere (Lacis *et al.*, 2013).

Adding an infrared absorber such as  $\text{CO}_2$ ,  $\text{CH}_4$ , or  $\text{N}_2\text{O}$  increases the atmosphere’s opacity, forcing an increase in  $Z_e$  (Fig. 2). Assuming an unchanged lapse rate, a doubling of  $\text{CO}_2$  raises  $Z_e$  by approximately 150 m (Held and

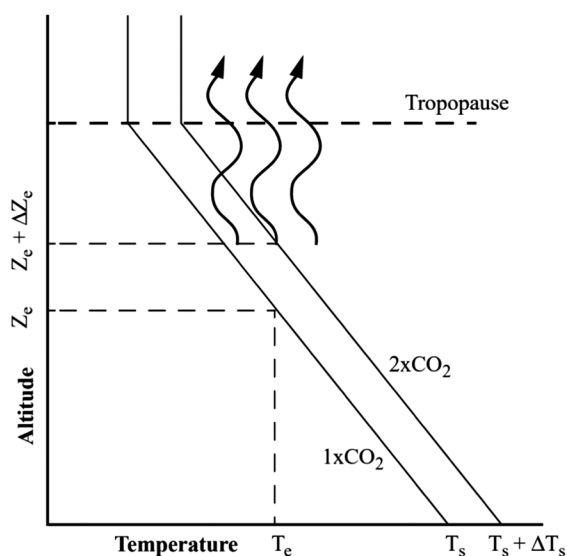


FIG. 2. Schematic illustrating how additions to atmospheric greenhouse gases, such as a doubling of  $\text{CO}_2$  concentration, change surface temperature. Assuming an unchanged lapse rate, additional longwave absorbers, and unchanged emission temperature ( $T_e$ ) forces radiation to space to come from a higher altitude, increasing the surface temperature ( $T_s$ ). From Held and Soden, 2000.

Soden, 2000) and thus increases the surface temperature by  $150 \text{ m} \times 6.5 \text{ K/km}$ , or  $\sim 1 \text{ K}$ . This warming, uniformly spread throughout the atmosphere and assuming a blackbody radiation according to the Stefan-Boltzmann law, increases the upward radiative flux at the TOA by  $\sim 4 \text{ W m}^{-2}$ , thereby balancing the reduced TOA outward flux induced by the increased  $\text{CO}_2$ .

This simple paradigm can be considered a no-feedback response, with only the vertically uniform Planck radiative damping operating (Bony *et al.*, 2006). This provides a first-order understanding of the planetary response to increased GHGs, with feedbacks including water vapor, lapse rate, clouds, and surface albedo then operating in addition to this basic response. These further modify  $Z_e$ ,  $\Gamma$ ,  $T_e$ , and  $T_s$ , through changes in the absorption or reflection of downward solar radiation, in lapse rate, and in the strength and vertical distribution of additional LW absorption (Held and Soden, 2000). Understanding these feedbacks, their underlying physical processes, their magnitude, and their interactions has been among the principal goals of climate research over the past five decades, as these set the fundamental sensitivity to greenhouse gases (Bony *et al.*, 2015).

As previously noted, early studies recognized the potential significance of the strong temperature dependence of the equilibrium vapor pressure of water as a feedback mechanism but lacked a clear quantification of its importance. A key insight from the RCMs was that if relative humidity stayed close to constant, water vapor feedback roughly doubled the previously described “no-feedback” warming (assuming no change in the lapse rate). The landmark study of Manabe and Wetherald (1967) deduced a consequent global surface temperature response to  $\text{CO}_2$  doubling of 2.3 K, a value well within the range of modern GCMs, and had a profound influence on subsequent research.<sup>2</sup> Of course, this was a 1D model only, ignoring many processes, such as the general circulation of the atmosphere, differing tropical or extratropical regions, ocean circulation, snow, sea ice, and land surface processes. Indeed, the assumption of constant relative humidity was born more out of necessity than strong theoretical or empirical support. Subsequent studies with 3D models showed that relative humidity does exhibit systematic changes regionally (Sherwood *et al.*, 2010a, 2010b); however, at the global scale the strong temperature dependence overwhelms the influence of regional variations in relative humidity. The basic tenets of water vapor feedback strength from 3D models substantiate the early 1D model estimates (Colman, 2001; Soden and Held, 2006; Boucher *et al.*, 2013). Given this central importance in amplifying anthropogenic climate change, water vapor feedback, along with the associated lapse rate feedback has undergone intense scrutiny over the past three decades from theoretical, observational, modeling, and process studies.

<sup>2</sup>A 2015 survey of climate scientists voted it as the most influential climate change paper of all time, being the “first proper computation of global warming ... from enhanced greenhouse gas concentrations, including atmospheric emission and water-vapour feedback” (<https://www.carbonbrief.org/the-most-influential-climate-change-papers-of-all-time>).

### III. GLOBAL RADIATIVE FEEDBACKS AND CLIMATE SENSITIVITY

#### A. A global feedback paradigm

The long-standing paradigm within the climate community for understanding the equilibrium climate response to forcing (Hansen *et al.*, 1984; Sherwood *et al.*, 2015) has been adapted from the classic model of the response of an electronic amplifier to perturbation (Bode, 1945).

Consider a radiative perturbation or forcing to the climate system, such as from a change in atmospheric CO<sub>2</sub>, that instantaneously affects the TOA<sup>3</sup> radiative balance by an amount  $\Delta F$ . Under the radiative imbalance,  $T_s$  responds, and with it a myriad of possible processes may be affected in the atmosphere and at the planetary surface, which in turn affects the TOA radiation balance  $R$ , by changing either the outgoing LW radiation (OLR) or the SW reflected radiation. Assuming that the net effect of the processes is related to global mean surface temperature,<sup>4</sup> we can then write

$$\Delta R = \Delta F + \lambda \Delta T_s, \quad (1)$$

where  $\lambda$  is defined as the climate feedback parameter and has units of  $\text{W m}^{-2} \text{K}^{-1}$ . Here we define the radiative flux<sup>5</sup> as downward positive (i.e., warming), although in fact there is no universal convention in the climate literature. Taking  $x$  as a vector of processes affecting  $R$ , following the formulation of Bony *et al.* (2006) and Knutti and Rugenstein (2015) we formally define the feedback parameter as

$$\lambda = \frac{\partial R}{\partial T_s} = \sum_x \frac{\partial R}{\partial x} \frac{\partial x}{\partial T_s} + \sum_x \sum_y \frac{\partial^2 R}{\partial x \partial y} + \dots \quad (2)$$

In the traditional feedback formulation, the most “fundamental” response of the climate system, analogous to open-loop gain in the electronic context, is the so-called Planck response,  $\Delta T_{s,P}$ . This is where the surface temperature and the overlying atmospheric temperature respond uniformly with height, with all other atmospheric and surface variables unchanged (Bony *et al.*, 2006). Assuming the Planck response only, we have

$$\Delta R = \Delta F + \lambda_P \Delta T_{s,P}, \quad (3)$$

<sup>3</sup>The imbalance is often specified at the tropopause rather than the TOA, but the difference between formulations is trivial since the stratosphere equilibrates to forcing on timescales of a few weeks (essentially instantaneous for climate change considerations) thereby equalizing TOA and tropopause imbalances (Hansen *et al.*, 1984).

<sup>4</sup>Other assumptions are possible: a recent proposal that feedbacks be better related to mean tropical 500 hPa temperatures (Dessler, Mauritsen, and Stevens, 2018) provides a different feedback formulation. We do not discuss this approach further, however, as little literature is yet available on feedbacks under this formalism.

<sup>5</sup>In the climate literature, the radiative *flux density* is typically referred to simply as radiative *flux*. In this review, we use the term *radiative flux* to refer to the spectrally integrated radiative power per unit area in units of  $\text{W m}^{-2}$ .

where  $\lambda_P = \partial R / \partial T_{s,P} \approx -4\sigma T_e^3 \approx -3.2 \text{ W m}^{-2} \text{K}^{-1}$ , where  $\sigma$  is the Stefan-Boltzmann constant. Note that this value of  $\lambda_P$ , obtained by simply differentiating the Stefan-Boltzmann law, is notably smaller than that calculated by climate models,  $\sim 4 \text{ W m}^{-2} \text{K}^{-1}$ , primarily because of the lack of stratospheric warming due to its decoupling from the surface (Cronin, 2020). A doubling of atmospheric CO<sub>2</sub>, corresponding to a radiative forcing of approximately  $4 \text{ W m}^{-2}$ , produces surface warming of around 1.2 K (Bony *et al.*, 2006). Note that, although horizontal uniformity of  $\Delta T_{s,P}$  is often also assumed for the Planck response, little difference occurs to this calculation if the temperature response varies geographically. For example, no fundamental difference occurs if the Planck warming is enhanced at high latitudes, as is normally the case in the GCM warming response to CO<sub>2</sub> forcing (Colman, 2004) (Sec. IV.I). Alternative no-feedback vertical temperature profiles have been proposed aside from a uniform increase with height (Schlesinger, Entwistle, and Li, 2012) but have not come into common usage, so they are not discussed further here.

In the presence of a non-Planck process such as temperature-dependent changes to water vapor, lapse rate, or clouds, we can express the final surface temperature change as  $\Delta T_s = (\lambda_P / \lambda) \Delta T_{s,P}$ . Ignoring the second- and higher-order terms in Eq. (2), we write

$$\lambda = \lambda_P + \sum_{x \neq P} \lambda_x, \quad (4)$$

where  $\lambda_x = (\partial R / \partial x) \partial x / \partial T_s$  and  $x \in \{q, \Gamma, \alpha, C\}$ , corresponding to water vapor, lapse rate, surface albedo, and cloud feedbacks, respectively. These are commonly referred to as the “fast” feedbacks of the climate system, as they respond to surface temperature changes on rapid timescales, in the case of water vapor, lapse rate, and clouds, on the order of hours to weeks, which is much shorter than, for example, adjustment timescales of the ocean. Beyond the fast feedbacks lie many other processes that eventually impact radiation. These include land and ocean carbon cycle feedbacks, ecosystem responses, vegetation albedo feedbacks, and many other processes that affect GHG concentration and TOA radiative balance; see Heinze *et al.* (2019), Tierney *et al.* (2020), and references therein. These are important for long (multidecadal or longer) timescale Earth system responses and will interact with fast feedbacks (Heinze *et al.*, 2019), but they are beyond the scope of this review.

For water vapor, given the close-to-logarithmic dependence of LW radiation on specific humidity and the roughly exponential rate of increase of saturation specific humidity with temperature (see Sec. IV.B), a pragmatic alternative can be to instead use  $\lambda_q = (\partial R / \partial \ln q) \partial \ln q / \partial T_s$  (Raval and Ramanathan, 1989; Soden and Held, 2006). This formulation has been widely used in the calculation and application of radiative kernels used for evaluating feedbacks in practice; see Appendix A.

Normalizing each feedback by the Planck response defines the gain from each feedback,  $g_x = -(\lambda_x / \lambda_P)$ , thereby allowing us to write

$$\Delta T_s = \frac{\Delta T_{s,P}}{1 - \sum_{x \neq P} g_x}. \quad (5)$$

Positive feedbacks then are viewed as those that oppose the Planck cooling, thus reducing the effectiveness of the planet below its simple blackbody cooling rate and therefore amplifying the global mean surface temperature response required to reach TOA balance. When  $\Delta F$  corresponds to a doubling of atmospheric  $\text{CO}_2$  concentrations, the equilibrated temperature  $\Delta T_{2\times\text{CO}_2} = -\Delta F_{2\times\text{CO}_2}/\lambda$  is referred to as the equilibrium climate sensitivity (ECS). ECS therefore considers only so-called fast climate feedbacks. ECS, although an idealized concept never fully realized in the real world, has been talismanic in climate science for more than 40 years as a benchmark measure of climate change (Charney *et al.*, 1979; Sherwood *et al.*, 2020) and remains an extremely useful parameter since it is proportional to the transient rate of warming projected by GCMs over the 21st century (Gregory, Andrews, and Good, 2015; Grose *et al.*, 2018).

Observational and modeling studies discussed in this review find that the water vapor and lapse rate feedbacks amplify global warming from  $\text{CO}_2$  and other GHGs by a factor of  $\sim 2$ , with a total gain of  $\sim 0.5$  (Bony *et al.*, 2006; Randall *et al.*, 2007). Other feedbacks in the climate system due to clouds and surface albedo (predominantly snow and sea ice) then operate “on top of” this enhanced warming and amplify or damp the response further. The critical nature of the combined water vapor + lapse rate feedback is apparent from this formalism. Because of the nonlinearity in Eq. (5), the 0.5 gain from water vapor and lapse rate acts to “sensitize” the climate response, giving greatly boosted warming from further positive feedback such as that due to surface albedo or clouds (Bony *et al.*, 2006; Zelinka *et al.*, 2020).

The nonlinear nature of feedback contribution to climate sensitivity in Eq. (5) indicates that apportioning fractional climate change (in this case the global mean surface temperature change) to individual feedbacks depends on the state of all other feedbacks (Held and Soden, 2000; Dufresne and Bony, 2008). Similarly, the uncertainty caused by any one feedback has the same state dependency. Therefore, although it is acknowledged that there is no unique way to achieve this subdivision, a useful methodology proposed by Dufresne and Bony (2008) follows the previously mentioned gain approach of normalizing each feedback by the strength of the Planck response, thereby reiterating the differing nature of the Planck response relative to the other feedbacks. Figure 3 shows the results for 12 models of the Coupled Model Intercomparison Project phase 3 (CMIP3) (Meehl *et al.*, 2007) ensemble. It shows a measure of the relative importance of the combined water vapor + lapse rate feedback on global temperature change and its uncertainty. Clouds dominate the overall projection uncertainty, although water vapor + lapse rate remains the second most important contributor and provides the greatest addition to temperature change over the basic Planck response.

## B. Alternate feedback formulations

Traditionally, water vapor and lapse rate feedbacks have been considered separate processes (Schlesinger, 1988). However, they are closely linked, and much can be gained from considering them a combined feedback (Soden and Held, 2006; Ingram, 2010; Held and Shell, 2012; Po-Chedley *et al.*, 2018). As discussed in Sec. IV.E, a strong anticorrelation is found

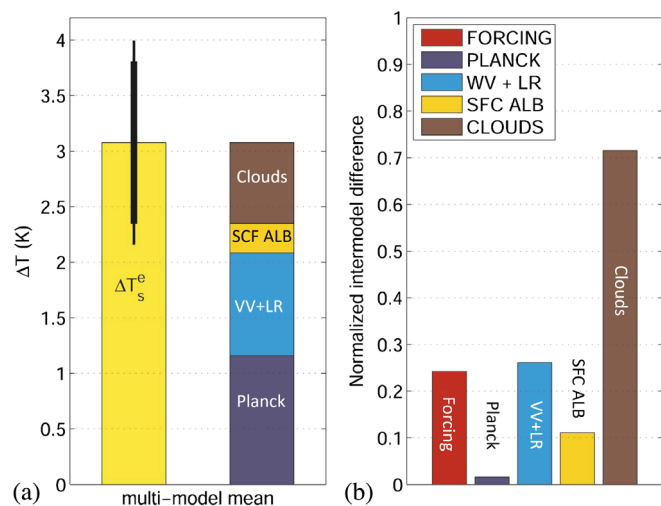


FIG. 3. (a) CMIP3 multimodel mean surface temperature change  $\Delta T_s^e$  [equivalent to  $\Delta T_s$  in Eq. (5)] under a doubling of  $\text{CO}_2$ . The thick and thin lines represent the 1 and 2 standard deviation ranges. Colored bars show the multimodel mean contribution to  $\Delta T_s^e$  from each of the feedbacks listed, according to gain factors in Eq. (5). (b) Contribution to the range in  $\Delta T_s^e$  of the different feedbacks, calculated as the standard deviation of the contribution to temperature change normalized by  $\Delta T_s^e$ . From Dufresne and Bony, 2008.

between water vapor and lapse rate feedbacks. Two approaches have been adopted to take consideration of this strong anticorrelation. The first is to simply sum the two feedbacks, resulting in a combined water vapor + lapse rate feedback, e.g., as assessed by the IPCC in the Fifth Assessment Report (Boucher *et al.*, 2013) and previously discussed when considering the relative contributions of feedbacks to the final temperature change (Fig. 3).

An alternative formulation from Held and Shell (2012) that drew on earlier work by Simpson (1929) and Ingram (2010, 2013a) posits that the assumption of a Planck response with unchanged specific humidity is fundamentally unphysical. This is because it implies large relative humidity drops with increasing temperatures, which were not seen either in observations (see Sec. V) or in GCMs (see Sec. VI). The subsequent “restoration” of an unchanged relative humidity with the Planck warming, which forms a large part of the water vapor feedback, is then seen as a physically artificial adjustment, leading by construct to a strong positive water vapor feedback, in turn opposed by a strong negative lapse rate feedback. Instead, a more fundamental Planck response can be considered one of fixed relative humidity. Under this assumption, following Held and Shell (2012) we construct the following modified Planck feedback:

$$\lambda'_P = \lambda_P + \lambda_{Pq}, \quad (6)$$

where  $\lambda_{Pq}$  corresponds to the radiative response from the water vapor changes required to maintain fixed relative humidity under the vertically uniform Planck temperature response. Under this formulation, the lapse rate feedback now also includes the radiative response from ensuring fixed relative humidity under the changed lapse rate, viz., as

$$\lambda'_{\Gamma} = \lambda_{\Gamma} + \lambda_{\Gamma q}. \quad (7)$$

The reformulated “water vapor feedback” now includes only relative humidity changes:

$$\lambda'_{H} = \lambda_q - \lambda_{Pq} - \lambda_{\Gamma q}. \quad (8)$$

Surface albedo and cloud feedbacks are unaffected by this transformation. The surface temperature response is now expressed as

$$\Delta T_s = \frac{\Delta T_{s,P'}}{1 - \sum_{x \neq P} g'_x}, \quad (9)$$

with  $g'_x = -\lambda'_x/\lambda'_P$  and  $x \in \{H, \Gamma, \alpha, C\}$ , where the symbols are as the same as in Eq. (4), with  $H$  representing the relative humidity and  $\Delta T_{s,P'} = -F/\lambda'_P$  (Held and Shell, 2012).

A comparison of traditionally defined Planck, water vapor and lapse rate feedbacks, and the relative humidity transformed feedbacks for the CMIP3 model ensemble are shown in Fig. 4 (Boucher *et al.*, 2013). It is immediately apparent that the relative humidity formulation removes the large offsetting feedbacks and reduces the intermodel spread.

In this review, we contend that both the traditional formulation and the relative-humidity-based formulation (hereafter called RH feedbacks) are useful, providing different insights into the nature of the feedbacks, their importance in determining large-scale response to forcing and the nature and importance of the feedback spread (Ingram, 2012, 2013b). Furthermore, within the traditional framework, the consideration of separate water vapor and lapse rate feedbacks and their simple sum are both useful approaches in different contexts. If the sum of water vapor and lapse rate feedbacks agrees between models, then this provides a pragmatic approach to narrowing

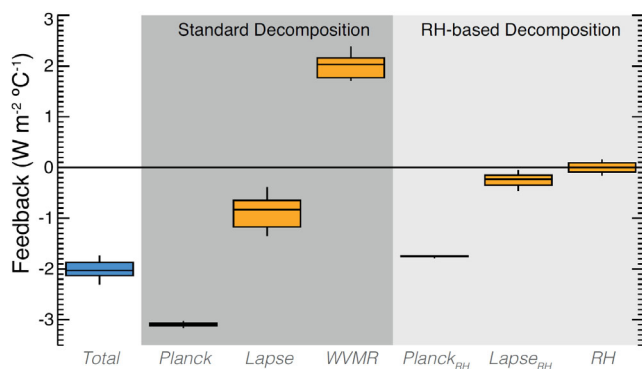


FIG. 4. Feedback parameters associated with water vapor or the lapse rate predicted by CMIP3 GCMs, with boxes showing interquartile range and whiskers showing extreme values. At left is the total radiative response including the Planck response. The darker-shaded region shows the traditional breakdown of this into a Planck response and individual feedbacks from water vapor (labeled WVMR) and lapse rate (labeled Lapse). The lighter-shaded region at the right depicts the equivalent three parameters calculated in the alternative, RH-based framework. In this framework all three components are both weaker and more consistent among the models. Data are from Held and Shell (2012). From Boucher *et al.*, 2013.

uncertainty in ECS and focuses research on cloud and surface albedo feedbacks that have a greater impact on ECS range. However, if different models produce the same net feedback balance through different mechanisms, this undermines confidence in models generally, and specifically for aspects of projections dependent on model representation of those processes. In practical terms too the overwhelming majority of studies in the last 40 years have considered traditional, separate feedbacks, so the focus of the research community has been strongly fixed on the traditional definitions. Finally, the sum of the modified lapse rate feedback [Eq. (7)], the RH feedback [Eq. (8)], and the term due to the humidity increase under a vertically uniform temperature increase with fixed relative humidity [ $\lambda_{Pq}$  in Eq. (6)] equals the traditionally defined water vapor + lapse rate feedbacks.

It may be asked how “separable” feedbacks are in practice, i.e., can they be divided into separate processes in practice, not just in theory? Strong support for this is provided by GCM studies where individual feedback loops are “cut” by suppressing their radiative impact; see Appendix A. Mauritsen *et al.* (2013) found for one such GCM that this yielded a “near-perfect decomposition of change into partial temperature contributions pertaining to forcing and each of the feedbacks,” including a separation of water vapor and lapse rate feedbacks according to the traditional framework.

### C. Feedbacks at Earth’s surface

The discussion thus far has focused on TOA forcing and feedback, as TOA radiative balance is fundamental to planetary equilibrium and response to forcing (Manabe and Wetherald, 1967). It can also be useful, however, to consider feedbacks from a surface perspective, which can provide additional insight into radiative impacts on processes such as evaporation, with consequences for changes to atmospheric temperature and rainfall (Andrews, Forster, and Gregory, 2009; Previdi, 2010). Under a small climate perturbation, the surface net radiative budget can be written as

$$\delta R = \delta R_P + \delta R_q + \delta R_{\Gamma} + \delta R_C + \delta R_{RF}, \quad (10)$$

where  $R$  is now the net surface radiation, RF is the surface radiative forcing, and the other surface radiation terms are from changes to the Planck term, water vapor, lapse rate, surface albedo, and clouds. Ignoring the small heat conduction term into the soil, the net surface heat balance  $W$  can be written as

$$\delta W = \delta R + \delta E + \delta S, \quad (11)$$

where  $E$  and  $S$  represent the evaporative and sensible heat turbulent fluxes, respectively (Colman, 2015). Surface feedbacks are discussed in Sec. IV.H.

## IV. PHYSICAL PROCESSES

### A. Radiative properties of water vapor

Water vapor has a profound impact on Earth’s outgoing LW radiation. It is responsible for around 50% of total absorption

and around 60% of the total clear-sky<sup>6</sup> “greenhouse effect” in the near infrared (Kiehl and Trenberth, 1997); see Fig. 5. Being a strongly polar molecule (in contrast to CO<sub>2</sub>, for example) water vapor has numerous absorption modes from rotation in three separate axes. These rotational modes combine with vibrational modes, producing a large number of absorbing bands in the near infrared and midinfrared. Molecular bending and symmetric or asymmetric stretching contribute to other absorption modes, often overlapping with the tones and overtones of other modes (Stevens and Bony, 2013). The result is bands consisting of thousands of closely packed narrow absorption lines (Goody and Robinson, 1951) (Fig. 5).<sup>7</sup> In addition, throughout the spectrum from the microwave to the visible lies a relatively smoothly varying absorption continuum (Brunt, 1932; Clough, Kneizys, and Davies, 1989; Tipping and Ma, 1995). This continuum is particularly important in the window zones between the bands, where it is the dominant source of absorption (Shine, Ptashnik, and Rädell, 2012; Stevens and Bony, 2013; Lechevallier *et al.*, 2018).

The source of the continuum has been debated for several decades [see the review by Shine, Ptashnik, and Rädell (2012) and references therein], with candidate mechanisms including “far-wing” effects from remote spectral lines and absorption by dimers. Uncertainties in the details of the physics underlying the continuum, albeit still an important research topic in the molecular spectroscopy community, have little impact on the strength of the water vapor feedback in the infrared (Huang, Ramaswamy, and Soden, 2007). This is as long as GCMs parametrize the essential features of both band and continuum absorption, as well as radiation codes in support of observations, including the satellite retrieval of features such as upper tropospheric humidity (Soden *et al.*, 2000). To this end, model radiation codes have been compared to detailed and sophisticated line by line radiation calculations in several major intermodel comparisons (Pincus, Forster, and Stevens, 2016). It was found that limitations in representation of radiation do not represent a material uncertainty in TOA radiation balance or water vapor feedbacks in models (Allan, 2012).

Typically, to a reasonable approximation the saturation of large parts of the water vapor spectrum mean that the addition of extra water vapor increases absorption not in the central part of the absorption lines but instead only in their far “wings.” This means that absorption is proportional to the logarithm of specific humidity (Lacis *et al.*, 2013). This is a key point that implies that absorption depends on relative humidity changes as temperatures increase (discussed later).<sup>8</sup>

<sup>6</sup>That is, radiation calculations performed when cloud amounts are set to zero.

<sup>7</sup>Figure 5 was taken from [https://upload.wikimedia.org/wikipedia/commons/7/7c/Atmospheric\\_Transmission.png](https://upload.wikimedia.org/wikipedia/commons/7/7c/Atmospheric_Transmission.png) following Goody and Robinson (1951).

<sup>8</sup>Note that there are some modest departures to the logarithmic absorption dependence: the remaining unsaturated weak lines have a linear dependence on the specific humidity (Lacis *et al.*, 2013), and continuum absorption in the spectral windows increases as the square of the water vapor density (Baranov *et al.*, 2008).

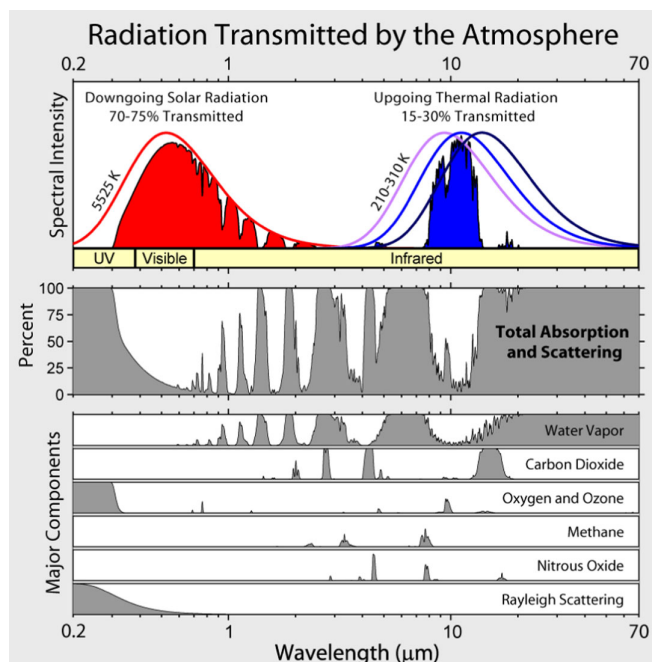


FIG. 5. Absorption spectra for total atmosphere and water vapor, CO<sub>2</sub>, and other atmospheric gases as a function of wavelength. Also shown are the blackbody curves of downward solar (SW) radiation and upward terrestrial (LW) radiation. Adapted from Goody and Robinson, 1951.

In the SW, although the cloud free atmosphere is mostly effectively transparent, water vapor is also the most important atmospheric constituent, responsible for more than 60% of the total absorption by atmospheric gases (Kiehl and Trenberth, 1997) (Fig. 5). Some questions regarding GCM representation of the SW absorption by water vapor remain. These uncertainties, particularly in the near infrared, may have important implications for the atmospheric energy balance and thus how precipitation changes in response to a moistening climate (DeAngelis *et al.*, 2015; Rädell, Shine, and Ptashnik, 2015). The uncertainties are less important for water vapor feedback (Takahashi, 2009; Allan, 2012), although there may be links to climate sensitivity through cloud impacts (Watanabe *et al.*, 2018).

In summary, the radiative properties of water vapor are well understood, and their representation in models is sufficiently accurate to rule out their contributing any significant uncertainty to water vapor feedback.

## B. Fundamentals of temperature and water vapor distributions in the atmosphere

### 1. Lapse rate

With limited exceptions, temperature decreases with height in the troposphere due to the absorption of the majority of the solar radiation at the surface and atmospheric cooling with altitude from expansion as parcels rise. Parcels raised from the surface, with no input or loss of heat (termed an adiabatic process), cool at the adiabatic lapse rate for dry air given by  $\Gamma_d = g/c_p \approx 10 \text{ K km}^{-1}$ , where  $g$  is the gravitational constant and  $c_p$  is the specific heat capacity of air. Another way of

thinking of this is the conservation of dry static energy,  $S = c_p T + gz$ , where  $z$  is the height above the surface.

The presence of water vapor, however, changes this profoundly. As water vapor in the parcel reaches saturation, further ascent results in condensation, with latent heat release offsetting some of the cooling. The moist, or saturated, lapse rate is given by

$$\Gamma_m \approx \Gamma_d \left[ \frac{1 + \frac{e^*}{P} \left( \frac{\beta}{T} \right)}{1 + \frac{e^* R_d}{P c_p} \left( \frac{\beta}{T} \right)^2} \right], \quad (12)$$

where  $e^*$  is the saturation vapor pressure [see Eq. (13)],  $P$  is the pressure,  $T$  is the temperature,  $R_d$  is the dry air specific gas constant, and  $\beta$  is a factor roughly equal to the ratio of the latent heat of vaporization at constant pressure to the water vapor gas constant (Stevens and Bony, 2013). Near the surface  $\Gamma_m \approx 4 \text{ K km}^{-1}$  but it approaches  $\Gamma_d$  aloft, where saturation vapor pressure becomes low as a result of low temperatures. In moist environments, if atmospheric lapse rates exceed the saturated adiabatic lapse rate, convection acts to stabilize the atmosphere. Above the tropopause (the upper limit of convection), the stratosphere lies in close to true radiative equilibrium and shows a largely unchanged or slightly increased temperature with height.

In the tropics, the atmosphere has been observed to be close to saturated adiabatic across broad regions (Xu and Emanuel, 1989; Sobel, Nilsson, and Polvani, 2001). This is due to convective stabilization in moist regions along with the fact that the Coriolis effect is small here. The latter means that dynamical circulations quickly erode horizontal temperature gradients, so the lapse rate is broadly set by the areas with the deepest convection (Neelin and Held, 1987; Lambert and Taylor, 2014).

In the midlatitudes baroclinic adjustment (associated with extratropical cyclones, anticyclones, and planetary scale waves) is a key process for setting the lapse rate (Stone, 1978; Stone and Carlson, 1979), although with some seasonal variation. In the summer hemisphere, in particular, convective cores within the warm parts of baroclinic eddies can result in a lapse rate similar to moist adiabatic (Juckes, 2000), with implications for amplified upper tropospheric warming under global temperature increase (Frierson, 2006).

At high latitudes the most common conceptual model of the basic state is one of “radiative-advective” equilibrium, with a balance between heat flux convergence from the lower latitudes (by atmospheric and/or oceanic processes), balanced by absorbed SW radiation, and LW cooling (Payne, Jansen, and Cronin, 2015; Cronin and Jansen, 2016). Vertical temperature profiles are set by the balance between surface and atmospheric SW absorption and commonly result in temperature inversions and stable atmospheric profiles: a cold surface layer overtopped by warmer air. The role of lapse rate feedback in controlling high latitude warming under radiative forcing is discussed in detail in Sec. IV.I.

## 2. Water vapor

Despite its profound radiative impact, water vapor accounts for only around 0.25% of the atmospheric mass (Stevens and Bony, 2013). For perspective, if all water in the atmospheric

column were precipitated, it would represent a globally averaged depth of only around 2.5 cm, which is dwarfed by an oceanic depth (globally distributed) of around 2.8 km. The vapor (gas) state comprises more than 99% of the total atmospheric water content (Stevens and Bony, 2013).

In a given air parcel, water vapor pressure in the presence of liquid water (such as water droplets) represents a balance between departure of individual molecules from the water surface and collision and coalescence of molecules within the surface. The departure process, in particular, is highly temperature dependent. When these rates are matched, the atmosphere is saturated with respect to the water vapor. This equilibrium or saturation vapor pressure  $e^*$  is described by the Clausius-Clapeyron equation:

$$\frac{de^*}{dT} = \frac{Le^*}{R_v T^2}, \quad (13)$$

where  $T$  is the temperature,  $R_v$  is the gas constant for water, and  $L$  is the latent heat of vaporization (or sublimation). The specific humidity  $h$  (used later) is related to the vapor pressure by  $h = e/R_v T$ . The relative humidity is given by  $e/e^*$ . Equation (13) implies that the rate of increase of saturation specific humidity with temperature is itself a function of temperature, increasing from 6% per kelvin at 35 °C, to 7% per kelvin at 0 °C, to 17% per kelvin with respect to ice at −85 °C (which are around the coldest tropospheric temperatures and occur near the tropical tropopause). This represents roughly a doubling with every 10 °C (Lacis *et al.*, 2013). Note that supersaturation with respect to liquid water is rare in the atmosphere due to an abundance of condensation nuclei (Sherwood *et al.*, 2010b), although such is not the case with ice saturation (Jensen *et al.*, 2005). Given the strong overall decrease of temperature with height, specific humidity drops by more than 4 orders of magnitude from the tropical surface to the tropopause.

## 3. Relative humidity distribution

Despite specific humidity decreasing roughly exponentially with height, relative humidity follows a far different profile, with large values in the boundary layer reducing to minima in the subtropical midtroposphere, then increasing again above that (Fig. 6). In the deep tropics relative humidity is high throughout the troposphere, with a secondary maximum of around 200–300 hPa. In mid to high latitudes relative humidity decreases with height, but only slowly, with high values persisting well into the mid-troposphere (Fig. 6).

An analytical model of the tropical troposphere by Romps (2014) was able to describe the main features of the vertical humidity profile. In the lower troposphere, a decreasing relative humidity with height resulted from a decreasing convective detrainment<sup>9</sup> coupled with subsidence “drying” (i.e., a decrease in the relative humidity as air parcels warm and the specific humidity is unchanged). On the other hand, the increase of relative humidity with height toward the upper

<sup>9</sup>“Detrainment” refers to the mixing of often saturated air within convective towers into surrounding air, causing increases in humidity in the region around the convection.

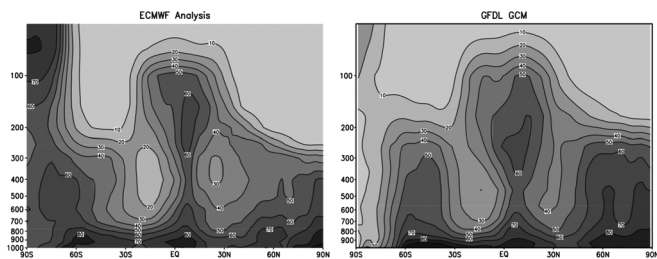


FIG. 6. Zonal mean distributions of relative humidity as a function of latitude and height in the European Centre for Medium-Range Weather Forecasts (ECMWF) reanalysis of July 1987 (left panel) and in a single GCM (right panel), that of the Geophysical Fluids Dynamics Laboratory. Vertical units are in hPa. From [Held and Soden, 2000](#).

troposphere was from the increased fractional convective detrainment, which increases rapidly as the mass flux (i.e., the total upward air transport) of convective systems dwindles ([Romps, 2014](#)). Midlatitude mixing also plays an important role ([Galewsky, Sobel, and Held, 2005](#)). These processes are described in more detail in Sec. IV.D. Overall, climate models can reproduce the features of large-scale relative humidity distribution with significant skill (Fig. 6; [Bates and Jackson, 1997](#); [Gaffen et al., 1997](#); [Randall et al., 2007](#); [Flato et al., 2013](#)). Climate models also show skill in reproducing the observed mean lapse rate in the tropics and elsewhere ([Flato et al., 2013](#)).

The principal questions that now follow concern how the distributions of temperature and water vapor change in a warming climate, such as one initiated by increases in  $\text{CO}_2$ , and how do these affect the TOA radiation?

### C. Spectrally dependent response to warming

Early studies of the outgoing terrestrial radiation ([Simpson, 1929](#)) noted a surprising insensitivity of the spectrally integrated OLR to surface warming if the atmosphere was allowed to moisten while conserving both lapse rate and relative humidity, sometimes referred to as Simpson's paradox ([Jeevanjee, 2018](#)). Such insensitivity is both counterintuitive, given the Planck function's strong dependence on temperature, and physically unrealistic, as it places the climate system in a perpetual runaway configuration ([Nakajima, Hayashi, and Abe, 1992](#); [Pierrehumbert, 2010](#)).

Resolution of this paradox comes by accounting for the spectral dependence of water vapor absorption, information that was not available at Simpson's time, as well as the influence of other absorbers, such as  $\text{CO}_2$  and clouds, on the atmospheric emission ([Ingram, 2010](#)). Indeed, further insight into the water vapor and lapse rate feedbacks can be gained by separating the outgoing longwave emission into two regions: one where water vapor absorption is optically thick and outgoing emission is insensitive to surface warming when relative humidity is conserved, and the other where it is optically thin and emission from the surface and atmosphere closely follows that of a blackbody ([Ingram, 2013a](#); [Jeevanjee, 2018](#)). This is sometimes referred to as a partly Simpsonian model.

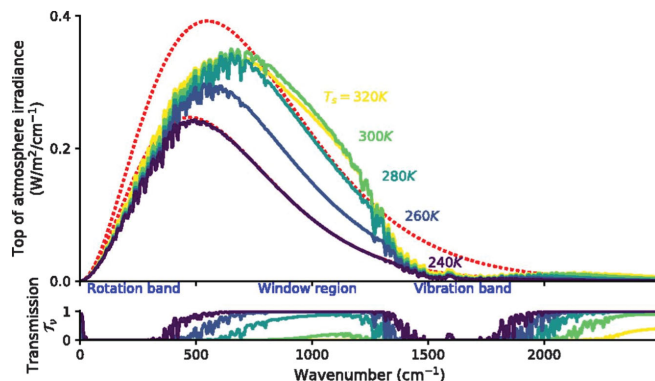


FIG. 7. Top panel: calculations of the spectrally resolved OLR as a function of temperature for idealized atmospheric profiles in radiative-convective equilibrium with constant relative humidity ( $r = 100\%$ ). Red curves show the surface's blackbody emission at 240 and 280 K. Bottom panel: spectrally resolved transmission between the surface and the top of atmosphere for each profile. From [Koll and Cronin, 2018](#).

Figure 7 from [Koll and Cronin \(2018\)](#) shows the spectrally resolved outgoing terrestrial radiation for a set of atmospheric profiles with constant relative humidity and moist adiabatic lapse rates, but varying surface temperature. Note that in the optically thick regions of the water vapor rotational (wave number  $1/1 < 500 \text{ cm}^{-1}$ ) and vibrational ( $1/1 > 1500 \text{ cm}^{-1}$ ) absorption bands, emission changes little with surface warming and the atmospheric transmissivity is near zero. [Jeevanjee, Lutsko, and Koll \(2021\)](#) showed that this insensitivity arises from a near-perfect cancellation between changes in blackbody emission and attenuation by water vapor at these wavelengths, thereby validating much of Simpson's original premise.

The large compensation between lapse rate and water vapor feedbacks originates from the tendency for models to conserve relative humidity, resulting in this spectral cancellation between emission and attenuation within the water vapor absorption bands. As noted by [Jeevanjee, Lutsko, and Koll \(2021\)](#), this cancellation is eliminated if the water vapor and lapse rate feedbacks are reformulated into the alternative relative-humidity-based framework (refer to Fig. 4), enabling greater insight into the processes responsible for the differences in climate sensitivity between models ([Po-Chedley et al., 2018](#); [Zelinka et al., 2020](#); [Zhang et al., 2020](#); [He, Kramer, and Soden, 2021](#)).

There are two basic consequences of the partly Simpsonian behavior of the atmosphere. The first is that the stabilization of Earth's climate to surface temperature change is achieved almost exclusively through radiative damping within the atmospheric window where water vapor absorption is negligible ([Slingo and Webb, 1997](#); [Koll and Cronin, 2018](#); [Seeley and Jeevanjee, 2021](#)).

This can be illustrated as follows using the partly Simpsonian model to decompose  $\lambda'_p$  from Eq. (6) into contributions from the atmospheric window ( $\lambda'^w_p$ ) and water vapor absorption band ( $\lambda'^{wv}_p$ ):

$$\lambda'_p = \lambda'^w_p + \lambda'^{wv}_p, \quad (14)$$

where, following Jeevanjee (2018),

$$\lambda_p^w = \int_{8 \mu\text{m}}^{12 \mu\text{m}} \pi \frac{dB(\lambda, T_s)}{dT_s} d\lambda \approx 2 \text{ W m}^{-2} \text{ K}^{-1} \quad (15)$$

and

$$\lambda_p^{wv} = \int_{\lambda \notin (8 \mu\text{m}, 12 \mu\text{m})} \pi \left( \frac{dB(\lambda, T_{em}(\lambda))}{dT_s} \right) d\lambda \approx 0, \quad (16)$$

assuming a partly Simpsonian atmosphere such that  $dT_{em}(\lambda)/dT_s \approx 0$  for  $\lambda \notin (8 \mu\text{m}, 12 \mu\text{m})$ . This simplification provides an excellent approximation for the values of  $\lambda_p$  simulated by GCMs (Ingram, 2013b; Zhang, Jeevanjee, and Fueglistaler, 2020). Errors arising from this approximation are largely the result of continuum absorption in the atmospheric window and pressure broadening of the water vapor absorption lines, both of which serve to make  $\lambda_p^{wv} < 0$  (Jeevanjee, Lutsko, and Koll, 2021). This is largely offset by terrestrial emission within the water vapor bands from clouds and the surface in dry polar regions, which causes  $\lambda_p^{wv} > 0$ .

The second is that changes in terrestrial emission within the water vapor absorption bands are dominated by changes in relative humidity ( $r$ ), not specific humidity or temperature (Möller, 1961). To a first approximation,  $dT_{em}(\lambda)/d \ln(r) \approx -8 \text{ K}$  within the water vapor absorption bands (Soden and Bretherton, 1996), so every doubling of relative humidity results in roughly an 8 K reduction in the water vapor emission temperature. This makes the climate system potentially quite sensitive to changes in relative humidity, particularly in the subtropical regions where  $r$  is small. However, theory, models, and observations all support the relative invariance in  $r$  under climate change, as discussed in Sec. IV.D.

#### D. Changes in temperature and water vapor under global warming and their radiative impact

##### 1. The importance of different regions for water vapor and lapse rate feedback

A key question then is, what changes in humidity and temperature can we expect in a warming climate? In the tropics, as the climate warms increasing latent heat released within rising parcels, from their increased moisture content, leads to a steepening saturated adiabatic lapse rate.<sup>10</sup> This means that temperature increases in the upper troposphere are greater than at the surface, increasing TOA OLR faster than implied by surface temperature change: a negative lapse rate feedback (Cubasch and Cess, 1990).

At the same time, warmer air can hold more moisture and the Clausius-Clapeyron equation dictates that saturation specific humidity increases exponentially with warming. A key

<sup>10</sup>The inability of the tropics to sustain strong tropospheric horizontal temperature gradients means that the tropical lapse rate is broadly set by the lapse rate in rising plumes within areas of active convection (Sec. IV.B). The expected slowing down of the tropical circulation under warming (Held and Soden, 2006) may reduce the net convective mass flux, but not the temperature structure of the convection that does occur, and therefore it would have little impact on broadscale lapse rate.

insight in the 1990s was that, because of the opacity of the lower troposphere to LW radiation and the increasing temperature contrast between the surface and atmosphere with height, upper tropospheric humidity changes, particularly in the tropics, have the greatest radiative impact on TOA radiation change (Lindzen, 1990; Shine and Sinha, 1991; Rind and Lacis, 1993; Spencer and Braswell, 1997; Inamdar, Ramanathan, and Loeb, 2004; Marsden and Valero, 2004). Furthermore, although for given specific humidity changes the LW effects are greatest in the tropical lower troposphere (Colman, 2001), it is the fractional increase in specific humidity that determines the LW radiative impact. This is greatest in the upper troposphere if relative humidity does not change much with warming (Held and Soden, 2000).

Models, theory, and observations (discussed later) suggest that relative humidity does remain close to unchanged, including in the upper troposphere, as the global temperature increases, thereby resulting in roughly exponential increases in saturation specific humidity with temperature under the Clausius-Clapeyron relationship. This implies a strong positive water vapor feedback (Held and Soden, 2000). This means that the upper troposphere, particularly in the tropics and subtropics, plays a disproportionate role in determining the global strength of LW water vapor feedback, as shown in Fig. 8.

By contrast, in the SW, which contributes around 15% to global water vapor feedback (Colman and McAvaney, 1997), it is water vapor changes in the lower troposphere and at high latitudes that are most important (Fig. 8). This is due to longer path lengths from highly reflective surfaces or clouds along with high summer insolation (Colman, Fraser, and Rotstajn, 2001; Soden *et al.*, 2008). Although the polar region SW feedback is consequently highly seasonal, compensation between hemispheres results in a fairly constant global SW feedback over the annual cycle (Colman, 2003b). In the LW the tropical dominance means the feedback also varies only weakly over the seasonal cycle (Colman, 2003b).

The geographical distribution of total water vapor feedback in a GCM is shown in Fig. 9(a) (Yoshimori, Yokohata, and Abe-Ouchi, 2009). The dominance of the low latitude LW contributions can be seen, as can the presence of individual maxima off the equator, along with relatively low values from high latitudes, particularly in the Southern Hemisphere.

The distribution of lapse rate feedback for the same GCM is shown in Fig. 9(b). Strong negative values are seen over the oceans throughout the tropics, consistent with convection maintaining the atmosphere at close to a saturated adiabatic lapse rate. Positive areas occur over sea ice and high latitude land corresponding to areas of low-level temperature inversions. The strength of lapse rate feedback in the tropics varies little with season but large changes occur at high latitudes, which is again associated with the strength of the surface temperature inversion (Colman, 2003b). These issues are discussed in more detail in Sec. IV.I.

In the midlatitudes, the presence of convective cores associated with baroclinic eddies also results in more warming in the upper troposphere than the lower troposphere under global warming. This effect is stronger in the summer hemisphere than the winter hemisphere, and in the Southern Hemisphere than the Northern Hemisphere (Frierson, 2006).

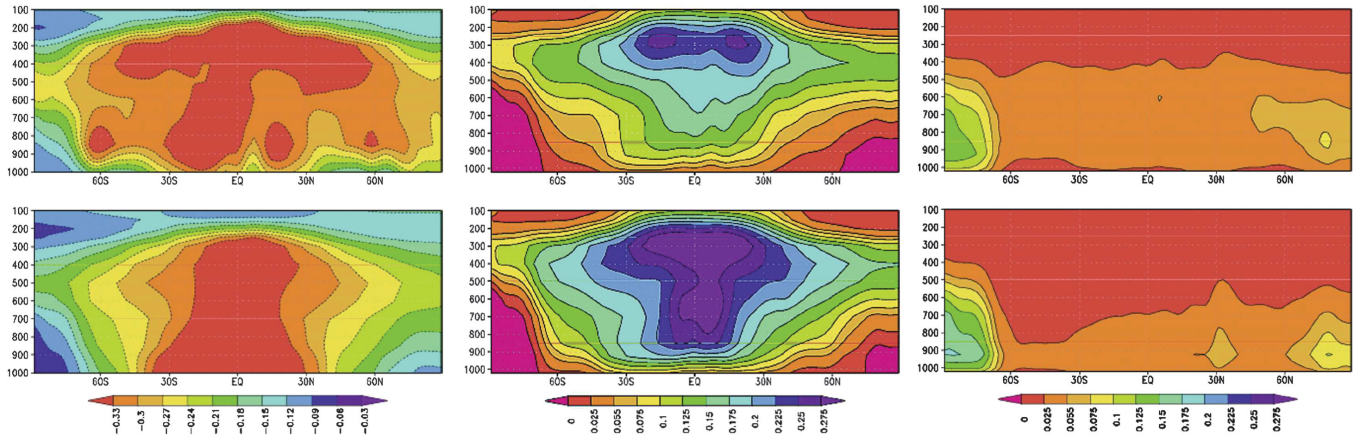


FIG. 8. Zonal mean radiative “kernels” (see Appendix A), in height (hPa) and latitude (deg), calculated using the Geophysical Fluids Dynamics Laboratory GCM. Shown are (left column) the LW TOA impact of 1 K temperature increases at each point and (center and right columns) the LW and SW TOA impacts of moisture increases corresponding to a 1 K temperature rise with fixed relative humidity. The top row shows “all-sky” conditions, i.e., those including the effect of clouds, while the bottom row shows “clear-sky” conditions, i.e., those with the removal of clouds at all levels. Units are in  $\text{W m}^{-2} \text{K}^{-1} 100 \text{ hPa}^{-1}$ . The importance of the tropical upper troposphere for LW water vapor feedback is apparent, whereas low levels and high latitudes are most important for the SW. From Soden *et al.*, 2008.

In summary, tropical and extratropical regions contribute differently to both water vapor and lapse rate feedbacks. However, given the importance of the tropical upper

troposphere for the globally dominant LW component of the water vapor feedback, many theoretical and observational studies over the past three decades have focused on understanding and evaluating humidity and temperature changes in this region.

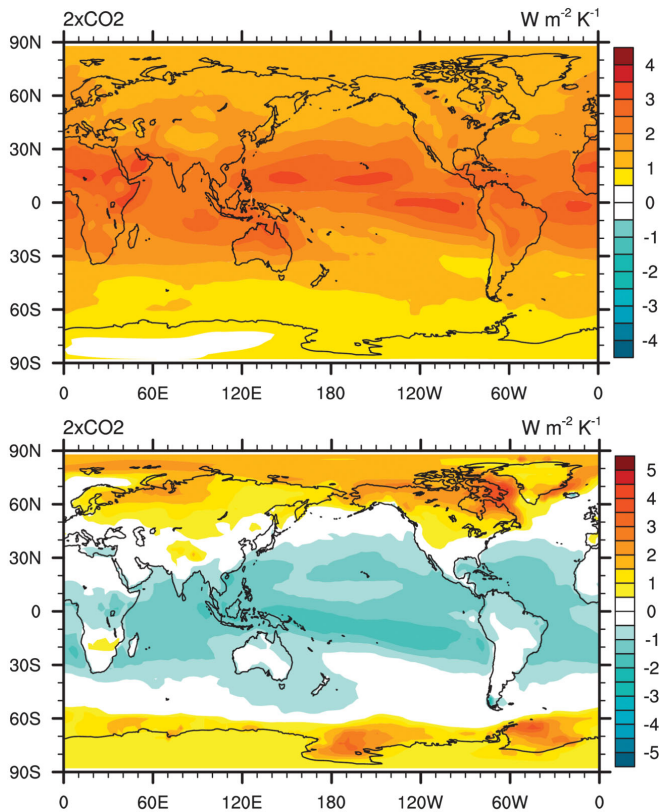


FIG. 9. Geographical distributions of water vapor (top panel) and lapse rate (bottom panel) feedbacks under  $2 \times \text{CO}_2$  forcing, as calculated using the PRP methodology (see Appendix A) applied to the CCSR/NIES/FRCGC/MIROC3.2(medres) Model for Interdisciplinary Research on Climate 3.2, medium-resolution version (Hasumi and Emori, 2004). From Yoshimori, Yokohata, and Abe-Ouchi, 2009.

## 2. Factors controlling relative humidity in a warming world

Processes which may control humidity distribution in the atmosphere are potentially complex. These include detrainment from convective systems, cloud microphysical processes, including cloud droplet formation and reevaporation, and turbulent mixing between clouds and ambient air, as well as large-scale advective processes (Emanuel and Pierrehumbert, 1996); see Fig. 10. The large descending subtropical areas are particularly important for water vapor feedback because they are relatively cloud free and relative humidity is low, so they play a major role in radiation to space, and changes under warming therefore can have a large impact on global OLR (Pierrehumbert, 1995; Held and Soden, 2000; Sherwood *et al.*, 2010a, 2010b). To establish the veracity of the feedbacks, particularly in the mid to upper troposphere, a combination of physical arguments and observational and modeling studies is needed.

## 3. Challenges to water vapor feedback “orthodoxy”: Convective drying and the role of microphysics

Given the complexity of the tropics and its importance for water vapor feedback, starting in the early 1990s some scientists raised challenges to the conventional role of water vapor feedback in climate change: that of its being a strong amplifying feedback. These challenges can be classified into four overall areas.

The first challenge postulated that with the primary source of free tropospheric moisture being detrainment from deep convection in the tropics (see Fig. 10), deeper tropical convection in a warming climate could cause air to detrain from higher, colder regions, thereby resulting in strong

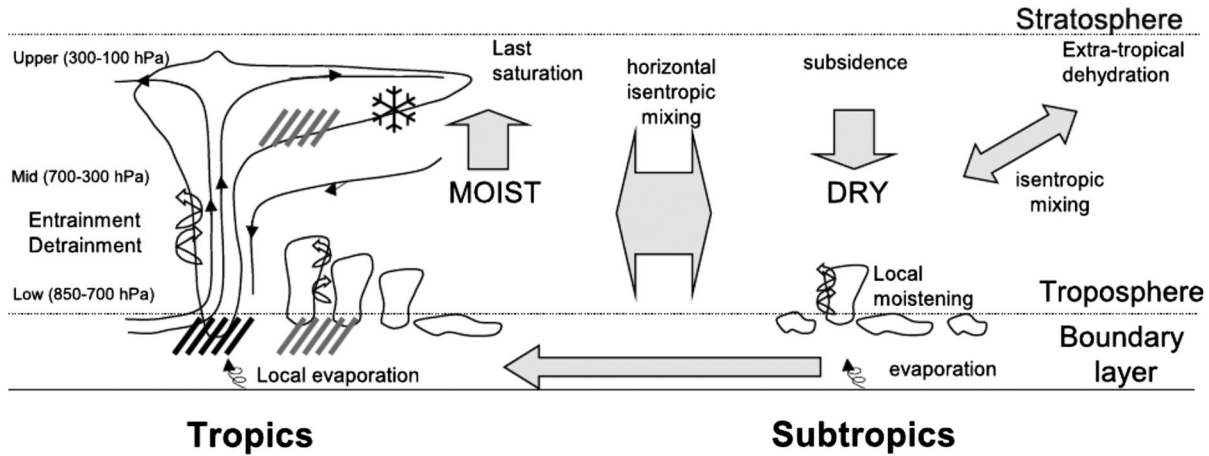


FIG. 10. Schematic of key processes involved in moisture transport in the tropics and subtropics. From Sherwood *et al.*, 2010b.

decreases in relative humidity throughout regions of broad-scale descent (Lindzen, 1990, 1994; Sun and Lindzen, 1993; Rennó, Emanuel, and Stone, 1994). This was postulated to lead to greatly weakened, or even negative, water vapor feedback (Lindzen, 1990). A second challenge was that hypothesized large decreases in the tropical high cloud fraction from convective outflows with warming could result in much drier air primarily affecting high cloud cover, but also reducing the strength of the water vapor feedback: the so-called iris effect (Lindzen, Chou, and Hou, 2001). Related to this was a third conjecture that condensate outflows could decrease with warming, causing upper tropospheric drying. A fourth was that microphysical changes such as increased precipitation efficiency inside convective towers could reduce moisture supply to the upper troposphere. These challenges helped prompt intense research over the following two decades.

Addressing the first point, the proposed simple model of detrainment from the tropical tropopause turns out to be too simplistic a view, with the atmosphere being moister than it would be if all detrainment occurred at these temperatures (Held and Soden, 2000). In response to warming, observations show increased tropospheric temperature exceeding the cooling effect from higher detrainment, resulting in increased water vapor, albeit with a small decrease in relative humidity (Minschwaner and Dessler, 2004; Minschwaner, Dessler, and Sawaengphokhai, 2006). A comparable, modest reduction in upper tropospheric relative humidity with warming has long been noted in climate models (Mitchell and Ingram, 1992; Held and Soden, 2000; Sherwood *et al.*, 2010a) (Fig. 11), and it is consistent with a water vapor feedback around 5% weaker than implied by unchanged relative humidity (Soden and Held, 2006) and in agreement with observations within uncertainties (Minschwaner, Dessler, and Sawaengphokhai, 2006); refer to Sec. V. This small reduction can be understood from temperature changes associated with convective outflow, which are in turn associated with the altitude of neutral buoyancy, and is a consequence of the vertical gradient of longwave cooling associated with decreasing water vapor concentration with altitude driven by the Clausius-Clapeyron relation (Allan, 2012; Zelinka and Hartmann, 2012). Additionally, not all the air in the driest subtropical descent regions is sourced from deep tropical convection. These

regions also contain air mixed in from the midlatitudes (Galewsky, Sobel, and Held, 2005), indicating a role for dehydration in midlatitude eddies as a source of subtropical dryness (Sherwood *et al.*, 2010b).

In summary, the “convective drying” in a warmer climate proposed by Lindzen (1990) is now known to contribute only a minor reduction below constant relative humidity.

On the question of an infrared iris, there is no observational or modeling evidence of decreases in tropical high clouds of the magnitude proposed (22% per kelvin of warming) (Chambers, Lin, and Young, 2002; Del Genio and Kovari, 2002; Hartmann and Michelsen, 2002; Lin *et al.*, 2002, 2004; Rapp *et al.*, 2005; Su *et al.*, 2008). Nor is there evidence of significantly drier air resulting from decreased cloud cover (Fu, Baker, and Hartmann, 2002). Just as with the first postulate (convective drying), the iris challenge was based in large part on simplified two box models of the tropics and

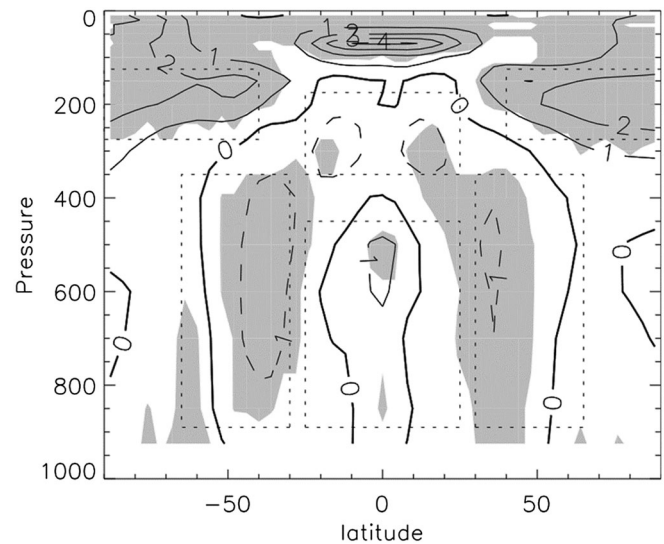


FIG. 11. Ensemble mean change in relative humidity per kelvin of surface warming under  $\text{CO}_2$  forcing, calculated from 18 CMIP5 GCMs. Axes are height (hPa) vs latitude (deg). Dashed contours indicate negative values, and shading represents areas of agreement on the sign of change by at least 90% of the models. From Sherwood *et al.*, 2010a.

postulated relationships among moisture, detrainment, and clouds not reproduced in GCMs or verified by observation.

The third and fourth challenges relate to the question of the role of cloud and convective “microphysics” in setting and changing upper tropospheric humidity under warming. Section IV.D.4 addresses this important issue.

#### 4. The role of model parametrizations in humidity distributions

Although in the 1990s no GCM had shown weak or negative water vapor feedback (as indeed remains the case today), it remained possible that all GCMs were “wrong” in the same way; in other words, all were missing or misrepresenting a certain key process. In particular, if details in the so-called microphysics<sup>11</sup> associated with convection and clouds are important for determining broadscale humidity distributions, then confidence in water vapor feedback would be substantially diminished considering the uncertainties in parametrizations of these processes in climate models (Randall *et al.*, 2007; Boucher *et al.*, 2013).

The reason why this question is so important is that confidence in models varies greatly for differing processes. It is high for the depiction of circulations of energy and moisture that are explicitly resolved by the model grid. GCMs used for climate modeling typically have grid sizes of around 50 to 100 km in the horizontal direction, and several hundred meters in the vertical direction.<sup>12</sup> However, many processes important for climate are not resolved on these scales, such as radiative interactions, convective plumes and entrainment, turbulent mixing, and cloud droplet aggregation and precipitation processes. Such processes need to be parametrized, that is, represented in approximate form, based on relationships between the time and area averaged effects of the unresolved process and grid-resolved (i.e., large-scale) variables. Parametrizations may include processes that are difficult to measure or observe or based on empirical, theoretical, or statistically derived values (Mauritsen *et al.*, 2012).

Uncertainties within parametrizations can have a substantial impact on climate response. For example, experiments where a range of parameter settings are systematically changed within “realistic” (often empirical or expert assessed) ranges can sometimes produce large differences in ECS (Murphy *et al.*, 2004; Stainforth *et al.*, 2005; Collins *et al.*, 2006; Klocke, Pincus, and Quaas, 2011; Lambert *et al.*, 2013; Tsushima *et al.*, 2020). If water vapor feedback is sensitive to such parameter perturbations, in particular, through control of the climatology or temperature dependency of upper tropospheric humidity, then confidence is reduced in the veracity of the feedback.

Evidence that parametrized microphysical processes are *not* critical for water vapor feedback come from several sources.

<sup>11</sup>Microphysics in this context refers to parametrized physical processes in cloud formation and convection, such as cloud droplet formation, coalescence, and precipitation.

<sup>12</sup>Finer grid spacing of ~10 km or less in the horizontal may be achieved with embedded regional climate models, but computational limitations generally prevent such fine scale for long global experiments, and these models still require relevant physical parametrizations.

The first is from “last saturation” simulations carried out using models without microphysics, showing that humidity distributions can be well represented using only evaporative and advective processes with 100% relative humidity limitation on parcels (Pierrehumbert and Roca, 1998; Dessler and Sherwood, 2000; Gettelman, Holton, and Douglass, 2000; Sherwood, 2006; Sherwood *et al.*, 2010b). This is an important area of research in its own right and is discussed further in Sec. IV.D.5.

The second is that strong positive water vapor feedback results from models with large numbers of different physical parametrizations and convection schemes (Colman and McAvaney, 1997; Ingram, 2002; Larson and Hartmann, 2003; Bony *et al.*, 2006; Sanderson, Shell, and Ingram, 2010), as well as cloud resolving models<sup>13</sup> (CRMs) (Tompkins and Craig, 1999), which have fewer unresolved convective processes than GCMs. For example, experiments using the Community Atmosphere Model (CAM4/5) suite of GCMs found that the magnitude of water vapor and lapse rate feedbacks were insensitive to a wide range of physical parametrization changes beyond the representation of deep convection. These included changes to moist boundary layer and shallow convection schemes, stratiform cloud microphysics, aerosol impacts on cloud droplet formation, and the model radiation code (Gettelman, 2012). Model climate sensitivity did change but was instead in response to changes in radiative forcing and tropical cloud feedbacks (Gettelman, 2012).

Large (by a factor of 15) changes in detrainment related microphysics settings, in concert with other parametrization changes, did alter the magnitude of water vapor feedback in a large, perturbed parameter experiment by roughly  $\pm 12\%$  (Sanderson, Shell, and Ingram, 2010). However, these setting changes were large compared to the range of change commonly applied in GCMs for tuning purposes (Colman *et al.*, 2019). Furthermore, there was strong offsetting from lapse rate feedback changes (Sanderson, Shell, and Ingram, 2010) and, consistent with that, another GCM showed little impact on climate sensitivity from convective detrainment changes (Mauritsen *et al.*, 2012).

There have been suggestions that insufficient vertical resolution in GCMs means that sensitivity to microphysics may be underrepresented (Emanuel and Živković-Rothman, 1999; Tompkins and Emanuel, 2000). This has proven to be unfounded, however, as experiments show insensitivity of water vapor feedback to large changes in vertical resolution in GCMs (Ingram, 2002). Furthermore, water vapor feedback strength has not changed significantly over generations of models, whereas vertical resolution has increased substantially, with models having up to ~100 layers in the vertical in the recent CMIP6 ensemble (Eyring *et al.*, 2016; Voldoire *et al.*, 2019).

Hints on the reasons for insensitivity of broadscale relative humidity distribution to microphysics come from studies in which atmospheric GCMs are forced by sea surface

<sup>13</sup>High-resolution models (down to around tens of meters) capable of simulating individual convective clouds (Guichard and Couvreux, 2017).

temperature (SST) and radiative perturbations to eliminate large-scale circulations such as the Hadley and Walker circulations and associated concentrated convective regions (Sherwood and Meyer, 2006). In this “boiling kettle” world, relative humidity in the upper troposphere was strongly affected by microphysical parameters determining precipitation efficiency. This was a factor that some had previously hypothesised might “rain out” extra moisture in the warmer world via convection, thereby decreasing relative humidity (Lindzen, Chou, and Hou, 2001; Lau and Wu, 2003). However, when convection was allowed to follow a more realistic, organized structure, the sensitivity to precipitation efficiency microphysics in the model was strongly decreased in the same GCM (Sherwood and Meyer, 2006). The experiments found that upper tropospheric relative humidity sensitivity to doubling convective precipitation efficiency was only a few percent, implying that the presence of convective organization makes the climate much less sensitive to the details of convective microphysics (Sherwood and Meyer, 2006).

The role of reevaporation from cirrus clouds in determining upper tropospheric humidity has been examined using cloud observations from the International Satellite Cloud Climatology Project and Television Infrared Observation Satellite (TIROS-N) Television Operational Vertical Sounder products and water vapor from combined infrared-microwave retrievals (Luo and Rossow, 2004). Results show that, although cirrus can be an important sink of water vapor, its total water content is too small to have a significant effect on upper tropospheric humidity through the subsequent reevaporation of condensate (Sherwood, 1999; Luo and Rossow, 2004; Soden, 2004; John and Soden, 2006). Instead, upper tropospheric moistening is associated with the same dynamical processes associated with the cirrus formation itself (Soden, 2004; Su *et al.*, 2006).

Outside the tropics, parametrized microphysical processes are also not expected to be important for water vapor distribution. Vertical mixing in baroclinic eddies (which are explicitly resolved in GCMs) act to maintain relative humidity profiles at around 30%–50% saturated throughout the year (Soden and Fu, 1995; Bates and Jackson, 1997; Stocker *et al.*, 2001).

In summary, multiple lines of evidence show that neither water vapor distribution nor feedback are significantly sensitive to parametrization choices in GCMs, including that of cloud or convection microphysics.

### 5. Simple models of water vapor distribution

Much understanding has been gained in the last two decades from application of the so-called advection-condensation (AC) approach. This idea poses perhaps the simplest possible explanation for humidity distribution within the atmosphere. It postulates that an air parcel’s specific humidity is conserved, being set by its last saturation, then subject only to large-scale advection, with no moisture gains or losses through small-scale mixing, condensed water evaporation, or further condensation (Pierrehumbert, Brogniez, and Roca, 2007). Specific humidity is therefore set by last contact with the surface (the ultimate source of all atmospheric moisture), with subsequent losses due to vertical transport or convection resulting in cooling, condensation, and precipitation from the parcel.

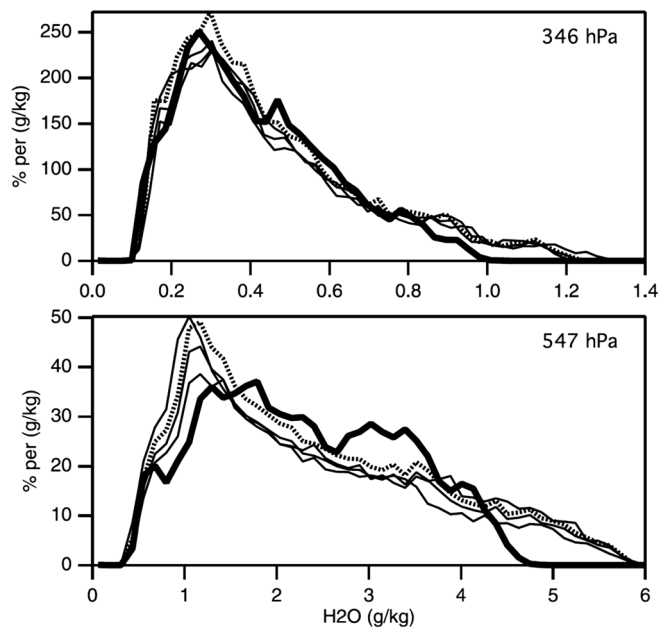


FIG. 12. Results from an advection-condensation (AC) simulation of annual average water vapor mixing ratio ( $\approx$ specific humidity) at 346 and 547 hPa using 50 day moisture advection trajectories. Thick solid lines represent AIRS satellite data. The three thin solid lines represent different configurations of the AC model, with different specified microphysics, in this case different convective thresholds whereby parcels mix with other sources of convection of different temperatures within rising plumes. Dashed lines show the AC model but with assumed relative humidity saturation limit of 90% instead of 100%. The close overall agreement with moisture distribution between the AC model and observations is apparent, as is the insensitivity of the AC model simulations to either microphysics specification, or even the precise definition of saturation. From Dessler and Minschwaner, 2007.

In the tropics the principal source of vertical advection is in convective regions associated with the upward branch of the Hadley circulation (Dessler and Minschwaner, 2007), with assumed saturation profiles, a feature supported by extensive observations (Bretherton, Peters, and Back, 2004; Holloway and Neelin, 2009). Outside the tropics final hydration is found to be sourced from air penetrating along isentropic surfaces to the midlatitudes (Dessler and Minschwaner, 2007). The AC approach explicitly excludes mixing on scales smaller than the resolved advective grid, and horizontal and vertical transport of condensed moisture (including processes such as reevaporation of cloud droplets).

A large number of studies followed and concluded that large-scale moisture distributions are generally well represented by this simple framework (Sherwood, 1996a, 1996b; Salathé and Hartmann, 1997; Pierrehumbert, 1998; Pierrehumbert and Roca, 1998; Dessler and Sherwood, 2000; Galewsky, Sobel, and Held, 2005; Hurley and Galewsky, 2010); see Fig. 12. Both Eulerian and Lagrangian advective schemes have been used and results are not sensitive to this choice. Without diffusive processes such as turbulent mixing, the latter results in filamentary structures that increase in time, eventually necessitating some degree of spatial or temporal averaging (Sherwood *et al.*, 2010b).

Supporting this insensitivity to microphysics, theoretical studies have argued that the detrainment profile and subsequent humidity distribution of upper tropospheric moisture can be understood in terms of a straightforward balance between moistening from convective detrainment and large-scale clear-sky cooling and subsidence drying (Folkens, Kelly, and Weinstock, 2002; Folkens and Martin, 2005). Both the vertical structure of relative humidity and its tendency to be conserved as the surface warms can be reproduced by a simple analytical model using only the Clausius-Clapeyron relation, the hydrostatic balance, and a bulk-plume water budget (Romps, 2014). This model provides the following analytic expression for the relative humidity  $r$ :

$$r = \frac{\delta}{\delta + \gamma}, \quad (17)$$

where  $\delta$  is the fractional detrainment and  $\gamma = -d \ln q / dz$  is the “water vapor lapse rate,” with  $q^*$  the saturated specific humidity.

Relative humidity is large in the tropical upper troposphere, where  $\delta \gg \gamma$  and convective moistening dominates over subsidence drying. Below this,  $r$  decreases due to increasing  $\gamma$  as one descends through the free troposphere. As the climate warms this simple analytical model predicts that  $\delta$  and  $\gamma$  dependences on ambient temperature are roughly independent of surface temperature, implying a close-to-unchanged relative humidity profile (Jeevanjee, 2018).

Challenges in the AC approach include uncertainties in verifying observations of both moisture and winds in the mid to upper troposphere, leading to several different approaches. A validation of results has occurred against a number of satellite products sensitive to upper tropospheric humidity, including 6.3  $\mu\text{m}$  High-Resolution Infrared Radiation Sounder (HIRS) brightness (Soden and Bretherton, 1996; Pierrehumbert and Roca, 1998), the Microwave Limb Sounder (Dessler and Sherwood, 2000; Ryoo, Igusa, and Waugh, 2009), Advanced Microwave Sounding Unit B (AMSU-B) (Brogniez and Pierrehumbert, 2006), and the Atmospheric Infrared Sounder (AIRS) (Dessler and Minschwaner, 2007).

AC studies have proved to be able to represent upper tropospheric relative humidity on a broad range of timescales including daily (Pierrehumbert and Roca, 1998), monthly (Dessler and Wong, 2009), and annual. The approach has also been found to skillfully represent GCM moisture fields using model winds (Salathé and Hartmann, 2000; Galewsky, Sobel, and Held, 2005). Nor is the skill adversely affected by the imposition of convective microphysical assumptions, or even to the level of relative humidity designated as saturated, e.g., reducing from 100% to 90% to account for mixed detrainment below relative humidities of 100% (Dessler and Minschwaner, 2007) (Fig. 12). An extensive review of the AC approach is provided by Sherwood *et al.* (2010b).

In summary, AC simulations can skillfully reproduce large-scale tropical humidity (particularly in the upper troposphere), typically to within 10% accuracy over a wide range of humidity levels and regimes (Sherwood *et al.*, 2010b) (Fig. 12). The reason they can do this appears to be because (i) at the large scale, free atmospheric parcel source regions of moisture can be effectively described as at or near saturation,

and (ii) additional sources of moisture such as condensed cloud water or ice are modest over parcel lifetime to next saturation (Sherwood *et al.*, 2010b).

The key importance of theoretical and AC studies is that they provide convincing evidence that convective or cloud microphysical settings have little impact on humidity distribution, meaning that it is unlikely that these uncertainties would substantially affect projected humidity changes under a warming climate. The only remaining possible sensitivity would be on the advecting winds themselves (Dessler and Minschwaner, 2007). As stated by Dessler and Sherwood (2000): “We see no evidence to suggest that accurate predictions of the humidity in this (upper tropospheric) region are dependent on accurate simulations of microphysical processes or on transport of ice or liquid water. Our results instead suggest that accurate predictions of the humidity primarily require realistic three-dimensional large-scale (greater than a few hundred kilometers) wind fields.”

## 6. Deviations from unchanged relative humidity

Climate models project that on broad scales relative humidity will be close to unchanged throughout much of the troposphere under global warming. This is not exact, however, and some systematic large-scale deviations from uniformity are apparent, as shown in Fig. 11 for the multi-model mean for 18 CMIP5 models. These deviations are important to understand in that they clarify model processes controlling moisture distribution, have a modest effect on the strength of the global (LW) feedback, and have a critical role in contributing to cloud feedback (Ceppi *et al.*, 2017; Sherwood *et al.*, 2020).

As the climate warms, models predict (Gettelman *et al.*, 2010; O’Gorman and Singh, 2013), and observations confirm (Santer, Sausen *et al.*, 2003; Santer, Wehner *et al.*, 2003), that there is an increase in the height of the tropopause. This is a consequence of the decreased effectiveness of thermal emission from water vapor below around 200 K (Hartmann and Larson, 2002). This increases relative humidity in the region of both the tropical and extratropical tropopause, i.e., at heights where formerly dry stratospheric air is replaced by moister tropospheric conditions (Boucher *et al.*, 2013). Both clouds and relative humidity shift upward following a fixed temperature coordinate (Po-Chedley *et al.*, 2019), which is consistent with that expected from a fixed temperature for convectively detrained clouds and moisture (Hartmann and Larson, 2002; Romps, 2014). Maximum zonal mean values of these changes are around 2%–4% of relative humidity per kelvin of warming (Fig. 11). This has important consequences for the increasing strength of water vapor feedback in warmer base climates (Sec. IV.G).

Other regions of increasing relative humidity are in the equatorial tropics (below about 400 hPa) and at high latitudes throughout the depth of the atmosphere. Decreases occur in the upper troposphere in the tropics, and through a broad depth in the subtropics to the midlatitudes. Notably, there is a marked symmetry between the two hemispheres, indicating that the circulation changes resulting in relative humidity perturbations are not sensitive to continental distribution (Sherwood *et al.*, 2010a). Furthermore, the presence of

modest increases and decreases results in close-to-unchanged relative humidity globally as the temperature rises.

What causes these large-scale humidity changes? The simplest possible explanation, the so-called shift hypothesis, postulates that they result from upward and poleward expansion of tropical circulations. That is, decreases are located where relative humidity in the current climate increases either with altitude, as it does in the tropical upper troposphere, or with latitude, as it does in the midlatitudes (Sherwood *et al.*, 2010a). Sherwood *et al.* (2010a), however, showed that midlatitude humidity changes are 2 to 3 times too large for this simple explanation. Instead, they postulated that air parcels in drying regions last experience saturation in regions of the atmosphere that are warming at a relatively slower rate; i.e., the humidity changes result from nonuniform rates of warming or wind change (Hurley and Galewsky, 2010).

These relative humidity differences are modest on global scales. Therefore, although they are important for cloud feedbacks, they have only a small impact on global water vapor feedback (Boucher *et al.*, 2013). Models simulate water vapor feedback that is around 5% weaker than that predicted by fixed relative humidity (Soden and Held, 2006), principally as a result of the reduction in upper tropospheric relative humidity (Vial, Dufresne, and Bony, 2013). High-resolution CRMs also find upward shifts in relative humidity with increasing temperature (Kuang and Hartmann, 2007), thus adding confidence to GCM processes.

In summary, small changes in relative humidity are found in models under global warming, partly caused by processes such as a rising tropopause and nonuniform rates of warming. Their net effect on water vapor feedback is to reduce it in strength by around 5%.

### 7. Water vapor feedback and convective aggregation

As the world warms, changes in “aggregation” (clustering) of tropical convection (Muller and Held, 2012) could potentially affect water vapor feedback strength. This is because changes in the way that convection is organized may affect broadscale humidity and, in particular, the area or dryness of large-scale descending regions. These large, relatively cloud free areas play a major role in global radiation balance (Pierrehumbert, 1999; Peters and Bretherton, 2005). Observations of changes in convective self-aggregation suggest an anticorrelation between aggregation and tropospheric humidity outside the boundary layer (Tobin, Bony, and Roca, 2012; Tobin *et al.*, 2013). Furthermore, drying of the free troposphere during periods of greater aggregation has been found to increase the clear-sky OLR over the tropics and constitutes the dominant factor controlling interannual variability of the tropical-mean radiation budget (Bony *et al.*, 2020).

A recent large multimodel ensemble using models ranging from GCMs to CRMs, the Radiative-Convective Equilibrium Model Intercomparison Project (Wing *et al.*, 2018), found that models widely exhibited self-aggregation, which acts to warm and dry the troposphere in the current climate (Wing *et al.*, 2020). Under global warming, however, there was no clear tendency in the degree of self-aggregation, although there was

some sensitivity in this result to the use of parametrized (GCM) convection versus CRMs (Wing *et al.*, 2020).

There remains some uncertainty then on how convective aggregation may change in response to a warming climate, and therefore as to what the net effect would be on water vapor feedback.

Recently a convection-related negative water vapor buoyancy feedback was proposed whereby the lightness of water vapor relative to other atmospheric constituents induces increased buoyancy in moist regions, compensated for by increased temperatures in dry regions (Seidel and Yang, 2020a). This was hypothesized to lead to increased OLR and to strengthen with warming, thereby producing a negative feedback (Seidel and Yang, 2020b). However, climate models explicitly represent the density impact of moisture and its effect on circulations, so this represents merely a different way of subdividing known feedback processes, rather than a new negative feedback.

### 8. Impact of water vapor or lapse rate changes on radiative forcing

Apart from temperature-related changes [Eq. (1)] the question arises as to whether rapid water vapor or lapse rate adjustments in response to the forcing itself (such as from a sudden increase in CO<sub>2</sub>) induce an additional TOA impact. Such *rapid responses* (i.e., fast, non-surface-temperature-related atmospheric adjustments) are important for clouds (Gregory and Webb, 2008; Sherwood *et al.*, 2015) and are regarded as contributing to the initial forcing.

However, there is little evidence on a global scale of rapid, radiatively important water vapor adjustments following CO<sub>2</sub> forcing (Colman and McAvaney, 2011; Block and Mauritsen, 2013; Vial, Dufresne, and Bony, 2013; Po-Chedley *et al.*, 2018). On a regional scale, positive and negative radiative responses can occur (Block and Mauritsen, 2013), although evidence of rapid responses over land has been linked to fast land warming, rather than atmospheric adjustments (Vial, Dufresne, and Bony, 2013). Together these studies mean that to a good approximation water vapor acts as a true feedback process coupled with global surface temperature change following external radiative forcing and contributes little to the original forcing.

Related to this issue, questions have also been raised as to whether human activities such as irrigation directly affect water vapor concentrations in the atmosphere, with consequent radiative impact. Idealized simulations by Boucher, Myhre, and Myhre (2004) indeed found that water vapor concentrations increase locally in irrigated regions, resulting in a global mean OLR impact of between 0.03 and 0.1 W m<sup>-2</sup>. This is a forcing process, not a feedback. However, it is unclear whether this is even truly a radiative forcing process, as local surface temperatures decreased, rather than increased, in their experiments due to surface evaporative and other changes (Boucher, Myhre, and Myhre, 2004). Furthermore, water vapor lifetime in the atmosphere is short, around two weeks (Zhang, Mapes, and Soden, 2003; Lacis *et al.*, 2013; Stevens and Bony, 2013), meaning that, without increased temperatures, injected water vapor will rapidly precipitate out.

Another source of direct water vapor injection, that from aviation, is estimated to have around an order of magnitude less impact than that from irrigation (Intergovernmental Panel on Climate Change, 1999), and therefore makes a negligible contribution to global radiative forcing.

The lapse rate response can be sensitive to the forcing agent due to differences in vertical forcing and the resultant rapid response differences in the large-scale tropospheric stability (Ceppi and Gregory, 2019). This includes changes in upper tropospheric temperature (Andrews and Forster, 2008). The global radiative impact on forcing for CO<sub>2</sub> increases, however, is small (Colman and McAvaney, 2011; Vial, Dufresne, and Bony, 2013).

## E. Relationship between water vapor and lapse rate feedbacks

### 1. What causes the (anti)correlation between water vapor and lapse rate feedbacks?

It has long been noted that there is a strong offsetting relationship between the traditionally defined water vapor and lapse rate feedbacks leading to a reduced overall range of feedbacks across multimodel ensembles (Cess, 1975; Colman, 2003a; Soden and Held, 2006; Held and Shell, 2012; Koll and Cronin, 2018). This occurs not only across different models but also within individual models when modifications such as parametrization changes are made (Zhang *et al.*, 1994). For example, a weakened lapse rate feedback was largely offset by a corresponding weakened water vapor feedback when moving from one version of the model to another of the Community Climate System Model (Bitz *et al.*, 2012), or when adjusting parameters as part of a large perturbed parameter ensemble within a single model (Sanderson, Shell, and Ingram, 2010). Figure 13 (Po-Chedley *et al.*, 2018) illustrates offsetting across Coupled Model Intercomparison Project phase 5 (CMIP5, Taylor, Stouffer, and Meehl, 2012) GCMs.

Our understanding of this anticorrelation has evolved significantly over time. The early focus emphasized the tropical upper troposphere, given its critical role in determining water vapor feedback strength. Enhanced warming in this region, it was argued, produces a stronger negative global lapse rate feedback, but it also strengthens water vapor feedback due to consequent increased specific humidity under the additional warming (Cess, 1975; Randall *et al.*, 2007; Huybers, 2010). However, a realization that both global water vapor (Soden and Held, 2006) and lapse rate feedback strength (Shell, 2013) are correlated with equator to pole temperature gradients hinted at another mechanism. While considering regional feedbacks, Armour, Bitz, and Roe (2013) found that the correlation between water vapor and lapse rate feedbacks in the tropics was in fact weak [Fig. 14(a)]. Furthermore, intermodel variation in the tropical water vapor feedback strength could be largely explained by changes in relative humidity rather than tropospheric temperature changes under a fixed relative humidity assumption (Vial, Dufresne, and Bony, 2013; Po-Chedley *et al.*, 2018). This is illustrated in Fig. 14(b), which shows the strong correlation between the classically defined tropical water vapor feedback  $\lambda_q$  [Eq. (4)] and the Held and Shell (2012) relative humidity

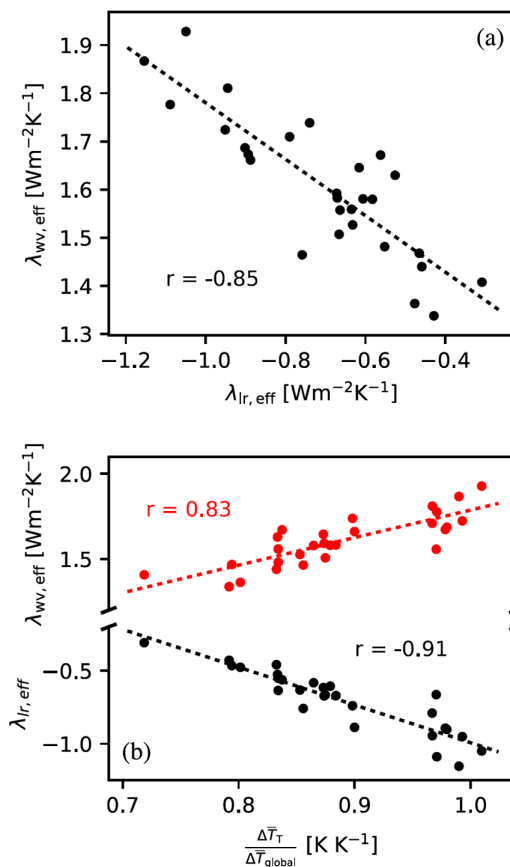


FIG. 13. (a) The relationship between global effective (viz., standardly defined) water vapor and lapse rate feedbacks for CMIP5 models. Each data point represents a GCM, and the correlation coefficient is shown. (b) Water vapor and lapse rate feedbacks plotted against the ratio of tropical to global surface temperature change. Note the discontinuity on the y axis. This shows the strong anticorrelation between water vapor and lapse rate feedbacks globally, and the close dependence of both feedbacks on the relative warming between the tropics and extratropics. From Po-Chedley *et al.*, 2018.

term  $\lambda'_H$  [Eq. (8)]. On the other hand, no link is found between changes in relative humidity and changes in tropical lapse rate feedback (Po-Chedley *et al.*, 2018). Hence, no common physical mechanism links variations in tropical mean water vapor and lapse rate feedback strengths, so little correlation would be expected (or is found) [Fig. 14(a)].

By contrast, in the extratropics strong anticorrelation is found between classically defined water vapor and lapse rate feedback, as shown in Fig. 14(a). The range in lapse rate feedback is greater in the Southern Hemisphere than the Northern Hemisphere by a factor of 3. Po-Chedley *et al.* (2018) showed that the asymmetry was due to contrasts in the spread in temperature pattern differences across models. Throughout the Northern Hemisphere, surface and atmospheric temperature changes are strongly coupled with the tropics. In the Southern Hemisphere extratropics, by contrast, temperature correlation with tropical changes is relatively weak and is instead dominated by patterns of surface temperature change and consequent local feedbacks (Po-Chedley *et al.*, 2018). Moreover, delayed warming in

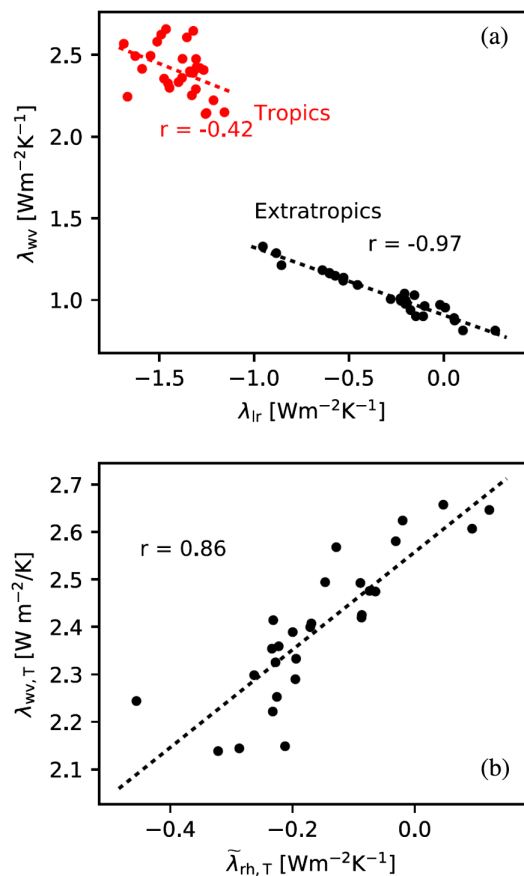


FIG. 14. (a) Relationship between global effective (viz., standardly defined) water vapor and lapse rate feedbacks for the CMIP5 models in the tropics (latitude  $<30^\circ$ ) and extratropics. (b) Tropical water vapor feedback shown against tropical relative humidity feedback [ $\lambda'_H$  in Eq. (8)], here denoted as  $\tilde{\lambda}_{rh}$ . From Po-Chedley *et al.*, 2018.

the Southern Hemisphere extratropical latitudes results in regional feedbacks that are sensitive to poleward-mixed warming and moistening from the tropics (Butler, Thompson, and Heikes, 2010; Rose and Rencurrel, 2016). It is differences then in both the magnitude and pattern of Southern Hemisphere extratropical warming, in turn related to differences such as Antarctic sea ice climatology (Feldl, Bordoni, and Merlis, 2017), that drive the intermodel range of feedback strengths and the global anticorrelation seen in Fig. 13(a).

Consistent with this, for the combined water vapor plus lapse rate feedback, a recent study of 31 CMIP5 models showed that relative humidity differences at the regional level contribute around 40% of the intermodel variance, in turn coupled with differences in patterns of tropical SST changes, with the remainder scaling closely with the difference between tropical-subtropical mean temperature change and that of the extratropics (Zhang *et al.*, 2020). This highlights the utility of the alternative RH-based feedback framework (Sec. III.B) for understanding the cause of intermodel spread in climate sensitivity.

Paleo studies reinforce the importance of the extratropics for the offsetting nature of water vapor and lapse rate feedbacks. In Last Glacial Maximum (LGM) (19–27 kyr ago)

experiments, Northern Hemisphere continental ice sheets push cold surfaces to much lower latitudes, weakening water vapor feedback but also rendering lapse rate feedback weakly positive globally, thereby resulting in virtually unchanged global water vapor plus lapse rate feedback (Yoshimori, Yokohata, and Abe-Ouchi, 2009).

The previous discussion relates to climate change timescale feedbacks. On shorter timescales, anticorrelations can also be found in the feedbacks. An evaluation of global lapse rate and water vapor feedbacks using accurate so-called partial radiation perturbation (PRP) methods (see Appendix A) every six hours for six consecutive years of model simulations showed only weak correlation on six hourly timescales, but strong anticorrelation between the feedbacks on three monthly (i.e., seasonal) timescales ( $r = 0.71$ ) (Klocke, Quaas, and Stevens, 2013). Different models have been found to produce similar interannual fluctuations in clear-sky (i.e., cloud free) OLR with surface temperature fluctuation when forced with observed SST changes, showing that their combined water vapor plus lapse rate feedbacks were similar, although both lapse rate changes and moisture distributions differed strongly, with significantly different upper tropospheric warming, suggesting contrasting mechanisms (Allan, Ramaswamy, and Slingo, 2002).

Regionally, however, there is little geographical (anti)correlation between the strength of water vapor and lapse rate feedbacks in either models (Taylor, Ellingson, and Cai, 2011) or observations (Ferraro *et al.*, 2015). This can be understood from the differing processes driving these feedbacks at regional or local scales. The close-to-ubiquitous saturated adiabatic lapse rate in the tropics and weak horizontal temperature gradients above about 700 hPa mean that local lapse rate feedback variations are primarily driven by surface temperature change patterns: stronger reduced OLR corresponds to greater temperature increases (Lambert and Taylor, 2014). Local water vapor feedback, on the other hand, is less tied to surface temperature increases. Over land, where surface temperature increases are greatest, relative humidity in the lower part of the atmosphere decreases because of reduced moisture availability (Fasullo, 2010). This modestly weakens local water vapor feedback (Lambert and Taylor, 2014). Over oceans local maxima in water vapor feedback are related only weakly to surface temperature changes and are instead strongly associated with areas of increased heavy precipitation (Lambert and Taylor, 2014). In summary, because of the differing processes driving regional changes in water vapor and lapse rate feedbacks, little (anti)correlation is found at these scales.

## 2. What causes the spread in combined water vapor + lapse rate feedbacks in models?

Section IV.E.1 addressed the reasons for the anticorrelation between separate water vapor and lapse rate feedbacks in GCMs. There is now also a much better understanding of the source of spread in the *combined* feedback. This is an important issue, as it is the combined feedback that underpins overall climate sensitivity and the uncertainty of the combined feedbacks that contributes to sensitivity spread (Fig. 3). Furthermore, the cause of the spread casts light on the spread that remains under the alternate RH-based formulation of

feedbacks described in Sec. III.B. The spread results from different processes at different latitudes.

In the tropics, the offsetting upper tropospheric contributions from water vapor and lapse rate changes ensure that the range in the combined feedback relates primarily to relative humidity changes, rather than changes to the vertical structure of temperature or moisture (Held and Shell, 2012; Vial, Dufresne, and Bony, 2013; Po-Chedley *et al.*, 2018). Theoretical support also comes from the realization that relative humidity changes alone are important for determining the combined feedback strength, provided that infrared absorption bands are close to saturated (Ingram, 2010, 2013a, 2013b), as they are throughout much of the atmosphere (Sec. IV.A).

The reasons for tropicswide differences in relative humidity changes in models are not fully understood but likely relate to differences in SST warming patterns (Armour, Bitz, and Roe, 2013; Andrews and Webb, 2018) or parametrization differences in processes such as deep convection (Po-Chedley *et al.*, 2018). Consistent with this, a recent parameter physics ensemble found that convective parameters determining the entrainment of environmental air into convective plumes controlled present-day climate clear-sky TOA LW fluxes (representing the clear-sky combination of Planck, water vapor, and lapse rate feedbacks), as well as their response to global warming (Tsushima *et al.*, 2020). Furthermore, there was a strong relationship between current climate tropical-mean clear-sky OLR and flux change (Tsushima *et al.*, 2020).

In the midlatitudes, relative humidity changes are not related to changes in the net feedback and models show little range in relative humidity changes over the poles (Vial, Dufresne, and Bony, 2013). Instead, the spread in the combined water vapor + lapse rate feedback in the midlatitude and polar regions depends on the spread in the lapse rate feedback (Vial, Dufresne, and Bony, 2013). As discussed in Sec. IV.E.1, the spread in absolute feedback strength in the extratropics depends upon local feedbacks in those regions (Po-Chedley *et al.*, 2018).

Cloud differences may also have an impact on combined feedback strength. The presence of clouds compared to clear-sky conditions has different impacts on LW and SW components of the water vapor feedback. In the smaller SW component, feedback is modestly strengthened (Zhang *et al.*, 1994) (Fig. 8), largely due to an increased path length from multiple reflections (Colman, Fraser, and Rotstayn, 2001; Soden *et al.*, 2008). For the dominant LW component, feedback is weakened (Fig. 8) due to midlevel and upper-level clouds partially obscuring the TOA radiative impacts of underlying water vapor changes (Soden, 2004). On the other hand, for lapse rate feedback, the presence of upper tropospheric clouds strengthens the impact of upper tropospheric temperature changes because clouds are stronger infrared emitters and absorbers than clear sky (Zhang *et al.*, 1994).

A covariance has been noted between CMIP3 model combined water vapor + lapse rate and cloud feedbacks (Huybers, 2010), with stronger feedback in one implying weaker feedback in the other. Although it remains possible that this is an artifact of feedback evaluation methodology or statistics, it may be related to physical processes such as convective differences between models resulting in different changes in tropical upper tropospheric relative humidity, with

compensation between water vapor feedback and changes in anvil cloud cover (Huybers, 2010). “Suppressed feedback” experiments in one GCM also noted interactions between water vapor, lapse rate, and cloud feedbacks (Mauritsen *et al.*, 2013). Extra upper tropospheric warming due to increased cloud cover strengthened water vapor feedback, but at the same time rising convective clouds strengthened negative tropical lapse rate feedback, damping the warming from cloud changes (Mauritsen *et al.*, 2013). These processes and correlations have received only limited attention, however, and further research is needed to understand their significance for net feedback strength and climate change.

In summary, the source of intermodel spread in combined, traditionally defined water vapor + lapse rate feedback is from tropicswide relative humidity differences in low latitudes, and from lapse rate feedback spread in the extratropics. Under the RH-based formulation (Sec. III.B), the tropical effect is included in the separate relative humidity feedback term, showing that there are benefits to this approach in identifying sources of intermodel feedback spread. Differences in cloud cover between models may also play a role in combined feedback spread, and there remain hints of correlations with cloud feedbacks that are not confirmed or fully understood.

## F. Stratospheric water vapor feedback

Traditionally, water vapor feedback was perceived as being confined to the troposphere, albeit with increasing tropopause height implying higher-level contributions in a warmer climate (Santer, Sausen *et al.*, 2003; Santer, Wehner *et al.*, 2003; Meraner, Mauritsen, and Voigt, 2013).

Enhanced climate forcing (a nonfeedback process) can occur from stratospheric methane oxidation (Forster and Shine, 1999; Forster *et al.*, 2007). Furthermore, model results suggest that stratospheric water vapor changes can amplify forcing from increases in lower stratospheric ozone. This occurs when increased stratospheric water vapor induces a secondary forcing (Stuber, Ponater, and Sausen, 2001). Stratospheric water vapor adjustments, however, have a negligible impact on CO<sub>2</sub> forcing and ozone forcing in the troposphere (Stuber, Ponater, and Sausen, 2001).

At first glance, however, we expect a relatively small role for the stratosphere in water vapor feedback. In contrast to the troposphere, there are no reasons *a priori* to expect, say, unchanged relative humidity in the stratosphere (Stuber, Ponater, and Sausen, 2001), and fractional changes in stratospheric water vapor have less impact radiatively than do those of the upper troposphere (Allan *et al.*, 1999).

Observations, however, do suggest that stratospheric increases in water vapor have affected TOA radiation over recent decades (Solomon *et al.*, 2010), and an examination of satellite and reanalyses data linked lower stratospheric water vapor changes with surface temperature changes, suggesting that it is operating as a true feedback (Dessler, 2013). It has long been thought that lower stratospheric water vapor enters through the tropical tropopause, with amounts controlled by minimum tropopause temperatures (Brewer, 1949; Rosenlof *et al.*, 1997; Joshi and Shine, 2003). Processes involved are a combination of convective and broadscale ascent

(Keith, 2000; Sherwood and Dessler, 2000; Rosenlof, 2003). However, more recent evidence reveals a broader picture, with water vapor entering the stratosphere through both the tropical and the extratropical tropopause (Dessler *et al.*, 2013) due to tropopause warming offsetting the freeze-drying process (Gettelman *et al.*, 2009; Smalley *et al.*, 2017). Models also suggest that for strong warming (e.g., that under  $8 \times \text{CO}_2$ ) large upper tropospheric warming greatly reduces the tropopause “cold trap,” leading to enhanced penetration of water into the lower stratosphere (Lacis *et al.*, 2013; Russell *et al.*, 2013).

CMIP5 models robustly show stratospheric moistening with global warming (Gettelman *et al.*, 2010; Smalley *et al.*, 2017). This produces significant additional radiative perturbations, peaking in the midlatitudes, with most of the contribution (over three quarters) resulting from extratropical lower stratospheric processes (Banerjee *et al.*, 2019). An estimate of the strength of the associated feedback is  $0.15 \pm 0.04 \text{ W m}^{-2} \text{ K}^{-1}$ , with a range of  $0.10 - 0.26 \text{ W m}^{-2} \text{ K}^{-1}$  (Banerjee *et al.*, 2019). The upper end of this multimodel estimate is comparable to the previous single model estimates of Stuber, Ponater, and Sausen (2001) and Dessler *et al.* (2013). A much lower CMIP5 multimodel estimate of  $0.02 \pm 0.01 \text{ W m}^{-2} \text{ K}^{-1}$  using a similar kernels-based methodology<sup>14</sup> (Huang *et al.*, 2016) appears to be unreliable because of the use of instantaneous radiative kernels, that is, ones that do not consider stratospheric temperature adjustments (Solomon *et al.*, 2010; Maycock and Shine, 2012; Banerjee *et al.*, 2019).

Recent work has aimed to understand the processes better, as well as limitations or biases in the models. It is important to note that some potentially important troposphere-stratosphere exchange processes appear to be underdone by models, such as the effect of the quasibiennial oscillation (QBO) on humidity in the lower stratosphere (Smalley *et al.*, 2017). This may be significant for the strength of the feedback, as the QBO plays an important role in modulating stratospheric water vapor through its effect on the tropical tropopause temperature (Tian *et al.*, 2019). Ozone effects on stratospheric water vapor feedback are also not well understood; experiments with partially prescribed rather than fully interactive ozone had the effect of increasing climate sensitivity through modification of the water vapor feedback strength (Nowack *et al.*, 2018).

Nor is the importance of the additional radiative effects of stratospheric water vapor feedback fully established. For example, it has been postulated that there are several radiation relevant processes from the increased stratospheric water vapor in a warmer climate. There is direct suppression of OLR from the additional atmospheric radiative opacity. Additionally, the stratosphere cools from the combined radiative effect of additional water vapor in both the troposphere and the stratosphere, which further reduces OLR (Wang and Huang, 2020). Offsetting this, ongoing tropospheric warming provides additional upwelling LW radiation, inducing stratospheric warming and increased OLR. The combined result may then result in negligible net TOA radiative

flux changes (Wang and Huang, 2020). A recent stratospheric water vapor “locking” experiment indeed found only a 2% increase in surface warming under  $4 \times \text{CO}_2$  forcing (Huang, Wang, and Huang, 2020) due to warming from increased stratospheric water vapor being compensated for by cooling from upper troposphere moisture and cloud responses. However, a similar experiment with a chemistry-climate model found a stratospheric water vapor feedback of  $0.11 \text{ W m}^{-2} \text{ K}^{-1}$ , contributing around 10% to global warming under  $\text{CO}_2$  quadrupling (Li and Newman, 2020).

The science remains unsettled in this area. It is clear from an examination of the CMIP5 ensemble that there is a significant LW impact of increased lower stratospheric water vapor with warming, and observational evidence indicates recent impacts on TOA radiation. However, evidence from single model experiments also suggests that compensating negative feedbacks in the troposphere from clouds or temperature changes may result in negligible net enhancement of global warming, although the results are somewhat inconsistent. Further research is needed to untangle and quantify these effects, particularly including a sampling of the results from multimodel ensembles.

### G. State and forcing dependence of water vapor and lapse rate feedbacks

Much of the research to date has focused on vapor and lapse rate feedbacks in the current climate. However, the climate is continually changing, and in recent years it has been demonstrated that there is a marked state dependency of climate sensitivity (Knutti and Rugenstein, 2015; Rugenstein *et al.*, 2020). Consequently, the concept of fixed strength feedbacks needs to be revisited. Indeed, the general paradigm of considering changing “equilibrium” feedbacks can overlook important dynamic and timescale components of their response (Hallegatte, Lahellec, and Grandpeix, 2006).

Water vapor and lapse rate feedbacks have been found to evolve on timescales ranging from decades to centuries, as GCMs slowly equilibrate in response to an impulsive doubling or quadrupling of  $\text{CO}_2$  (Armour, Bitz, and Roe, 2013). This evolution in turn is the result not only of global mean temperature change but also of changing meridional surface temperature patterns, such as delayed warming in the Southern Ocean and southern high latitudes, which affect the balance between low and high latitude feedback contributions (Armour, Bitz, and Roe, 2013; Shell, 2013; Andrews, Gregory, and Webb, 2015; Dessler, 2020). On extremely long (millennial) timescales, GCM clear-sky LW feedback (a combination of Planck, lapse rate, and water vapor) becomes steadily less stabilizing. This is sourced mainly in the tropics and the Northern Hemisphere midlatitudes, which is consistent with strengthening water vapor feedback and an increasing tropopause height (Rugenstein *et al.*, 2019).

Paleo climates provide the opportunity to test water vapor and lapse rate feedback under different base conditions, and under different forcing. For example, during the LGM  $\text{CO}_2$  concentrations were around 2/3 of preindustrial levels (along with reduced amounts of other GHGs), and there was additional forcing from vegetation changes and extensive ice sheet coverage of northern continents (Masson-Delmotte *et al.*, 2013).

<sup>14</sup>See Appendix A for a description.

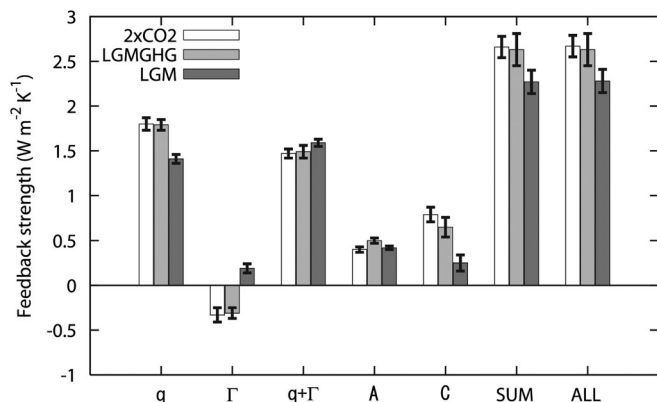


FIG. 15. Feedbacks derived from the Model for Interdisciplinary Research on Climate 3.2, medium-resolution version [MIROC3.2(medres)] GCM under  $2 \times \text{CO}_2$  forcing above current climate, as well as from Last Glacial Maximum (LGM) changes, compared with the current climate. LGM forcing includes ice sheets over northern continents and  $\text{CO}_2$  levels of 185 ppm ( $\sim 65\%$  of the current value) along with reduced values of  $\text{CH}_4$  and  $\text{N}_2\text{O}$ . LGMGHG denotes an experiment with current climate ice sheets, but with LGM-level greenhouse gases. Feedback notation is as in Eq. (4), with the addition of “A” for surface albedo. Error bars represent 1 standard deviation of different ten-year samples that are calculated using PRP; see Appendix A. This shows the weakened water vapor feedback in the colder climate, and a small positive lapse rate feedback due to low latitude ice sheets; however, the combined feedback is close to that of  $2 \times \text{CO}_2$ . From Yoshimori, Yokohata, and Abe-Ouchi, 2009.

State dependency is apparent across different paleo regimes (Berger *et al.*, 1993; Crucifix, 2006; Lariviere *et al.*, 2012), with positive feedbacks (other than those from surface albedo) overall becoming stronger as the climate warms. In a modeling study comparing modern-day and early Paleogene ( $\sim 6.5\text{--}3.5 \times 10^7$  yr ago) times, in which the global mean temperature changed by  $12^\circ\text{C}$ , this strengthening was attributed largely to cloud feedback, as increasingly strong water vapor feedback was close to offset by increasingly negative lapse rate feedback (Caballero and Huber, 2013).

A GCM experiment with current-day surface properties but LGM-level  $\text{CO}_2$ ,  $\text{CH}_4$ , and  $\text{N}_2\text{O}$  reveals little difference in the strength of water vapor and lapse rate feedbacks (Yoshimori, Yokohata, and Abe-Ouchi, 2009) (Fig. 15). Adding LGM ice sheets does not change SW water vapor feedback but has a profound effect in the LW, reducing it by around 25% and overall feedback by roughly 22%; see Fig. 15. This is largely because resultant extratropical temperature changes are much greater than tropical ones, and these are regions of relatively weak water vapor feedback (Yoshimori, Yokohata, and Abe-Ouchi, 2009). Lapse rate feedback in the LGM experiment is globally *positive* (see Fig. 15) because cold, ice covered surfaces extend to relatively low latitudes, causing positive lapse rate feedback in these regions to outweigh negative tropical contributions (Yoshimori, Yokohata, and Abe-Ouchi, 2009). As found in many other scenarios, offsetting changes in water vapor and lapse rate feedback result in a close-to-unchanged combined feedback (Fig. 15). This offsetting means that a RH-based formulation of the feedbacks would

suggest little change to the Planck or lapse rate terms across all experiments.

When the “base climate” itself is cold (as in the LGM), perturbations away from that climate can show a weaker combined water vapor + lapse rate feedback than under the present climate. This results from weaker (less positive) high latitude feedbacks at high latitudes (Yoshimori *et al.*, 2011).

There is ample evidence that water vapor feedback strengthens as the model base state warms from the current climate (Hu *et al.*, 2017). Model experiments undertaken with mixed layer oceans (which equilibrate more rapidly than full ocean-atmosphere GCMs) find an increase of roughly 30% in feedback strength under forcing increasing from  $2 \times$  to  $16 \times \text{CO}_2$  (Meraner, Mauritsen, and Voigt, 2013), at a rate across the range slightly higher than implied by fixed relative humidity (Colman and McAvaney, 2009). This increase has been shown to be due to a narrowing of the atmospheric window due to increased continuum absorption from water vapor (Seeley and Jeevanjee, 2021). At the same time negative lapse rate feedback strengthens too (Colman and McAvaney, 2009; Meraner, Mauritsen, and Voigt, 2013), at least partially offsetting water vapor feedback increases (Jonko *et al.*, 2013; Klufft *et al.*, 2019). The lapse rate changes stem from strengthening negative tropical feedback from a continually steepening saturated adiabatic lapse rate and increased emission from upper tropospheric  $\text{CO}_2$  (Seeley and Jeevanjee, 2021). The reduction and then disappearance of high latitude positive feedbacks with accelerated loss of snow and sea ice cover with warming also strengthen the lapse rate feedback (Colman and McAvaney, 2009). This offsetting has been attributed for models not projecting a runaway due to water vapor feedback even under extremely strong forcing, such as an increase in the solar constant of 25% (Boer, Hamilton, and Zhu, 2005) or of  $\text{CO}_2$  by a factor of 32 (Colman and McAvaney, 2009), as lapse rate feedback compensations result in a much more stable combined feedback (Colman and McAvaney, 2009).

The processes behind strengthening water vapor feedback with temperature are now better understood. Using a combination of GCMs and a 1D RCM, Meraner, Mauritsen, and Voigt (2013) found that the increase in tropopause height with temperature is critical, a finding similar to that of Rugenstein *et al.* (2019), although close-to-unchanged relative humidity remains an important process. Given the greater appreciation of the importance of processes around the tropopause, there may now be some caveats on earlier results (Boer, Hamilton, and Zhu, 2005; Colman and McAvaney, 2009) from model experiments with relatively coarse vertical resolution (Meraner, Mauritsen, and Voigt, 2013).

The increased understanding of the spectral dependence of OLR with increasing temperature (see Sec. IV.C) also casts light on critical processes as surface temperature increases. Increasing  $\text{CO}_2$  at high levels of warming can dominate spectral cooling windows, thereby coupling OLR to tropospheric temperatures helping to stabilize global temperatures (Seeley and Jeevanjee, 2021). Note also that parametrized radiation schemes can become insufficiently accurate to properly resolve these processes as surface temperatures exceed around 310 K (Klufft *et al.*, 2021).

Water vapor and lapse rate feedbacks also show sensitivity to forcing *type*. In part this can originate from differences in horizontal and vertical forcing distributions but can also be affected by differences in absorption spectra, for example, from less overlap of the  $O_3$  absorption spectrum with water vapor compared to that of  $CO_2$  (Yoshimori and Broccoli, 2008). Volcanic ejecta and sulphate forcing produce slightly weakened lapse rate and water vapor feedbacks, but again with the compensation producing close-to-unchanged combined feedback (Yoshimori and Broccoli, 2008). Other forcing agents including black carbon and tropospheric  $O_3$  strengthen negative lapse rate feedback relative to  $CO_2$  forcing, although again with substantial compensation from water vapor feedback changes (Rieger, Dietmüller, and Ponater, 2017). Water vapor feedback is stronger for globally equivalent solar forcing than it is for  $CO_2$ , as the forcing is more strongly weighted to lower latitudes where feedback is strong, although again with some compensation from increased lapse rate feedback (Yoshimori and Broccoli, 2008). Although these studies used the traditional feedback decomposition, the compensating effects of water vapor and lapse rate feedbacks suggest that the alternative RH-based formulation would show little change in the Planck and lapse rate terms from the different forcings.

Low latitude lapse rate changes can be sensitive to the details of forcing, with evidence that changes in recent decades have been affected by the pattern of the anthropogenic and volcanic aerosol forcing (Santer *et al.*, 2017). At high latitudes, different lapse rate responses may be induced by different radiative forcing, as, for example, found with  $CO_2$  increases paired with reduced insolation from solar radiation management GCM results from the Geoengineering Model Intercomparison Project (Robock, Kravitz, and Boucher, 2011). The  $CO_2$  forcing produces a bottom heavy warming that outweighs the lapse rate response to the more uniform solar forced change, or to advective changes (Henry and Merlis, 2020). High latitude feedbacks are particularly complex and are discussed at length in Sec. IV.I.

#### H. A surface perspective on feedbacks

The conventional view of feedbacks is considered at the TOA, as this is fundamental to long-term planetary energy balance (Manabe and Strickler, 1964; Manabe and Wetherald, 1967); see Sec. II. It is instructive, however, to also consider feedbacks at Earth's surface, as these provide different perspective and physical insights and clarify the impact of feedbacks on features such as rainfall change under climate warming. The different components are listed in Eqs. (9) and (10).

Zonally averaged surface and TOA feedbacks from one GCM are shown in Fig. 16 (Colman, 2015). In the LW, surface water vapor feedback is around 30%–50% stronger than at the TOA (Pendergrass and Hartmann, 2014; Colman, 2015), which essentially renders the surface in radiative “runaway greenhouse” conditions as it exceeds the net cooling from the combination of surface blackbody cooling plus atmospheric downward Planck warming. The strong surface radiative warming is offset mainly by increased evaporation, which is a key process driving global precipitation increases with

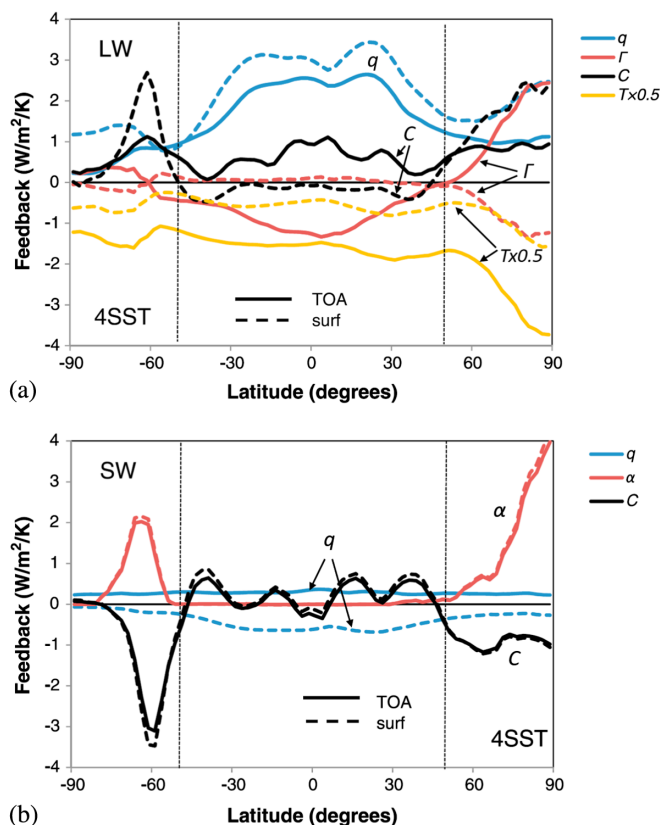


FIG. 16. Latitude mean, annual radiative feedbacks defined at the TOA (solid lines) and at the surface (dashed lines) calculated for a GCM forced by SSTs from a equilibrium warming  $4 \times CO_2$  forcing experiment (4SST) for the (a) LW and (b) SW. Notation for feedbacks is as in Eq. (4), except that  $T$  denotes the Planck feedback  $P$  and is scaled by a factor of 0.5 for display purposes. This shows that at the surface (compared with TOA) SW water vapor feedback is reversed in sign, lapse rate feedback is close to zero except at high latitudes, and LW water vapor feedback is consistently stronger. From Colman, 2015.

temperature (Andrews, Forster, and Gregory, 2009; Previdi, 2010; Pendergrass and Hartmann, 2014). From an atmospheric energy balance perspective, differences between TOA and surface feedbacks result in a change in net radiative heating requiring latent and sensible heat changes (coupled directly with surface evaporative adjustments) to restore heat balance (Previdi and Liepert, 2012).

In contrast to TOA water vapor feedback, which is dominated by changes in the mid to upper troposphere, the contributions to surface feedback are strongly peaked in the lowest parts of the atmosphere, with negligible contributions above 500 hPa (Previdi, 2010; Colman, 2015; Pendergrass, Conley, and Vitt, 2018; Dacie *et al.*, 2019; Kramer, Soden, and Pendergrass, 2019). This is a consequence of the high LW opacity of the lower atmosphere (Shine and Sinha, 1991). This also means that surface feedbacks are relatively insensitive to changes in factors such as convective parametrization, upwelling circulations, and ozone distribution (Dacie *et al.*, 2019). As for the TOA, surface water vapor feedback in models scales closely with unchanged relative humidity under warming (Pendergrass and Hartmann, 2014).

Observations support a strong positive surface water vapor feedback. A global study based on a National Centers for Environmental Prediction–National Center for Atmospheric Research reanalysis with an off-line radiation calculation found confirming evidence of positive water vapor feedback at the surface where temperatures exceeded approximately 2 °C (Lindberg, 2003). Radiation trend measurements from the European Alpine Surface Radiation Budget ground station network, combined with correlations between surface temperature and ECMWF reanalysis (ERA)-40 integrated water vapor, confirm GHG warming accompanied by strong water vapor feedback at the surface (Philipona *et al.*, 2004, 2005). Radiosonde trends in lower tropospheric water from 1964–1990, combined with temperature changes and surface radiative transfer calculations, also suggest strong positive water vapor feedback over this period (Prata, 2008).

Except at high latitudes, classically defined lapse rate feedback is weak at the surface (Colman, 2015; Kramer, Soden, and Pendergrass, 2019) (Fig. 16), as the opacity of the lower atmosphere prevents mid to upper tropospheric warming from having a direct surface radiative impact. There is some evidence of indirect surface impacts, though, as enhanced upper tropospheric warming can contribute to increases in moisture in the lower troposphere, which affects the surface radiation balance (Xiang *et al.*, 2014).

As a result of weakness in lapse rate feedback, the offsetting water vapor–lapse rate relationship found at the TOA is absent at the surface, so both feedbacks contribute to intermodel spread in the net surface radiative response to forcing (Kramer, Soden, and Pendergrass, 2019), and hence to impacts such as changes in precipitation. In the SW, water vapor feedback provides a surface cooling due to increased atmospheric absorption, of a magnitude slightly stronger than that of TOA warming (Colman, 2015) (Fig. 16). Note that it remains unclear what different insights a RH-based surface feedback analysis would provide, as this promising approach has yet to be explored.

## I. The role of lapse rate and water vapor feedbacks in regional climate variability and change

### 1. Polar amplification of warming

Greater than global average warming at high latitudes, so-called polar amplification, is a ubiquitous feature in GCMs (Holland and Bitz, 2003) and is also found in observations (Intergovernmental Panel on Climate Change, 2019) and paleo records (Masson-Delmotte *et al.*, 2006). For example, in years 100–150 after a CO<sub>2</sub> quadrupling in CMIP5 models, Arctic (60° to 90° north) warming averages 11.2 °C, compared to 4.3 °C for the tropics (Pithan and Mauritsen, 2014) (Fig. 17), with winter Arctic warming roughly double that of the summer. There is strong evidence that lapse rate feedback, in particular, plays a strong role in this amplification.

Polar amplification is of major consequence due to regional impacts from the accelerated warming (Intergovernmental Panel on Climate Change, 2019) and indeed has become emblematic of climate change (Boé, Hall, and Qu, 2009).

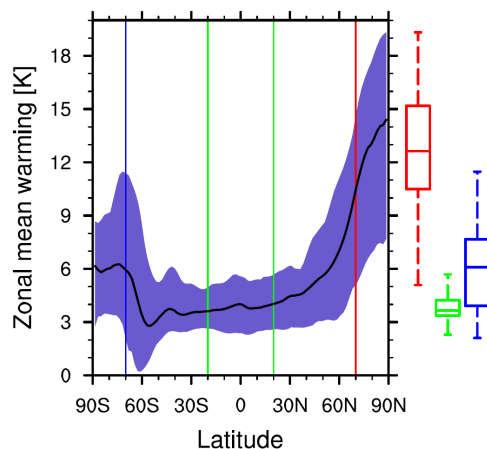


FIG. 17. Surface temperature change from 14 CMIP5 models as a function of latitude, in years 100–150 after an abrupt  $4 \times \text{CO}_2$  forcing, showing the “amplification” in surface warming that occurs in the high latitudes, particularly in the Arctic. The thick black line is the model average, and the shading shows the full model range. Box-whisker plots from left to right denote the warming averaged over the Arctic poleward of 70°N, the Antarctic poleward of 70°S, and the tropics 20°N–20°S. Box whiskers represent 25th to 75th percentile and minimum, median, and maximum values. From Block *et al.*, 2020.

Moreover, the high latitude feedbacks and warming also have substantial global effects. Differences in strength between models in the surface albedo and lapse rate feedbacks at high latitudes in turn affect meridional temperature gradients and associated heat fluxes, thereby contributing to differences in low latitude circulation such as Hadley cell overturning (Feldl, Bordoni, and Merlis, 2017). Furthermore, large volumes of consequential land ice melting could lead to a large sea level rise (Intergovernmental Panel on Climate Change, 2019).

The reasons for polar amplification are complex, involving a balance between changes in surface albedo, lapse rate, water vapor, and cloud feedbacks, as well as in atmospheric and oceanic poleward fluxes, and these can vary widely between models (Ramanathan, 1977; Curry *et al.*, 1995; Crook, Forster, and Stuber, 2011; Ghatak and Miller, 2013; Graverson, Langen, and Mauritsen, 2014a; Pithan and Mauritsen, 2014; Payne, Jansen, and Cronin, 2015; Mokhov, Akperov, and Dembitskaya, 2016; Feldl, Anderson, and Bordoni, 2017; Feldl, Bordoni, and Merlis, 2017; Stuecker *et al.*, 2018; Block *et al.*, 2020). Considering feedbacks from both a regional and a hemispheric perspective provides valuable insights into processes important for poleward amplification and its variation across GCMs (Feldl and Roe, 2013).

From a hemispheric and TOA perspective, a key driver is changes in radiative imbalances induced by latitudinal variation in feedbacks, which in turn affect poleward atmospheric and oceanic heat fluxes (Zelinka and Hartmann, 2012). From this perspective lapse rate feedback has been shown to be the greatest contributor to annual mean polar amplification in CMIP5 models, as it cools the tropics but warms high latitudes (Pithan and Mauritsen, 2014; Stuecker *et al.*, 2018) [Figs. 9(b) and 18(a)].

The Planck feedback has also been hypothesized to contribute to amplification because of the strong dependence of OLR increase per degree of warming in the warm tropics relative to the cold high latitudes (Pithan and Mauritsen, 2014). However, this has been challenged by other studies that point to the importance of atmospheric emission temperatures relative to those at the surface, suggesting that the Planck feedback gradient may even reduce polar amplification (Feldl and Roe, 2013; Henry and Merlis, 2019). Considering feedbacks in the fixed relative humidity framework (Held and Shell, 2012) [Eqs. (6)–(8)] retains the alternative lapse rate feedback as the most important contributor to polar amplification, but the redefined Planck feedback contribution is then small (Pithan and Mauritsen, 2014).

From the hemispheric TOA viewpoint, water vapor feedback, although warming the Arctic in absolute terms, opposes polar amplification since it is much stronger at low latitudes than at high latitudes (Langen, Graversen, and Mauritsen, 2012; Zelinka and Hartmann, 2012; Taylor *et al.*, 2013).

At high latitudes the presence of cold dense air near the surface (particularly during the cool seasons) can induce weak coupling between the surface and the free atmosphere. Lapse rate feedback is therefore a key contributor to polar amplification (particularly during the winter) because the highly stable lapse rate acts to trap warming in the lowest atmospheric levels, thereby increasing surface warming relative to the layers above (Manabe and Wetherald, 1975). This vertical decoupling means that it is important to also consider both a surface and a regional feedback view in understanding feedback contribution to polar amplification (Taylor *et al.*, 2013; Pithan and Mauritsen, 2014; Laîné, Yoshimori, and Abe-Ouchi, 2016). From this perspective, the largest Arctic

warming results from greater downward than upward LW at the surface, again due to the nonlinear dependence on temperature of blackbody emissions (Pithan and Mauritsen, 2014; Sejas and Cai, 2016), and again from this perspective water vapor feedback reduces polar amplification.

Model experiments find that at a regional level high latitude lapse rate and surface albedo feedbacks interact to amplify each other: strengthened surface albedo feedback results in a warmer surface and stronger positive lapse rate feedback, which can strengthen surface warming and lead to further melting snow and sea ice (Döscher, Vihma, and Maksimovich, 2014; Graversen, Langen, and Mauritsen, 2014a). Although the surface albedo feedback is important, Arctic amplification can occur without it (Hall, 2004; Graversen and Wang, 2009; Kim *et al.*, 2018; Russotto and Biasutti, 2020), and LW feedbacks are known to play a dominant role in the region in coupled models (Winton, 2006). Suppression of the lapse rate feedback by locking lapse rates in a GCM reduced Arctic amplification of warming by 15%, and Antarctic amplification by 20%, although interaction with surface albedo feedback meant that it could not be properly considered a separate feedback process (Graversen, Langen, and Mauritsen, 2014b).

The role of heat transport by atmosphere and ocean, and its interaction with feedbacks, has also been intensively investigated. Although poleward heat transports are important to maintaining energy balance and contribute to warming, model spread in polar amplification is primarily due to differences in feedbacks (Hwang, Frierson, and Kay, 2011; Stuecker *et al.*, 2018). Atmospheric heat flux changes in fact act to reduce model spread by opposing radiatively induced differences, and ocean heat transport changes are not correlated with warming across models (Pithan and Mauritsen, 2014).

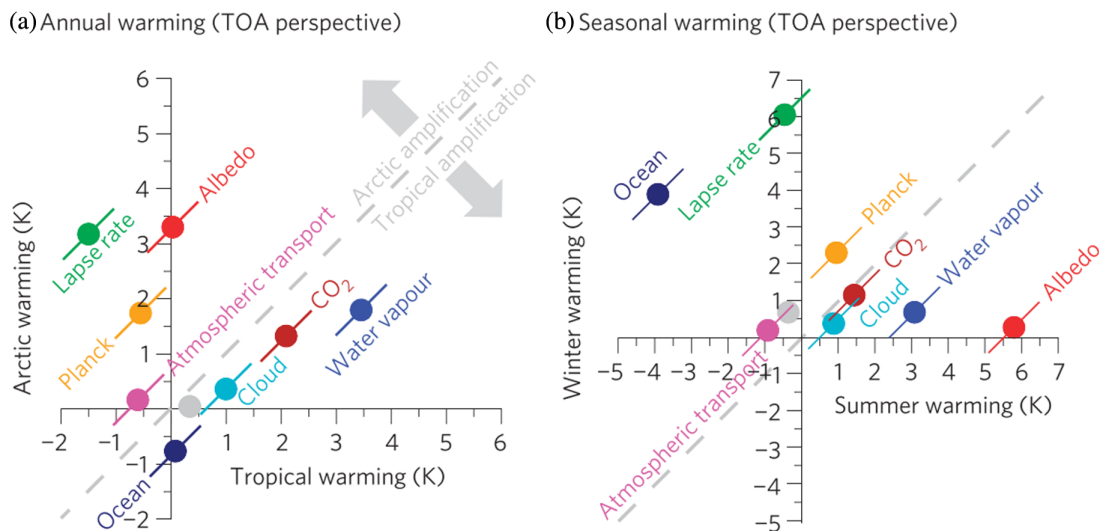


FIG. 18. (a) Contribution to Arctic warming vs tropical warming in 16 CMIP5 models from diagnosed TOA feedbacks (lapse rate, water vapor, Planck, surface albedo, and cloud) from changes in atmospheric transport and ocean uptake or transport, and from the latitudinal dependence of CO<sub>2</sub> forcing. Values to the top left of the gray dashed line increase polar amplification, and those to the bottom right decrease it. The importance of lapse rate feedback is apparent from its warming of the Arctic vs tropical cooling, whereas water vapor feedback warms the tropics more. (b) Seasonal variation shown by winter vs summer warming from each of the processes in (a). The contrasting seasonal roles of lapse rate (winter) and water vapor (summer) are apparent. The gray dot represents the residual from total warming minus the addition of the individual components. From Pithan and Mauritsen, 2014.

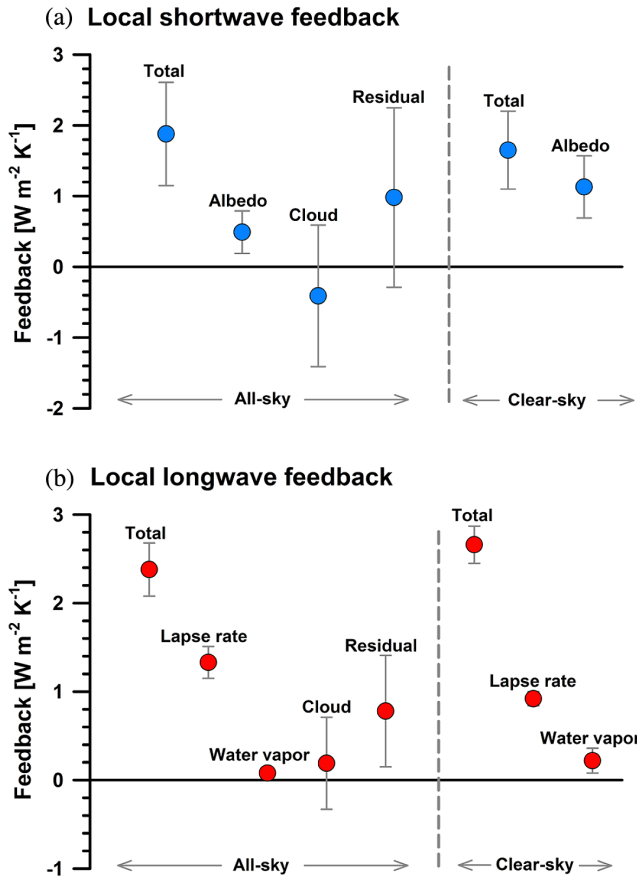


FIG. 19. Radiative feedbacks diagnosed using 2000–2014 Clouds and the Earth’s Radiant Energy System (CERES) (Wielicki *et al.*, 1996) TOA SW and LW fluxes combined with surface temperature and vertical profiles of temperature and humidity taken from ERA-Interim reanalyses (Dee *et al.*, 2011). Values shown are calculated using linear regression of TOA fluxes with regional surface temperature and kernels applied to temperature and moisture profiles to diagnose individual feedbacks. Error bars show the standard error from regressions combined with estimated CERES uncertainties. Clear sky represents results with all cloud effects removed. The importance of lapse rate feedback is apparent in regional warming, whereas water vapor contributions are diagnosed as small. From Hwang *et al.*, 2018.

Observations of feedbacks poleward of  $60^{\circ}\text{N}$  for the period 2000 to 2014 indeed find a dominant role for lapse rate feedback in the positive LW feedback, with little contribution from water vapor (Hwang *et al.*, 2018); see Fig. 19. Hwang *et al.* (2018) explained the weakness of the water vapor feedback as due to moistening being confined to the lower parts of the atmosphere, whereas lapse rate feedback is strong due to temperature differentials between the surface and atmospheric upper levels. Observations also suggest that on short timescales (monthly to inter-annual) lapse rate and surface albedo feedbacks are of comparable magnitude, but that lapse rate feedback makes the greatest contribution to high latitude amplification and water vapor feedback opposes it (Zhang *et al.*, 2018). The strength of lapse rate feedback along with other feedbacks can be expected to further change under the

ongoing loss of Arctic sea ice (Dekker, Bintanja, and Severijns, 2019).

Model studies find that the magnitude of the polar amplification and the role of different feedbacks change throughout the year (Block *et al.*, 2020). Polar lapse rate feedback is positive and reinforces amplification in the winter and spring, when the atmosphere is dominated by inversions, but is negative and weakens amplification in the summer and autumn, when surface inversions are weaker or absent (Colman, 2003b; Pithan and Mauritsen, 2014; Kim *et al.*, 2018) [Fig. 18(b)]. Differences in climatological polar cloud fractions, for example from cloud parametrization changes, can also strongly affect the seasonality of both lapse rate and water vapor feedbacks (Kim *et al.*, 2016).

The strength of the high latitude lapse rate feedback depends not only on season, however, but also on the magnitude of the high latitude warming (Feldl, Anderson, and Bordoni, 2017). If warming is strong, a more positive lapse rate feedback further enhances surface temperature increase and polar amplification. If surface warming is only moderate, then flux convergence from atmospheric eddies contributes to regional stabilization and neutral (or even negative) high latitude lapse rate feedback.

The polar lapse rate feedback contribution to warming also depends on the nature and profile of the forcing, as it is not uniquely dependent of the surface temperature: it also depends on other regional processes (Cronin and Jansen, 2016; Henry and Merlis, 2020). Lapse rate response differs between surface forcing, such as that from  $\text{CO}_2$  changes, a reduction in surface albedo, or an increase in oceanic heat transport relative to forcing such as that from increased poleward advection or increased atmospheric SW absorption (Cronin and Jansen, 2016). This implies that advective heat fluxes from lower latitudes can also play an important part in regional heat balance adjustment. If additional atmospheric heat flux convergence from lower latitudes “wins out” over SW surface warming from reduced albedo, this can result in surface stabilization and a negative lapse rate feedback (Cronin and Jansen, 2016). Consistent with this, investigation of the impact of  $\text{CO}_2$  forcing, offset by “geoengineered” SW flux reductions found positive lapse rate feedback associated with the bottom heavy warming from the  $\text{CO}_2$  response won out over the atmospheric SW-induced changes, meaning that polar amplification persisted despite the global radiative balance (Henry and Merlis, 2020)

Despite the major role of lapse rate feedback in causing polar amplification in the models, when looking across models the *spread* in net radiative feedback in the Arctic arises more from differences in Planck and albedo feedbacks than from the lapse rate (Block *et al.*, 2020). Other feedbacks may also play a role. The cloud feedback impact on polar amplification appears to be modest (Pithan and Mauritsen, 2014) (Fig. 18), but clouds interact to strengthen or weaken lapse rate feedback from changes in downward LW radiation (Tan and Storelvmo, 2019). The role of the stratosphere in polar amplification has received relatively little study. A recent GCM experiment found that stratospheric water vapor feedback was 3 times stronger at high latitudes than at low latitudes, contributing around 14% to Arctic amplification (Li and Newman, 2020).

Models consistently project a greater amplification in the Arctic than the Antarctic under transient climate change (Manabe *et al.*, 1991) (Fig. 17), in part due to deep mixing in the Southern Ocean that slows the warming (Intergovernmental Panel on Climate Change, 2019). Experiments both with and without Antarctic ice sheet elevation indicate equilibrium amplification comparable to that in the Arctic with no Antarctic topography (Salzmann, 2017; Hahn *et al.*, 2020), with the implication that smaller equilibrium amplification in the Antarctic results from a weaker, shallower temperature inversion related to topographic damping of meridional heat fluxes and cooling from katabatic winds (Hahn *et al.*, 2020). Consequently, lapse rate feedback plays a smaller role in seasonal variation in Antarctic temperature amplification (Hahn *et al.*, 2020).

In summary, observations and a large number of modeling studies confirm that lapse rate feedback is a critical factor in polar amplification both for its global-scale TOA structure (negative feedback at low latitudes, positive feedback at high latitudes) and for its regional-scale surface impacts and interactions. Water vapor feedback, although important for broadscale warming, generally opposes the amplification, largely due to its greater strength at low latitudes than at high latitudes. A large number of methodological approaches and differences in models and datasets produce somewhat different quantifications of these processes, however, and preclude a simple unifying conceptual framework and unambiguous quantification of feedback impact. Further refining this understanding and framework remains an ongoing challenge (Russotto and Biasutti, 2020).

## 2. Climate features and regional variability

Apart from global-scale or broadscale radiation changes, such as those over high latitudes, there is ample evidence that water vapor and/or lapse rate feedback can play important roles in the characteristics of modes of variability (i.e., of preferred patterns of large-scale spatiotemporal variability).

One example is the El Niño–Southern Oscillation (ENSO), where the presence of a water vapor–LW interaction affects the vertical structure of radiative heating associated with surface temperature anomalies in the tropics and acts to amplify ENSO variability (Hall and Manabe, 2000a).

The seasonal movement of the Intertropical Convergence Zone (ITCZ)<sup>15</sup> provides a second example in which water vapor feedback plays a role. Water vapor feedback processes have been found to roughly double the seasonal movement of the ITCZ (Clark *et al.*, 2018), which was traced to changes in the interhemispheric asymmetry of subtropical relative humidity (Peterson and Boos, 2020). Water vapor and lapse rate feedbacks also play a role in maintaining the Hadley circulation response to asymmetric forcing, such as hemispheric warming (Yoshimori and Broccoli, 2009). Aqua planet experiments using radiation suppression found that, under CO<sub>2</sub> forcing, water vapor feedback widens the

monsoon region and increases monsoon-associated moisture and rainfall by warming and moistening the region (Byrne and Zanna, 2020). There is also evidence that regional water vapor feedback plays an important role in the persistence of anomalously high winter SSTs into subsequent seasons in the tropical North Atlantic region, which is mainly responsible for the genesis of hurricanes (Wang, Liu, and Foltz, 2017), on top of well-known cloud-SST and wind-evaporation-SST feedbacks.

Moisture-radiative feedbacks also play an important role in the dynamics of some tropical intraseasonal processes (Bony and Emanuel, 2005). Regional water vapor and lapse rate feedbacks are important in the propagation and magnitude of the Madden-Julian oscillation (MJO), a near equatorial ~30–60 day wave featuring coupling between convective and circulation processes (Hendon and Salby, 1994; Madden and Julian, 1994). This includes enabling the MJO to penetrate further into the Maritime Continent (Indonesian region) barrier due to stronger heating resulting from water vapor feedback coincident with the convective envelope (Zhang, Kramer, and Soden, 2019).

There is some evidence that regional water vapor feedback may also amplify regional surface responses to warming. Elevation-dependent water vapor feedback has been proposed as being partly responsible (along with surface albedo feedback and other processes) for observed amplification of climate change warming with altitude in mountainous regions (Pepin *et al.*, 2015). The hypothesized physical process is that due to decreasing water vapor with altitude, absorption bands are undersaturated (because of less overlying total water vapor), resulting in larger additional downwelling LW radiation under surface warming (Rangwala, Miller, and Xu, 2009; Rangwala *et al.*, 2010; Rangwala, 2013; Rangwala, Sinsky, and Miller, 2013; Palazzi, Filippi, and von Hardenberg, 2017). The feedback loop is evidenced by statistical relationships between water vapor, downwelling LW radiation and surface warming (Rangwala, Miller, and Xu, 2009). These findings must be treated with some caution, however, as a recent high-resolution study of warming in the Rocky Mountains using a regional climate model (RCM) found no evidence of amplification by elevation-dependent water vapor feedback (Minder, Letcher, and Liu, 2018).

Similarly, local surface water vapor feedback has been hypothesized to play a role in regional temperature variability, such as in response to ENSO (Zhang *et al.*, 2011) and temperature extremes such as heat waves (Oueslati *et al.*, 2017). There is also some evidence that, despite low humidity, surface water vapor feedback enhances the dryness of desert regions from strong coupling between the surface and the lower atmosphere, and the particular sensitivity of downward LW radiation to water vapor increases in dry environments (Zhou, 2016; Zhou *et al.*, 2016; Wei *et al.*, 2017).

It is not clear to what extent the latter processes are fully established, or indeed truly closed loop feedbacks, rather than water vapor responses to or drivers of large-scale forcing and variability, and they are not discussed further here. Further research is needed to fully establish their veracity and importance.

<sup>15</sup>The region of enhanced convection, lying close to the equator, representing the upward branch of the Hadley circulation.

## V. OBSERVATIONAL EVIDENCE FOR WATER VAPOR AND LAPSE RATE FEEDBACK

### A. Moisture trends and variability in the lower atmosphere

As global temperature has risen by around 0.5°C since 1990 (Masson-Delmotte *et al.*, 2018), we might expect to see changes in the global water vapor amount and distribution under that warming.

Water vapor changes in the lower atmosphere are strongly coupled to the surface (Trenberth, Fasullo, and Smith, 2005), and expected strong increases with temperature have been confirmed by observations. Globally, satellite, and radiosonde analyses confirm (lower tropospheric dominated) total precipitable water<sup>16</sup> variations consistent with close-to-unchanged relative humidity under interannual variability (Wentz and Schabel, 2000; Dai *et al.*, 2011; Trenberth *et al.*, 2015).

Over oceans, energy balance arguments suggest that only small changes of lower atmosphere relative humidity would be expected with increased temperature (Jeevanjee, 2018). This is because significant shifts in relative humidity would imply large changes in evaporation (in the absence of large changes in wind or stability), which cannot be sustained energetically, as the subsequent latent heat release in the troposphere cannot be matched by radiative cooling (Allen and Ingram, 2002; Held and Soden, 2006). Consistent with this, models project only a small trend in lower tropospheric relative humidity with secular warming, that of modest increases (Byrne and O’Gorman, 2013). Observations provide strong evidence for increases in total precipitable water over ocean regions from satellite-based Special Sensor Microwave Imager data (Santer *et al.*, 2007; Wentz *et al.*, 2007). Trends in relative humidity over oceans are less clear (Willett *et al.*, 2008) but appear to be broadly consistent, with unchanged relative humidity that is in line with underlying SSTs (Byrne and O’Gorman, 2013; Hartmann *et al.*, 2013). Two-hourly Global Positioning System (GPS) (see Sec. V.B) measurements show an increase in precipitable water from 1995 to 2011 that is also roughly in line with unchanging relative humidity, along with change that is larger at night than during the daytime (Wang, Dai, and Mears, 2016).

Over most land areas, models predict decreasing relative humidity in the lowest parts of the atmosphere, particularly during the warm season (O’Gorman and Muller, 2010; Byrne and O’Gorman, 2016). Observations broadly confirm this trend, except for some regions in the tropics and high northern latitudes (Willett *et al.*, 2014).

### B. Upper tropospheric moisture

Although these robust responses in the lower troposphere provide important confirmation of increasing specific humidity with a warming climate, it is mid to upper tropospheric humidity that is most important for water vapor feedback (Sec. IV.D), and water vapor trends in this region are less straightforward to measure. In recent decades several different observational approaches have been taken to monitor variability and change in this challenging region. Confidence in

the results depends upon the robustness of the measurement methodology, so they are reviewed here.

### 1. Methods of measuring upper tropospheric humidity

There are three principal observational sources for monitoring trends and variability of upper tropospheric humidity: the radiosonde network, satellite measurements, and atmospheric reanalyses.

*The radiosonde network* of balloon-borne soundings was established long ago to provide vertical profiles of temperature and moisture for input into operational numerical weather prediction systems. In principle, radiosondes can measure changes in humidity at a much finer vertical resolution than satellites. However, attempts to use the radiosonde network for long-term climate monitoring and detection purposes have encountered several major challenges.

The first has been moisture biases, including the temporal and spatial variation of biases from instrumental and measurement technique differences between countries and changes over time (Parker and Cox, 1995; Seidel *et al.*, 2009). Accuracy problems are widespread. For example, even in recent decades dry biases of up to 20% have been evident in the middle troposphere from commonly used radiosondes (Miloshevich *et al.*, 2009), and biases can also result from the emergence of radiosondes from saturated regions into much drier overlying layers (Held and Soden, 2000). A further issue is the inherently data sparse nature of the radiosonde network, which leaves large tropical and oceanic regions, for example, severely undersampled (Müller *et al.*, 2016). Sampling is particularly limited in the stratosphere (Hurst *et al.*, 2011; Hegglin *et al.*, 2014).

To address these issues there have been several separate efforts to homogenize global operational radiosonde observations (Durre *et al.*, 2009; McCarthy, Thorne, and Titchner, 2009; Dai *et al.*, 2011). Indeed, the limitations inherent with the radiosonde network, together with the recognized importance of monitoring upper tropospheric and lower stratospheric water vapor have led to calls for the development of global, carefully calibrated, and long-term balloon-borne upper troposphere water measurement program (Müller *et al.*, 2016).

*Satellite measurements* have been increasingly used in recent decades to estimate variability and trends in relative humidity. Upper troposphere humidity can be inferred from instruments such as the 6.7  $\mu\text{m}$  radiance channel from HIRS, which is sensitive to moisture in a deep upper troposphere layer from roughly 200 to 500 hPa (Soden *et al.*, 2000). HIRS measurements have been made for over 40 years, since the launch of TIROS-N in 1978 (Shi and Bates, 2011). A break in the TIROS-N record occurred in 2005, when the central wavelength of the HIRS instrument was changed from 6.7 to 6.5  $\mu\text{m}$ , thus limiting the record to 27 years (1979–2005) (Chung *et al.*, 2014), although comparable measurements have been available from the microwave sounder SAPHIR from 2011 (Brogniez, Clain, and Roca, 2015). Since the purpose of the HIRS mission was weather prediction, not climate monitoring, producing long, multisatellite trends is challenging because of intersatellite biases (John *et al.*, 2011), and careful bias correction has been needed to produce a continuous, consistent dataset suited to climate applications

<sup>16</sup>Vertically integrated water vapor content.

(Bates and Jackson, 2001; Jackson and Soden, 2007; Shi and Bates, 2011). The difference between microwave sounding unit/advanced microwave sounding unit (MSU/AMSU) channel 2 brightness temperatures and HIRS channel 12 is also useful for removing defective temperature changes on the upper troposphere to produce a cleaner measure of upper troposphere relative humidity (Chung *et al.*, 2014).

Other important satellite datasets derive from the Microwave Limb Sounder (MLS), and the newer Cross-track Infrared Sounder. These instruments provide high-quality temperature and water vapor profiles from as early as 2002, and these measurements have been used extensively to study water vapor variability and trends (Dessler and Minschwaner, 2007; Liu *et al.*, 2018).

Global Positioning System networks can also be exploited to produce water vapor datasets, essentially measuring the integrated temperature and humidity along the GPS path length (Jin, Chang, and Wang, 2007; Wang *et al.*, 2007; Wang and Zhang, 2008; Vergados *et al.*, 2016; Wang, Dai, and Mears, 2016). This is a relatively new and short dataset, with around 100 ground stations established in 1997. The GPS technique has inherent advantages, including no requirement of calibration and being essentially unaffected by clouds (Sherwood *et al.*, 2010b). Trends derived from GPS data indicate moistening Ho *et al.* (2018)); however, these can be sensitive to beginning and end values (i.e., variability) given the shortness of the GPS time series (Hartmann *et al.*, 2013).

Atmospheric reanalyses provide a source of what might be considered pseudo-observations. These are produced by running recent-version numerical weather prediction models on observations from past years and decades retrieved from extensive archived data sources. By exploiting advanced data assimilation techniques, they produce a climate as closely as possible constrained by those observations (Slingo, Pamment, and Webb, 1998). As such, they represent a “fixed model” representation of past climate but remain subject to inherent model deficiencies, particularly in data sparse areas, and are subject to a greatly varying input dataset in terms of observational instrumentation, coverage, and accuracy (Thorne and Vose, 2010; Fujiwara *et al.*, 2017). Because of these changes in the observational network, or because of limitations on data ingestion or data quality, trends must be treated with some caution (Dessler, Zhang, and Yang, 2008; Dessler and Davis, 2010). Nevertheless, they produce a convenient and comprehensive, observationally constrained, and physically consistent estimate of past climate gleaned from a vast store of observational datasets.

## 2. Trends in upper tropospheric humidity

A range of studies have concluded that long-term trends are consistent with near unchanged relative humidity in the upper troposphere (Allan, Ringer, and Slingo, 2003; Cess, 2005; Soden *et al.*, 2005; Ferraro *et al.*, 2015). After careful homogenization and bias correction of the HIRS brightness temperatures from both the TIROS-N and Metop-A satellites, Shi and Bates (2011) found little change in equatorial tropical upper tropospheric relative humidity over the 30-year period spanning from 1979 to 2008. On top of such broadscale specific humidity trends lie superimposed regional

and latitudinal changes due to changes in circulation (Bates and Jackson, 2001). Allowing for these is important in understanding long-term broadscale water vapor feedback, and extreme caution must be exercised when one considers limited-region data and extrapolating to global means (Dai *et al.*, 2011).

An examination of four more recent reanalysis products [ERA-40, Japanese Reanalysis (JRA), Modern-Era Retrospective Analysis for Research and Applications (MERRA) (Rienecker *et al.*, 2011), and the European Centre for Medium-Range Weather Forecasts (ECMWF)-interim reanalyses (Dee *et al.*, 2011)] found unanimous agreement on increasing specific humidity between 1984 and 2009 as well as with ENSO-induced warm interannual fluctuations (Dessler and Davis, 2010; Dessler, Zhang, and Yang, 2008).

But is the moistening due to human activities? An attribution study by Chung *et al.* (2014) considered satellite-derived tropical upper tropospheric humidity trends over 27 years (to 2005) with CMIP5 model simulations (Fig. 20). They concluded that observed changes were consistent only with the models in which the forcing applied included anthropogenic GHGs; i.e., changes were absent when models saw natural

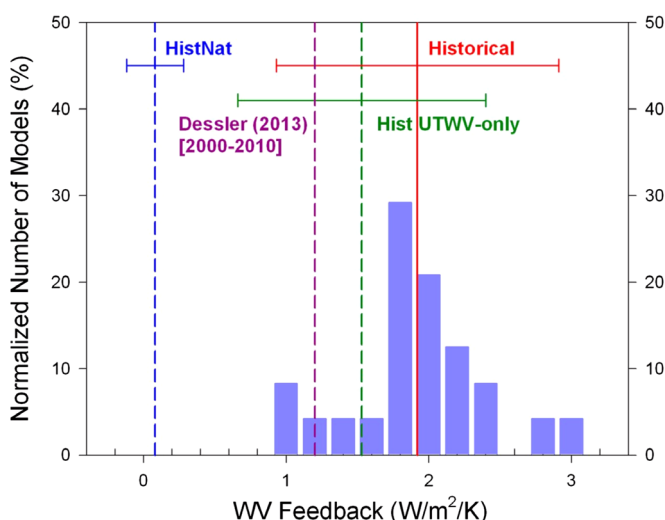


FIG. 20. Graphic attributing observed water vapor feedback to anthropogenic greenhouse gas emissions. Bars show water vapor feedback between the periods 1979–1988 and 1989–1998 from CMIP5 experiments forced by natural forcing agents due to solar and volcanic changes only (HistNat) and anthropogenic greenhouse gases and aerosols as well as natural forcings (Historical). A third calculation (Hist UTWV only) is derived from the historical runs but uses only humidity changes occurring above 600 hPa. One estimate of water vapor feedback from reanalyses (Dessler, 2013) is marked in purple. Differences between Historical and HistNat show that models do not match observational estimates of water vapor feedback unless anthropogenic greenhouse gas forcing is included: i.e., this feedback can be attributed to anthropogenic emissions. Differences between Historical and Hist UTWV only values demonstrate the dominance of the upper troposphere, in that around 80% of the feedback strength can be attributed to upper humidity changes in this region. See Tables I and III for other estimates of water vapor feedback from unforced variability and climate change. From Chung *et al.*, 2014.

forcing by volcanic sulphates and solar changes alone. Historical feedbacks are also consistent with feedbacks calculated while assuming fixed upper tropospheric relative humidity (Fig. 20) (Chung *et al.*, 2014). This result is important because it provides strong evidence not only that water vapor feedback is occurring and is strongly related to upper tropospheric humidity trends but also that it is operating in response to human-induced warming.

### C. Use of variability analogues for evaluating water vapor feedback

In addition to measurements of humidity trends, many observational studies have been made for the relative humidity response under natural (i.e., unforced) variability, including that from the seasonal cycle and interannual and decadal variability. This has the advantage of providing observable tests for water vapor response to temperature change and avoids possible pitfalls in deriving reliable, long-term homogeneous data series and detecting modest trends. Caution is needed, however, as discussed later, in interpreting the resultant feedback as analogs for water vapor feedback seen under long-term climate change, largely because of differences in SST patterns associated with global temperature changes.

On the seasonal cycle, large hemispheric-scale changes in temperature occur, with observed winter-summer water vapor changes consistent with close-to-unchanged relative humidity, including in the upper troposphere (Rind *et al.*, 1991). Satellite-derived OLR changes show radiative damping (below Planck cooling) from strong positive water vapor feedback (Tsushima, Abe-Ouchi, and Manabe, 2005). Seasonal cycle water vapor feedback from ERA-40 and MERRA reanalyses are of comparable strength to that of CMIP5 GCMs, both globally and on hemispheric scales (Colman and Hanson, 2013) [Fig. 21(d)]. These results are all consistent with a feedback from unchanged relative humidity. A caveat, however, is that the large hemispheric temperature swings do not bear a close resemblance to patterns of change under global warming, and the large, compensating positive and negative radiative responses in the warmer and cooler hemispheres result in a relatively weak global net feedback (Colman and Hanson, 2013) [Fig. 21(b)].

Caution must also be exercised on interannual timescales, as the pattern of warming associated with global temperature change differs between climate change warming and unforced variability. Regional relative humidity fluctuations and associated TOA radiative changes in the tropics follow large-scale interannual circulation changes, such as those associated with ENSO (Bates *et al.*, 2001; Blankenship and Wilheit, 2001; Brown *et al.*, 2016; Tian *et al.*, 2019) or planetary scale midlatitude atmospheric waves (Bates and Jackson, 2001). Consequently, ENSO-driven interannual surface temperature fluctuations peak much more strongly close to the equator than temperature increases under global warming (Hurley and Galewsky, 2010; Colman and Hanson, 2013; Dessler, 2013). These result in a strong low latitude peak in the LW water vapor radiative response (Dessler and Wong, 2009), as shown in Fig. 22.

Since much of the variability in upper tropospheric humidity is driven by ENSO-related migration of convective

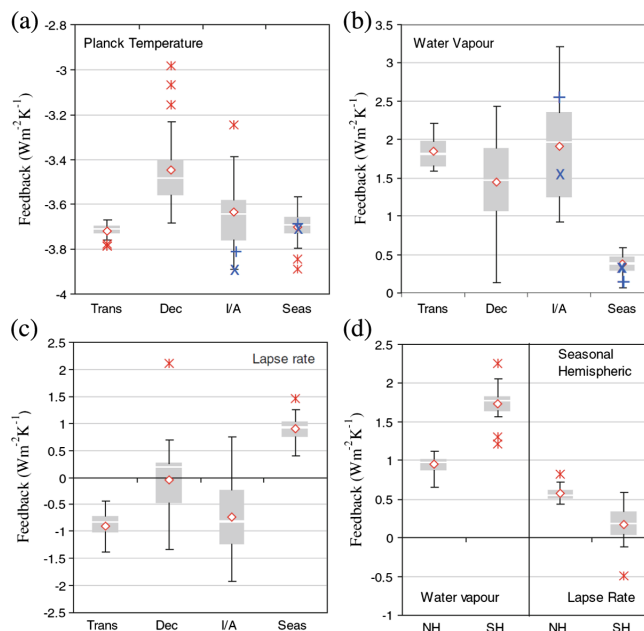


FIG. 21. (a)–(c) Planck, water vapor, and lapse rate feedbacks from CMIP5 models for transient (i.e., secular) response to increased  $\text{CO}_2$  (Trans) and from unforced decadal (Dec), interannual (I/A), and seasonal (Seas) variability. In (d) the seasonal feedback is broken up into separate Northern and Southern hemispheres. Box-whisker plots show median 25th–75th percentiles, ranges within 1.5 interquartiles, and outliers (stars). X's (plus signs) show results calculated from ERA-40 (MERRA) reanalyses. From Colman and Hanson, 2013.

features such as the ITCZ (Xavier *et al.*, 2010) and modified regionally by deep convection (Su *et al.*, 2006), it is important to consider changes over large areas that include both rising and descending regions. When calculated over such large spatial scales, the data are consistent with close-to-constant relative humidity (Dessler, Zhang, and Yang, 2008; Gettelman and Fu, 2008; Chung, Yeomans, and Soden, 2010). Averaging over the entire tropics,  $6.7 \mu\text{m}$  HIRS brightness temperature responses are also consistent with close-to-unchanged relative humidity (Allan, Ringer, and Slingo, 2003; McCarthy and Toumi, 2004), although another study using the HALOE MLS found modest decreases in tropics-averaged relative humidity associated with temperature increases in convective regions (Minschwaner and Dessler, 2004). A recent comparison of tropical-mean 200 hPa specific humidity variations with temperature as measured from three datasets, GPS refractive indices, AIRS satellite retrievals, and the MERRA reanalysis, also found values consistent with small reductions in relative humidity (Vergados *et al.*, 2016) (Fig. 23). Together these studies make an overwhelming case for broadscale upper tropospheric humidity responding to global surface temperature perturbations close to, or slightly below, fixed relative humidity values.

Because of the more peaked tropical warming, radiative response under interannual variability may be expected to exaggerate the strength of the resultant feedback relative to climate change feedback (Dessler, 2013; Colman and Hanson, 2017; Po-Chedley *et al.*, 2018)—contrast Figs. 16(a) and 22(a). In fact, results show roughly

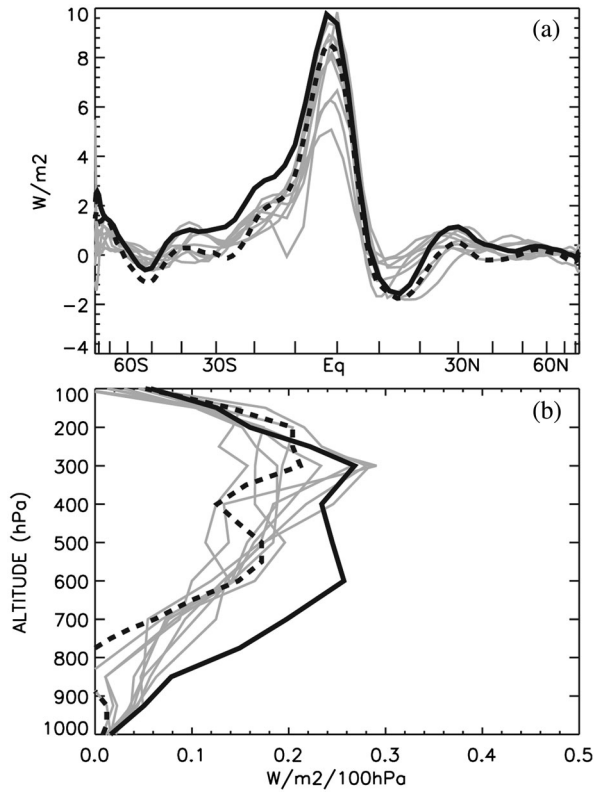


FIG. 22. (a) Longitudinally averaged TOA flux responses (positive is increased downward flux) from water vapor changes over an ENSO cycle as depicted by 12 CMIP3 models (gray lines) and derived from two reanalyses: MERRA (dashed black line) and ERA-40 (solid black line). (b) Flux changes (in  $\text{W m}^{-2} 100 \text{ hPa}^{-1}$ ) from water vapor perturbations as a function of altitude. From Dessler and Wong, 2009.

comparable strength in global water vapor feedback from interannual and secular climate change, albeit with some showing somewhat stronger interannual feedback (Colman

and Hanson, 2013) (Fig. 21) and others showing slightly weaker interannual feedback (Koumoutsaris, 2013; Liu *et al.*, 2018). Much more limited literature suggests slightly weaker decadal water vapor feedback than for interannual feedback (Colman and Hanson, 2013); see Fig. 21.

Another possible difference is that the contribution to the interannual TOA radiative response may peak less strongly in the upper troposphere than for climate change (Hall and Manabe, 1999; Dessler and Wong, 2009; Colman and Power, 2010); see Fig. 22. However, some studies find strong upper tropospheric peaking for interannual feedback (Colman and Hanson, 2013) and reanalysis-derived feedbacks can diverge strongly (Dessler and Wong, 2009) (Fig. 22), so this possible structural difference remains unclear.

Despite the differences in geographical and perhaps vertical structure, an important finding has been that a modest correlation exists between individual CMIP5 model interannual and climate change LW water vapor feedbacks (Dalton and Shell, 2013; Gordon *et al.*, 2013; Takahashi, Su, and Jiang, 2016; Colman and Hanson, 2017; Liu *et al.*, 2018). This provides strong motivation to estimate water vapor feedback from observations, as it may allow a semidirect evaluation of climate change feedback in addition to providing a key test of water vapor processes in models via the strength and structure of their interannual feedbacks.

A significant number of estimates of the strength of interannual water vapor feedback have now been made, as summarized in Table I. Published estimates show substantial divergence in diagnosed feedback magnitude, although they agree on a strong positive feedback on interannual timescales.

The range shown in Table I is unsurprising given the diversity of approaches adopted across the studies. Some consider different phase strong ENSO events alone (Dessler and Wong, 2009), while others perform regressions of radiative changes with monthly (Dessler, 2013; Gordon *et al.*, 2013; Liu *et al.*, 2018) or annual (Colman and Hanson, 2013) temperature across multiple years irrespective of ENSO activity. Regression

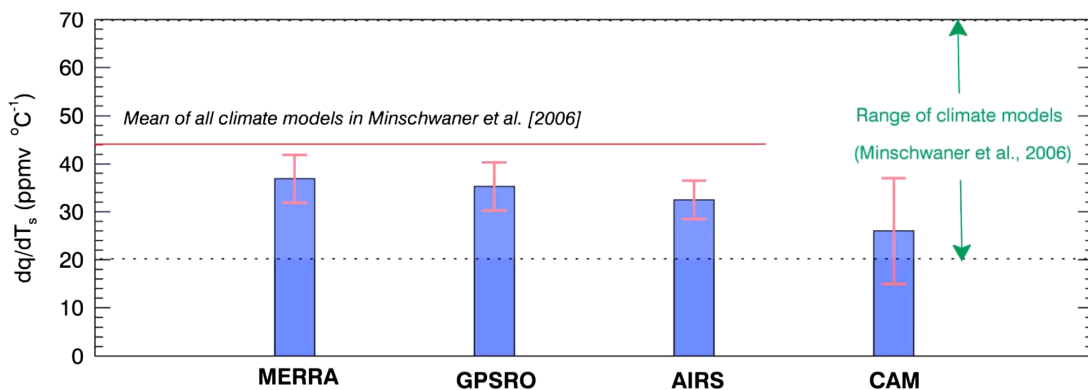


FIG. 23. Estimated specific humidity variations with temperature averaged over the tropics from MERRA (Rienecker *et al.*, 2011), Atmospheric Infrared Sounder (AIRS) satellite retrievals, and 1.2–1.6 GHz Global Positioning System Radio Occultation (GPSRO) measurements at 250 hPa during the period 2007–2010. This shows close agreement among the three observational measurements. The values of  $dq/dT_s$  indicate moistening with temperature at slightly below the rate implied by unchanged relative humidity. Error bars represent 1 standard deviation estimation uncertainty from linear regressions. Also shown are calculations from a single GCM, the Community Atmosphere Model (CAM) (Gettelman and Fu, 2008). The solid line and the region between the horizontal dotted lines represent the mean and spread of  $dq/dT_s$  in 42 CMIP5 GCMs from Minschwaner, Dessler, and Sawaengphokhai (2006) and show overall consistency between models and observations, albeit with wide model spread and a mean model value that is slightly larger than observational estimates. From Vergados *et al.*, 2016.

TABLE I. Summary of estimates of water vapor feedback (and one of lapse rate) from interannual variability. LW = longwave feedback, SW = shortwave feedback, and net = LW + SW. The range of values shown is  $\pm 2\sigma$ .

Reference	Dataset(s)	Analysis period	Water vapor	Value ( $\text{W m}^{-2} \text{K}^{-1}$ )
Dessler and Wong (2009)	ERA-40 (Uppala <i>et al.</i> , 2005) MERRA	ENSO warm and cold phases, 1980–2000		3.7 (net)
				4.7 (net)
Dessler (2013)	ERA-Interim (Dee <i>et al.</i> , 2011) MERRA (Rienecker <i>et al.</i> , 2011)	2000–2010		1.35 (net)
				1.12 (net)
Colman and Hanson (2013)	ERA-Interim MERRA	1960–1998		1.6 (LW)
		1980–2008		2.5 (LW)
Gordon <i>et al.</i> (2013)	Atmospheric Infrared Sounder (AIRS)-MLS	2002–2009		$2.2 \pm 0.4$ (net)
Koumoutsaris (2013)	JRA-25 (Onogi <i>et al.</i> , 2007) ERA-Interim	1979–2009		$0.86 \pm 0.14$ (net)
		1979–2009		$1.37 \pm 0.16$ (net)
Liu <i>et al.</i> (2018)	AIRS-MLS	2004–2016		$1.46 \pm 0.22$ (LW)
				$0.09 \pm 0.01$ (SW)
				$1.55 \pm 0.23$ (net)
Lapse rate				
Koumoutsaris (2013)	JRA-25 ERA-Interim	1979–2009		$0.34 \pm 0.20$
		1979–2009		$0.11 \pm 0.16$

methodology can also make a significant difference and, in particular, explains much of the large variation in feedback strength found between the related studies of Dessler and Wong (2009) and Dessler (2013). Differences can also arise because of the choice of radiative kernels used (Liu *et al.*, 2018), along with one study applying the PRP technique (Colman and Hanson, 2013); see Appendix A. Estimates using reanalyses must also contend with shortcomings in representation of moisture over dry subtropical ocean regions in some reanalysis datasets (Allan, 2004) and substantial differences between the reanalyses themselves arising from differing Numerical Weather Prediction models and assimilated datasets (Koumoutsaris, 2013).

All but one study (Dessler, 2013) evaluated only traditional water vapor feedback [Eq. (4)]. Using the alternate fixed relative humidity formulation [Eqs. (6)–(8)], Dessler (2013) found, as expected, that the disagreement between the results of two reanalyses decreased, giving common values of the  $\lambda'_P$  term of  $-1.92 \text{ W m}^{-2} \text{ K}^{-1}$ , and the  $\lambda'_H$  term of  $\sim -0.06 \text{ W m}^{-2} \text{ K}^{-1}$ . However, not all disagreement disappeared, with the  $\lambda'_T$  term varying significantly from 0.09 to  $0.26 \text{ W m}^{-2} \text{ K}^{-1}$  (Dessler, 2013).

A key remaining difference between the studies is their choice of time periods for feedback evaluation. The effect of this can be great and poses an additional challenge for determining interannual water vapor feedback from observations. Liu *et al.* (2018) showed that sampling 19 different 12-year segments (corresponding to the length of the available AIRS-MLS dataset) from 30-year periods from CMIP5 models gave widely varying estimates of feedback strength; see Fig. 24. Further, the mean of the 19 samples could differ strongly from results from the entire 30-year period (Fig. 24). An investigation of five different 20-year samples over the entire 20th century from CMIP3 models (Dalton and Shell, 2013) backs this up. It found substantial variation in the analyzed interannual variability feedback from the five samples, although despite this it showed modest cross model correlation between variability-derived water vapor feedback and secular water vapor feedback over the entire century

(Dalton and Shell, 2013). This high sensitivity to time sampling in calculating interannual water vapor feedback needs to be borne in mind, for example, when considering values such as those of Gordon *et al.* (2013), which are based

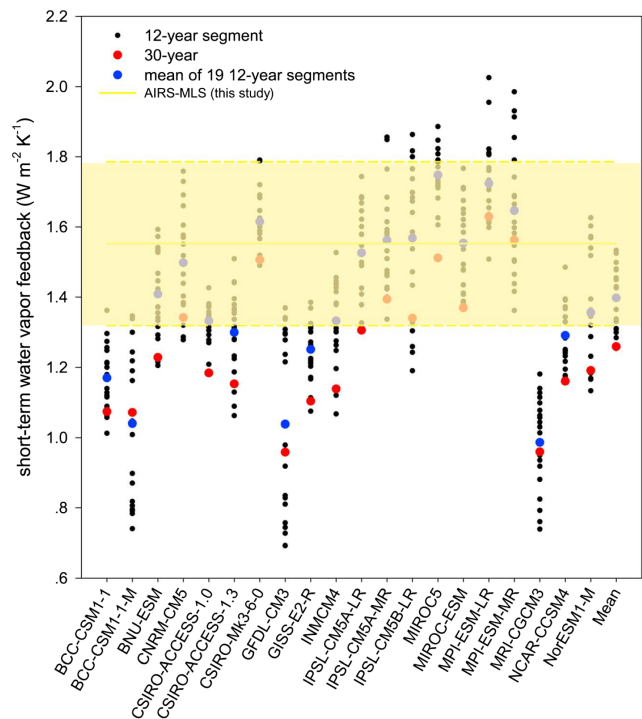


FIG. 24. Water vapor feedback calculated from interannual variability from CMIP5 GCMs forced by observed SSTs over the period 1979–2008. Red (larger) dots show feedbacks calculated over the entire 30-year period, black dots from 19 different 12-year segments within this period, and blue dots the mean of all 12-year segments. Shading shows AIRS-MLS sounding observations from 2004 to 2016. It is clear that an enormous spread of results from estimation of water vapor feedback can be expected if taken from relatively short (approximately decadal) time periods of models or observations. From Liu *et al.*, 2018.

on only 88 months of observations (which was the limit of the AIRS data available).

In summary, seasonal, interannual, and longer timescales provide important information and tests on water vapor feedback, although they do not provide direct analogs for climate change feedback. There remains considerable observational uncertainty in the value of interannual water vapor feedback, and there are major challenges in refining it. However, if the range of estimates could be better understood and narrowed, potential constraints may be possible using model-derived correlations between interannual (and longer term) feedbacks and feedbacks under secular climate change (Dalton and Shell, 2013; Gordon *et al.*, 2013; Takahashi, Su, and Jiang, 2016; Colman and Hanson, 2017; Liu *et al.*, 2018).

#### D. Volcanoes and water vapor feedback

Volcanic eruptions provide another potential analog for long-term climate change. Large explosive volcanoes can emit vast quantities of aerosols into the stratosphere, blocking sunlight for extended periods and causing a multiyear

transient cooling of the order of a few tenths of a °C (Robock and Mao, 1995; Kirtman *et al.*, 2013). The most recent large, climatologically significant eruption, that of Mount Pinatubo in 1991, provides a natural experiment for testing water vapor feedback and its role in climate response.

Observed  $6.7\ \mu\text{m}$  channel radiances (sensitive to relative humidity averaged over roughly 200 to 500 hPa) showed modest reductions in the years immediately following the eruption [black line in Fig. 25(a), which was taken from Soden *et al.* (2002)]. GCM simulated emission temperatures show good agreement with observations (blue and green lines) calculated either directly from the model or while assuming constant relative humidity. However, they show roughly doubled observed  $6.7\ \mu\text{m}$  emission temperature reduction if no relative-humidity-induced drying occurred (red line). Together this provides direct evidence that roughly unchanged upper tropospheric relative humidities occur under the cooling found in response to Mount Pinatubo (Soden *et al.*, 2002).

To investigate the impact of water vapor feedback on the global cooling that followed, Soden *et al.* (2002) used a

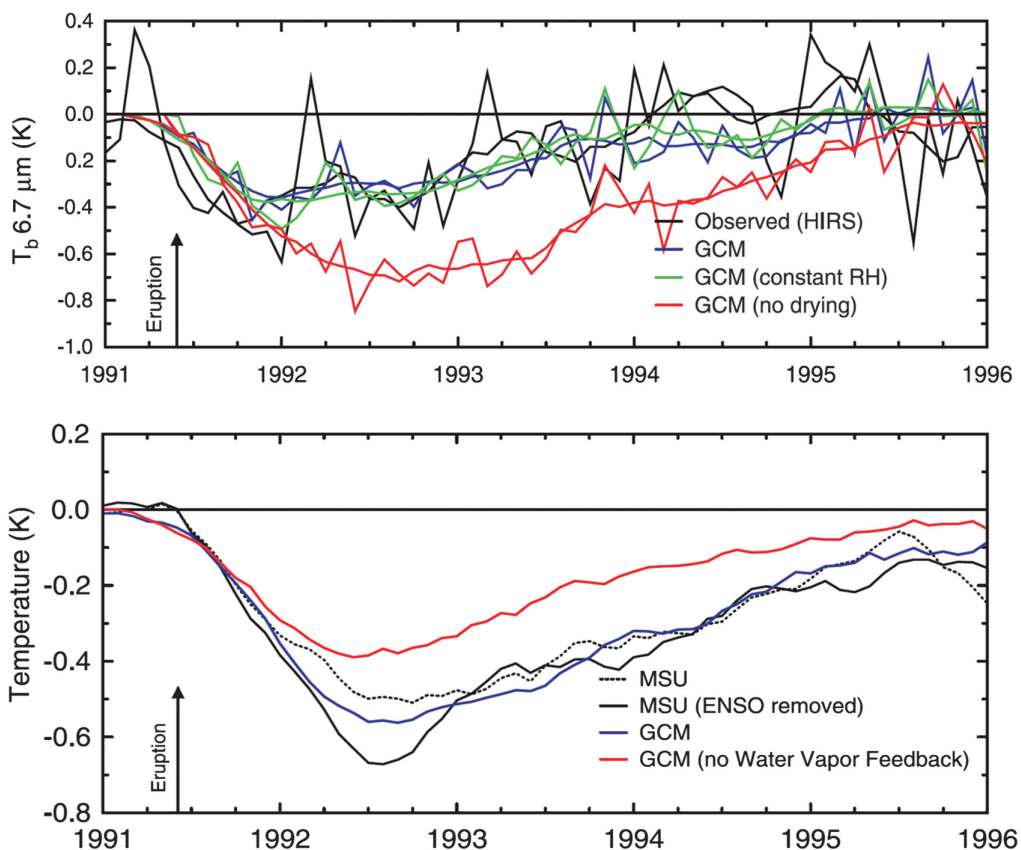


FIG. 25. Top panel: changes in global mean  $6.7\ \mu\text{m}$  brightness temperatures from High-Resolution Infrared Radiation Sounder (HIRS) observations (black line) and as simulated by the Geophysical Fluid Dynamics Laboratory GCM (blue line) following the Mount Pinatubo eruption. Anomalies are expressed relative to preeruption values (January–May 1991). The green line represents the GCM with unchanged relative humidity, and the red line represents the GCM with unchanging specific humidity (corresponding to no upper tropospheric drying). Thick lines are seven month running means. This shows that unchanging relative humidity, not specific humidity, enables the model to match observations. Bottom panel: observed global cooling in the lower troposphere following the Mount Pinatubo eruption as measured by the microwave sounding unit (MSU) (black lines) and model predicted temperature (blue line). The red line shows the temperature trace of the GCM with suppressed water vapor feedback. This shows that strong positive water vapor feedback was necessary for the GCM to reproduce observed cooling. From Soden *et al.*, 2002.

modified GCM that suppressed the terrestrial radiative response to water vapor changes. They showed that, whereas an unmodified version of the GCM was able to represent the magnitude of post–Mount Pinatubo global cooling (peaking at around  $-0.5^{\circ}\text{C}$ ), the GCM without water vapor feedback produced much weaker cooling [Fig. 25(b)].

An extension by Forster and Collins (2004) considered the vertical and meridional distribution of water vapor changes in response to Mount Pinatubo using satellite-derived vertical water vapor observations. Calculating the radiative effect, they estimated a value of the water vapor feedback of  $1.6 \text{ W m}^{-2} \text{ K}^{-1}$ , with a 5%–95% range progressing from 0.9 to  $2.5 \text{ W m}^{-2} \text{ K}^{-1}$ . Parallel calculations from a large model ensemble forced by stratospheric aerosol observations produced a comparable average of  $2.0 \text{ W m}^{-2} \text{ K}^{-1}$  (range of 0.4 to  $3.6 \text{ W m}^{-2} \text{ K}^{-1}$ ). Caution must be exercised in interpreting the results. No vertical profile from the GCM ensemble closely matched the observations, and natural variability unrelated to the volcanic forcing caused considerable spread in both the observational and model results (Forster and Collins, 2004).

Together these studies provide compelling evidence for strong positive water vapor feedback following climate forcing (Del Genio, 2002). Some differences in water vapor feedback strength may be possible from volcanic aerosol forcing, as distinguished from GHG forcing. However, GCM experiments considering both volcanic aerosol and  $\text{CO}_2$  forcings find only small differences in the net clear-sky response (Yokohata *et al.*, 2005) or the water vapor feedback itself (Yoshimori and Broccoli, 2008).

### E. Paleo evidence

Paleo climates provide another line of evidence for the magnitude of water vapor feedback. Paleo reconstruction and modeling evidence indicates that a strong positive water vapor feedback is needed to explain both colder (Berger *et al.*, 1993; Crucifix, 2006) and warmer (Lariviere *et al.*, 2012) paleo climates. For example, 2D modeling sensitivity studies by Berger *et al.* (1993) found that water vapor feedback was responsible for around 40% of the cooling during the LGM. Strong positive water vapor feedback has also been found to help explain impacts of LGM continental ice sheet thicknesses on high latitude temperatures (Liakka and Lofverstrom, 2018).

A study using six CMIP5–Paleo Model Intercomparison Project phase 3 models found that water vapor feedback was responsible for around 29% of the global cooling during the Little Ice Age, 1600–1850 CE (Atwood *et al.*, 2016).

A consideration of reconstructed 800 000-year temperatures from ice-core data (across multiple glacial and interglacial cycles) shows self-consistency for climate sensitivity of 3 K, which is consistent with strong positive net water vapor + lapse rate feedback (Hansen *et al.*, 2008; Lacis *et al.*, 2013).

Together these studies provide important, albeit indirect, supporting evidence for strong positive water vapor (and water vapor + lapse rate) feedback, which has acted to amplify past climate change.

### F. Observed lapse rate changes and variability

The section has concentrated thus far largely on water vapor changes. Since lapse rate feedback is dominated by tropical changes in saturated adiabatic lapse rate, we would expect to observe warming in the upper troposphere that has exceeded surface warming in recent decades. However, there has been controversy over the past 30 years on observed global or tropical-mean lapse rate changes, starting with suggestions in the early 1990s that models have overstated upper tropospheric temperature increases relative to observed changes (Spencer and Christy, 1990). The implication was that models may be missing or misrepresenting processes driving lapse rate responses under projected climate change. A lengthy debate has taken place on the significance and cause of differences, including uncertainties in the observations (Flato *et al.*, 2013).

Behind much of this uncertainty has been the fact that both satellite and radiosonde observations are characterized by time varying biases and discontinuities (Po-Chedley, Thorsen, and Fu, 2015), with the radiosonde network also featuring regional inhomogeneities and large data sparse regions. For example, producing long-term tropical time series from AMSU measurements has been challenging, with different estimates depending on factors such as the proper treatment of different satellites and diurnal cycle corrections (Po-Chedley, Thorsen, and Fu, 2015). The removal of temperature biases has also proven to be sensitive to methodology (Thorne *et al.*, 2011).

There is evidence that tropical upper tropospheric warming in GCMs overall has exceeded observations of the last several decades (Santer *et al.*, 2017; McKittrick and Christy, 2018), although some of the CMIP5 models agree with the observations within error estimates (Flato *et al.*, 2013). Decadal timescale variability may explain some of the disagreement, but deficiencies in the forcing applied to models, such as that from volcanic eruptions (Santer *et al.*, 2014) or from other atmospheric aerosol changes (Santer *et al.*, 2017), have also been found to contribute. Despite possible observational and model disagreements, however, observed trends in mid to upper tropospheric temperatures (Santer *et al.*, 2013) and trends in the seasonality of atmospheric temperatures (Santer *et al.*, 2018) are incompatible with natural variability alone, indicating a human influence.

Patterns of SST changes also influence the strength of lapse rate feedback diagnosed from observations and models. Warming, as has occurred in the observed trend (enhanced western Pacific compared to eastern Pacific warming) (Hartmann *et al.*, 2013), results in a stronger negative lapse rate feedback in models than for more uniform warming such as that under equilibrium (i.e., long-term) climate change (Andrews and Webb, 2018). This pattern of warming is important, as it also has impacts on net climate sensitivity as it affects Pacific-wide cloud changes, particularly for low clouds in the east (Andrews and Webb, 2018).

Studies using models forced by observed SSTs (rather than fully coupled models) provide a promising “cleaner” comparison with observed upper tropospheric warming (Mitchell *et al.*, 2013). Model results can vary between different SST datasets, however, so possible observational SST errors add further uncertainty (Flannaghan *et al.*, 2014). Furthermore, results can differ substantially between models for a given

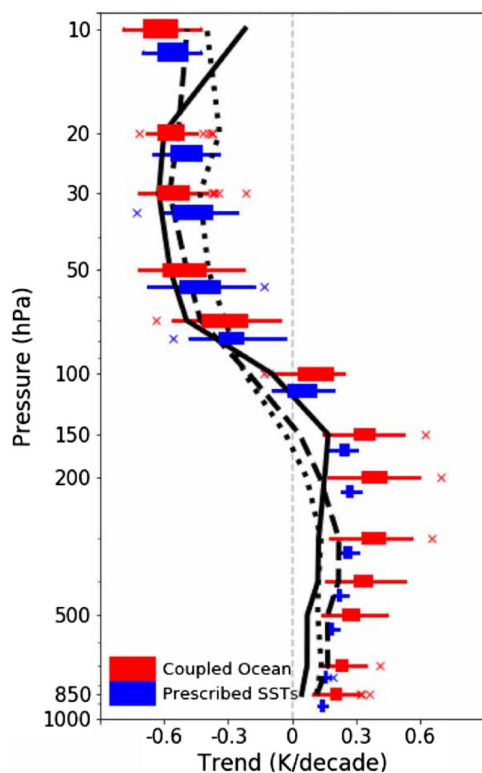


FIG. 26. Comparisons of CMIP6 model vertical temperature trends ( $20^{\circ}\text{N}/20^{\circ}\text{S}$ ) to observations from two radiosonde datasets (RICH1.7 and RAOBCORE1.7) and the ERA5/5.1 reanalysis (black lines) for the period 1979–2014. Box-whisker plots show the 25%–75% intermodel range, while bars and crosses represent the 1.5 quartile range and then outliers beyond that. Red (upper) boxes represent 48 fully coupled ocean-atmosphere CMIP6 GCMs forced by anthropogenic greenhouse gases and aerosols as well as estimated natural forcing, and blue (lower) boxes represent a subset of 28 atmosphere-only GCMs forced by observed SST changes. Blue (lower) lines are displaced vertically for plotting purposes. In the troposphere, models show much less spread, and better agreement with observations when forced by SSTs that match observed, rather than those simulated under a “freewheeling” experiment, indicating that much of the apparent disagreement between model and observed lapse rate changes may be due to different trends in model surface temperatures. From Mitchell *et al.*, 2020.

SST dataset due to differing precipitation pattern responses (Fueglistaler, Radley, and Held, 2015).

A recent study of Coupled Model Intercomparison Project phase 6 (CMIP6) (Eyring *et al.*, 2016) models showed that, as in the two previous model generations (Fu, Manabe, and Johanson, 2011; Po-Chedley and Fu, 2012), there remains an overestimate of upper tropospheric warming relative to observations—in this case radiosondes and ECMWF reanalyses (Mitchell *et al.*, 2020) (Fig. 26). However, much of the overestimate can be linked to biases in surface temperature increases, rather than lapse rate change deficiencies, as tropospheric temperature agreement is much closer when models are forced by observed SST changes; see Fig. 26.

Confidence in models is also reinforced by variability studies. On monthly to interannual timescales, a range of observations including radiosondes and MSU satellite

observations show an amplification of warming with altitude, in a manner that agrees with theory and climate model simulations (Santer *et al.*, 2005).

Further details of the debate on upper tropospheric warming in models versus observations are beyond the scope of this review. An extensive review, albeit not recently updated, was provided by Thorne *et al.* (2011); see also the Fourth and Fifth IPCC Assessment Reports (Hegerl *et al.*, 2007; Hartmann *et al.*, 2013) for further discussion.

Regardless, the offsetting nature of temperature and water vapor responses in the tropical upper troposphere means that combined tropical water vapor plus lapse rate feedbacks are insensitive to such differences (Boucher *et al.*, 2013; Ingram, 2013a, 2013b; Po-Chedley *et al.*, 2018). Therefore, the uncertainties of tropical lapse rate changes, although important for understanding the individual feedbacks and the representation of processes in models, do not significantly decrease confidence in the strength of combined water vapor and lapse rate feedbacks in GCMs.

## VI. MODEL REPRESENTATION OF FEEDBACKS AND FEEDBACK PROCESSES

Section V described the extensive observational evidence supporting water vapor and lapse rate feedbacks. Models, in combination with observations, are fundamental to our understanding of feedback processes and for providing quantitative estimates of their strength. Models represent our primary tool for projections of future climate change. The extensive research presented in this section therefore focuses on the evaluation and assessment of models and model processes underpinning water vapor and lapse rate feedbacks.

### A. Quantification of feedbacks in models

Limitations in the understanding and evaluation of water vapor and lapse rate feedbacks in GCMs through the 1990s and early 2000s in part related to challenges in their quantification in models and observations. A critical advance in this area in the last 40 years and particularly over the past 20 years has been the development of methods for calculating and comparing model feedbacks and determining feedbacks from observations. These methodologies are described in Appendix A.

### B. Model representation of water vapor distribution, variability, and trends and their radiative impact

For the mean climate, models represent with skill large-scale features of the observed relative humidity field and associated OLR (Bates and Jackson, 1997). For example, comparison with observations from AIRS showed that CMIP5 models overall represented distributions of tropospheric specific humidity and temperature well (Tian *et al.*, 2013). There were, however, some notable biases, including a cold bias of around  $2^{\circ}\text{C}$  in the extratropical upper troposphere, and a moist bias in the tropical upper troposphere (Tian *et al.*, 2013). Comparison of CMIP5 model specific humidity with NASA A-train moisture retrievals show agreement to within 10% in the low to mid troposphere (Jiang *et al.*, 2012). In the upper troposphere, however, a larger range is found in models, from

around 1% to twice the observed value (Jiang *et al.*, 2012). This represented a limited advancement from the earlier generation of CMIP3 models, which on average had a bias of over 100% in free tropospheric specific humidity (John and Soden, 2007; Jiang *et al.*, 2012). Further modest improvement has been found in CMIP6 compared to CMIP5 (Jiang *et al.*, 2021). Although some of these biases remain substantial, *fractional* change in water vapor rather than absolute change is critical for the feedback. Therefore, such “present climate” biases should not be crucial to net feedback strength (Held and Soden, 2000; John and Soden, 2007), and indeed biases in the current climate are not correlated with the magnitude of model water vapor feedback (John and Soden, 2007).

The observed tropical “bimodality” in the humidity distribution is represented with widely varying skill in GCMs (Zhang, Mapes, and Soden, 2003; Pierrehumbert, Brogniez, and Roca, 2007). Bimodality is indicative of sharp moisture gradients, and of parcel mixing timescales being longer than moisture residence times in the tropical atmosphere (Zhang, Mapes, and Soden, 2003). However, the importance of this feature for feedback processes and the representation in models is unclear (Randall *et al.*, 2007), and no evidence has established that this issue adversely affects model representation of water vapor feedback.

Although, as previously discussed, feedback strengths under interannual or decadal variability are not direct analogs for secular climate change feedback, skillful representation of observed variability can nevertheless bolster confidence that models represent key processes controlling upper tropospheric humidity on these timescales, and under these temperature forcings (Randall *et al.*, 2007).

Studies show that models can reproduce observed interannual variations in lower tropospheric moisture, which is itself consistent with approximately invariant relative humidity (Soden and Schroeder, 2000; Allan, Ringer, and Slingo, 2003; Trenberth, Fasullo, and Smith, 2005); see Sec. V.A. This is an important test for model representation of moisture variability generally but is unsurprising, given the tight coupling between surface and lower troposphere and the widespread availability of surface water (Bony *et al.*, 2006).

For the upper troposphere, models show skill in the representation of OLR and observed water vapor variations from seasonal changes (Inamdar and Ramanathan, 1998; Tsushima, Abe-Ouchi, and Manabe, 2005). Many studies have also found overall model skill in representing interannual moisture variations and associated radiation changes (Soden, 1997, 2000; Kiehl, Hack, and Hurrell, 1998; Dessler and Sherwood, 2000; Gettelman and Fu, 2008; Dessler and Wong, 2009). For example, models reproduce interannual water vapor feedbacks derived from reanalysis temperature and moisture data (Slingo *et al.*, 2000; Dessler and Wong, 2009; Colman and Hanson, 2013; Dessler, 2013) and show a modest decrease in relative humidity with temperature within the error bars of observations at 215 hPa (Minschwaner, Dessler, and Sawaengphokhai, 2006). A recent study found tropical-mean 200 hPa specific humidity variations with temperature measured using three methodologies, GPS refractive indices, AIRS satellite retrievals, and the MERRA reanalysis, to lie well within the range simulated by CMIP5 models, albeit slightly below the multi-model mean (Vergados *et al.*, 2016) (Fig. 23).

Figure 22 shows TOA radiation perturbations due to water vapor changes over ENSO events for 12 CMIP3 models and two reanalyses. It confirms that models represent interannual fluctuations in moisture and radiation response that are similar to estimates from observations in both the meridional and vertical dimensions. CMIP3 models have also been found to straddle two reanalysis estimates for both interannual and seasonal water vapor feedback (Colman and Hanson, 2017) and 20 CMIP5 models with values calculated using AIRS-MLS satellite observations from 2004 to 2016 (Liu *et al.*, 2018). Feedbacks from fully coupled models, however, are on average slightly weaker than those from models forced by observed SSTs (Liu *et al.*, 2018).

Critically, models also show trends of upper tropospheric humidity that are consistent with satellite observations over the period 1982–2004 (Soden *et al.*, 2005). Results using satellite “emulators”<sup>17</sup> within models of upper tropospheric humidity-dependent radiances, such as those of HIRS 14  $\mu\text{m}$  wavelength, find model skill in the representation of interannual and decadal variability and long-term trends (Allan, Ringer, and Slingo, 2003). Similarly, a more recent study found CMIP5 models overall reproduced satellite-derived tropical upper tropospheric humidity trends over a 27-year period ending in 2005 (Chung *et al.*, 2014).

In summary, models show significant skill in reproducing observed trends and the variability of relative humidity in both the upper and lower tropospheres, and consequently of water vapor feedback under secular change and interannual variability. Models overall have skill in representing large-scale mean distributions of humidity, but with biases in some regions. Because of the logarithmic dependence of radiation changes on specific humidity however, these biases do not affect model estimates of water vapor feedback. Together these findings strongly reinforce confidence in model representations of water vapor feedback.

### C. Conclusions on feedback impacts on global variability

In addition to observations of variability providing exacting tests for models, studies presented in Secs. V.B and VI.B provide overwhelming evidence that water vapor feedback (and combined water vapor + lapse rate feedback) amplify global temperature variability across a wide range of timescales.

Observations and models confirm that water vapor feedback reinforces the annual cycle (Hu, 1996; Tsushima, Abe-Ouchi, and Manabe, 2005; Wu, Karoly, and North, 2008), with large positive values in individual summer hemispheres (Colman and Hanson, 2013) (Fig. 21), although with relatively weak annual mean values because of strong seasonal hemispheric offsetting. Based on more limited evidence, models suggest that lapse rate feedback also amplifies both global (Colman and Hanson, 2013) (Fig. 21) and midlatitude (Hu, 1996) seasonal cycles.

Models and observations are also unanimous on the amplification of interannual global temperature variability; see the discussion in Secs. V.C and VI.B. In addition to the

<sup>17</sup>An emulator is model code that simulates the radiances as they would be directly seen by a satellite.

TABLE II. IPCC assessments of water vapor and lapse rate feedbacks for the First (FAR), Second (SAR), Third (TAR), Fourth (AR4), Fifth (AR5), and Sixth (AR6) Assessment Reports and for the Supplementary Report.

Report	Assessment
FAR (Cubasch and Cess, 1990)	The best understood feedback mechanism is water vapor feedback, and this is intuitively easy to comprehend.
Supplementary Report (Gates <i>et al.</i> , 1992)	There is no compelling evidence that water vapor feedback is anything other than positive, although there may be difficulties with upper tropospheric water vapor.
SAR (Dickinson <i>et al.</i> , 1995)	Feedback from the redistribution of water vapor remains a substantial source of uncertainty in climate models. Much of the current debate has been on addressing feedback from the tropical upper troposphere, where the feedback appears likely to be positive. However, this has not yet been convincingly established: much further evaluation of climate models with regard to the observed processes is needed. Changes in lapse rate act as an additional feedback that can also be substantial and that generally opposes the water vapor feedback.
TAR (Stocker <i>et al.</i> , 2001)	Models are capable of simulating the moist and dry regions observed in the tropics and subtropics and how they evolve with the seasons and from year to year....While reassuring, this does not provide a definitive check of the feedbacks, although the balance of evidence favors a positive clear-sky water vapor feedback of a magnitude comparable to that found in simulations.
AR4 (Randall <i>et al.</i> , 2007)	New evidence from both observations and models has reinforced the conventional view of a roughly unchanged relative humidity response to warming.... Taken together, the evidence strongly favors a combined water vapor–lapse rate feedback of around the strength found in GCMs.
AR5 (Boucher <i>et al.</i> , 2013)	The net feedback from water vapor and lapse rate changes combined, as traditionally defined, is extremely likely (more than 95% confidence) to be positive. Values in this range ( $0.9 - 1.3 \text{ W m}^{-2} \text{ K}^{-1}$ ) are supported by a steadily growing body of observational evidence, model tests, and physical reasoning.
AR6 (Forster <i>et al.</i> , 2021)	The combined water vapor plus lapse rate feedback is positive. The main physical processes that drive this feedback are well understood and supported by multiple lines of evidence, including models, theory, and observations. The combined water vapor plus lapse rate feedback parameter is assessed at $1.30 \text{ W m}^{-2} \text{ K}^{-1}$ , with a highly likely range of 1.1 to $1.5 \text{ W m}^{-2} \text{ K}^{-1}$ and a likely range of 1.2 to $1.4 \text{ W m}^{-2} \text{ K}^{-1}$ with high confidence.

overwhelming diagnostic evidence presented in those sections, direct evidence comes from suppressed water vapor feedback experiments in models, which find that removal of water vapor feedback decreases unforced interannual temperature fluctuations (Hall and Manabe, 1999, 2000b). Lapse rate feedback impact on interannual variability has been evaluated more rarely, with findings that it remains a negative feedback thereby suppressing interannual variability (Colman and Hanson, 2013, Koumoutsaris, 2013) (Fig. 21).

More limited evidence on decadal variability indicates that water vapor also increases temperature variations on those timescales (Allan, Ringer, and Slingo, 2003; Colman and Hanson, 2013; Colman and Power, 2018), but that lapse rate feedback dampens them (Colman and Hanson, 2013, 2017). Limited available evidence also suggests that decadal feedback is modestly weaker in magnitude on average than is the case under long-term climate change (Fig. 21).

## VII. EVALUATION AND ASSESSMENT OF WATER VAPOR AND LAPSE RATE FEEDBACKS

### A. IPCC assessment of water vapor and lapse rate feedbacks

The IPCC has made prominent assessments of the magnitude of, and overall confidence in, water vapor and combined water vapor + lapse rate feedbacks. The importance of the IPCC assessments is that they strive to represent a climate

communitywide evaluation of relevant evidence. The IPCC process facilitates this through a broadly representative lead and contributing author list and three review stages consisting of expert, community, and government reviewing (InterAcademy Council, 2010). Table II lists the headline assessments of the First through Sixth Assessment Reports. The IPCC has only more recently explicitly estimated the value of water vapor–lapse rate feedbacks, with earlier reports providing qualitative or semiquantitative statements about their strength, the ability of models to faithfully represent key processes, and the overall assessed confidence level.

A close examination of Table II is instructive on the progress of confidence in water vapor and lapse rate feedbacks over the past 30 years. In the First Assessment Report (1990) it was deemed self-evident that water vapor feedback was strong and positive. However, the scientific challenges to the mainstream view in the early 1990s (see Sec. IV.D) pointing out the critical nature of the (then poorly understood) tropical upper tropospheric moisture changes, and the central role of convective detrainment and associated uncertainties (Lindzen, 1990, 1994) caused a reexamination of confidence in the nature and strength of the feedback. This resulted in the much more ambivalent statements in the Supplementary Report (1992) and the Second Assessment Report (1995), featuring an emphasis on poorly understood processes governing upper tropospheric humidity changes.

An accumulation of research on theory, processes, modeling, and observational studies in subsequent years has led to a steady increase in confidence in the sign and strength of the combined feedbacks through the Third, Fourth, Fifth, and Sixth Assessment Reports. It pays to now reflect upon a timely challenge to those arguing for weak or negative water vapor feedback, issued by the Third Assessment Report (Stocker *et al.*, 2001). That challenge was to develop a GCM that reproduces the observed climate, and yet has a substantially weaker water vapor feedback than contemporary GCMs. No such model has ever been produced.

### B. Summary “best” estimate of feedback strengths and uncertainty ranges

Many studies have provided estimates of water vapor, lapse rate, and combined water vapor plus lapse rate feedbacks, either from models or derived from observations. A list of estimates including the methodology and references is provided in Table III in Appendix B. A summary of the feedback estimates is provided in Fig. 27.

An early estimate was made from the IPCC First Assessment Report (Cubasch and Cess, 1990) based largely on published studies by Cess *et al.* (1989) and Raval and Ramanathan (1989) that considered observations of temperature sensitivity of OLR, as well as modeling studies from 14 GCMs under simplified forcing. That estimate ( $1.2 \text{ W m}^{-2} \text{ K}^{-1}$ ) now sits well below the range of subsequent estimates. Other IPCC Assessment Reports have generally not provided evaluations of the magnitude of water vapor or lapse rate feedback apart from those in the literature, except for the AR5, which provided an estimate of the combined feedback of  $1.1$  ( $0.9$  to  $1.3$ , 90% range)  $\text{W m}^{-2} \text{ K}^{-1}$  and the AR6 with a combined estimate of  $1.30 \text{ W m}^{-2} \text{ K}^{-1}$  ( $1.1 - 1.5 \text{ W m}^{-2} \text{ K}^{-1}$ , 90% range).

Purely modeling-based estimates of feedback strength have a long history. A study by Colman (2001) assembled already published model results from RCMs and GCM studies and derived a multimodel combined feedback estimate of  $1.37 \pm 0.4 \text{ W m}^{-2} \text{ K}^{-1}$ . This is a higher number than other estimates, such as that from the AR5 or AR6, although it included a diverse range of models including RCMs. Other multimodel estimates have typically been calculated using radiative kernels applied to a range of CMIP experiments; see Table III. As a result, we have estimates from the CMIP2, 3, 5, and 6 ensembles (Soden and Held, 2006; Koumoutsaris, 2013; Vial, Dufresne, and Bony, 2013; Caldwell *et al.*, 2016; Colman and Hanson, 2017; Zelinka *et al.*, 2020). It is noteworthy that there have been high levels of overall consistency down the years between different model generations, despite two decades of model development and a dramatic increase in horizontal and vertical resolution, albeit with the suggestion of slightly stronger water vapor feedback in the last two generations of models (Table III and Fig. 27). It is also notable that overall consistency between generations holds despite a significant increase in ECS from CMIP5 to CMIP6, including some models with sensitivities of over 6 K (Zelinka *et al.*, 2020).

A caveat on such comparisons is that different climate change experiments produce slightly different feedback strengths, as can be seen by comparing water vapor and lapse

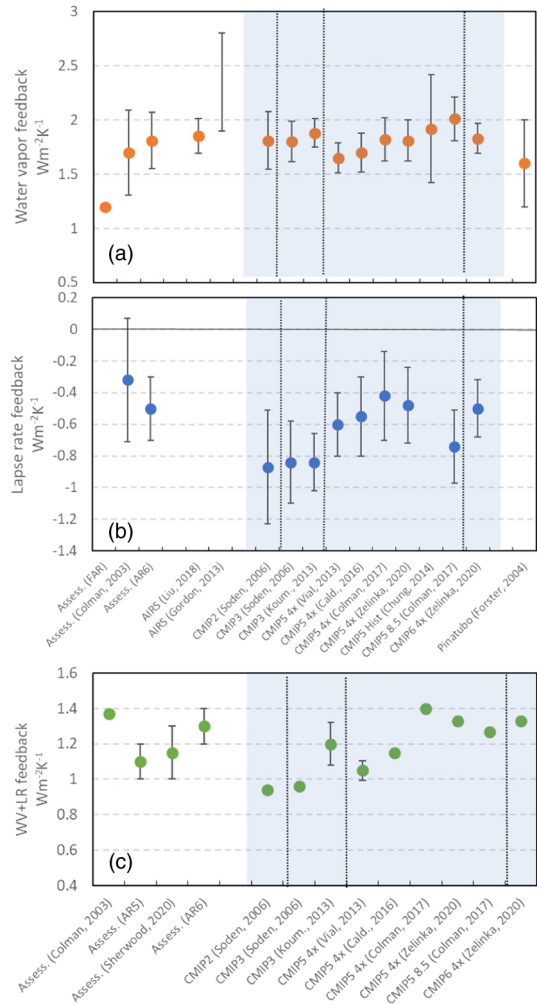


FIG. 27. Values of (a) water vapor, (b) lapse rate, and (c) combined water vapor plus lapse rate feedbacks taken from the studies listed in Table III. Error bars show a  $\pm 1\sigma$  range of the estimates (where available). Assess. refers to an evaluation carried out from published literature. Experiments referred to are  $4\times$ ,  $4\times \text{CO}_2$ ; Hist, CMIP Historical simulations; 8.5, CMIP RCP8.5 experiments. Shaded areas denote CMIP-based analyses, with the vertical lines differentiating CMIP2, 3, 5, and 6. AIRS are determinations from Atmospheric Infrared Sounder observations of interannual feedback, scaled by the ratio between climate change and interannual feedbacks derived from model ensembles. AR6 water vapor values are the average of the reported model and observational estimates.

rate feedback estimates for CMIP5 from Historical, abrupt  $4\times \text{CO}_2$ , and RCP 8.5 projection experiments (Colman and Hanson, 2017); see Fig. 27. This is not surprising given the sensitivity of water vapor and lapse rate feedbacks to SST warming patterns, as discussed in Sec. IV.G. Furthermore, different kernels can produce somewhat different feedback strengths (Vial, Dufresne, and Bony, 2013).

Another approach to estimating climate change feedbacks has been to use observations to estimate interannual feedback, then employ model-derived correlations between interannual and climate change feedbacks. This method was used by Gordon *et al.* (2013) and Liu *et al.* (2018) to estimate climate change feedback using AIRS-MLS based interannual

feedback measurements. The appeal of this approach is that it has a basis in observations rather than models alone. The disadvantages are that the relatively short time periods available for the observations inevitably result in significant sampling uncertainties in the strength of the feedback (Sec. V.C), and the technique also relies on the validity and accuracy of the correlation between interannual and climate change feedbacks in GCMs. Finally, another observational approach is that of [Forster and Collins \(2004\)](#), who used the cooling following the Mount Pinatubo eruption to estimate a water vapor feedback of  $\sim 1.6 \text{ W m}^{-2} \text{ K}^{-1}$ .

A recent review of variations in ECS across models by [Sherwood \*et al.\* \(2020\)](#) compared water vapor, lapse rate, surface albedo, and cloud feedbacks across models and observations. This included estimates from two separate model ensembles, CMIP 5 ([Taylor, Stouffer, and Meehl, 2012](#)) and CMIP 6 ([Eyring \*et al.\*, 2016](#)), as well as estimates from interannual variability using ERA reanalyses ([Dessler, 2013](#)).

[Sherwood \*et al.\* \(2020\)](#) demonstrated that uncertainty in cloud feedbacks remains the biggest source of uncertainty in model ECS. The final estimate of water vapor plus lapse rate feedback strength made by [Sherwood \*et al.\* \(2020\)](#) was  $1.15 \pm 0.15 \text{ W m}^{-2} \text{ K}^{-1}$  (the range representing 1 standard deviation), which lies between the estimate from the IPCC AR5 of 1.1 (0.9 to 1.3, 90% range)  $\text{W m}^{-2} \text{ K}^{-1}$  and the AR6 of 1.3 (1.1 to 1.5, 90% range). In estimating water vapor feedback we need to consider possible stratospheric water vapor feedback. Estimates of this are much fewer and contain considerable uncertainty (Sec. IV.F), with a recent calculated CMIP5 range of 0.10 to 0.26  $\text{W m}^{-2} \text{ K}^{-1}$  ([Banerjee \*et al.\*, 2019](#)), although compensating temperature feedbacks may largely offset much of this (Sec. IV.F).

From this review, our best estimate of overall strength of combined water vapor + lapse rate feedbacks is  $1.25 \pm 0.15 \text{ W m}^{-2} \text{ K}^{-1}$  (the range being 1 standard deviation), based on expert judgment from the range of results in the literature. This is a value slightly larger than that of [Boucher \*et al.\* \(2013\)](#) and [Sherwood \*et al.\* \(2020\)](#), taking under consideration the higher feedback strength from the last two generations of CMIP models (Fig. 27) and the evidence for at least a modest positive stratospheric contribution. It is close to (marginally below) the estimate of [Forster \*et al.\* \(2021\)](#); see Table III.

The RH-based feedback approach (Sec. III.B) provides a second and related perspective on this estimate. Adding the component of the Planck term in Eq. (6) that corresponds to the radiative effect of the humidity increase from uniform warming to the modified lapse rate, and relative humidity feedbacks equals the traditionally defined water vapor + lapse rate feedback.

## VIII. CONCLUSIONS

### A. On the strength and consistency of evidence for water vapor and lapse rate feedbacks

Significant progress in understanding water vapor and lapse rate feedbacks has been made in the past three decades, as well as in their observation and the understanding and representation of processes in climate models. This research has transformed our understanding of these feedbacks and established

beyond doubt that the water vapor feedback (as traditionally defined; see Sec. III.A) operates as a strong positive feedback in the climate system, on its own roughly doubling the response to GHG forcing compared to a hypothetical climate system without feedbacks, i.e., with Planck cooling alone. This research has also established that lapse rate feedback is a moderate negative climate feedback and, beyond doubt, that the combined water vapor plus lapse rate feedback is a strong positive feedback in the climate system.

For confidence in water vapor feedback, an understanding of the processes controlling humidity distributions and their change under global warming is critical. Overall, these physical processes are now well understood. Theoretical understanding points to an overall unchanged relative humidity with warming. Further, the “partly Simpsonian” explanation of the spectral dependence of TOA radiation on surface temperature has provided a firm theoretical basis for understanding the water vapor feedback.

Large-scale humidity structures in the mid to upper tropical troposphere can be traced to detrainment and mixing from convection advected by winds, along with moisture mixed in from midlatitude intrusions. To first order, broadscale relative humidity is unchanged under global warming, although upon closer inspection there are widespread modest projected relative humidity changes ( $\sim 1\%$  to  $2\%/K$  of warming), including decreases in the tropical upper troposphere and at midlatitudes, with increases in the tropical lower troposphere. These modest decreases in the mid to upper troposphere are found in both models and observations and weaken water vapor feedback by roughly 5% compared to fixed relative humidity.

The broadscale humidity distribution, and its change with temperature, is not sensitive to uncertainties stemming from model convection or cloud microphysics. This is evidenced by similar water vapor feedback being found in multiple generations of models with widely varying resolution and physical parametrizations: no GCM described in the peer-reviewed literature has ever been constructed with small or negative water vapor feedback. It has also been demonstrated that the broadscale observed and modeled humidity distributions can be well represented by advection-condensation models that eschew microphysics altogether but instead prescribe only conservation of last saturation humidity sourced from rising convective regions, then advection by broadscale winds. The large-scale organization of the atmosphere into concentrated rising regions rather than widespread small-scale convective cells appears to be central to this insensitivity to convective-cloud microphysics. On top of this there is no evidence of significant moistening resulting from evaporation of advective precipitated water, such as that from clouds, further reinforcing the position that the details of cloud microphysics are not important for overall humidity distribution.

This coherent view, which combines theory, observations, and simple and complex modeling studies, establishes confidence in water vapor providing a strong positive feedback and in its being of about the strength found in GCMs. Other lines of evidence in support come from the observed and modeled response to volcanic eruptions, and from paleo reconstructions that provide evidence that a strong positive water vapor feedback is required to explain global and regional temperature changes in past warmer and colder climates. Although not an

exact analog for climate change, the close-to-unchanged relative humidity observed and modeled on large scales under natural variability further reinforces the picture.

New observational datasets and modeling studies suggest there may be significant contributions to water vapor feedback from the stratosphere through temperature-dependent penetration of moisture from the midlatitude and tropical upper troposphere into the lower stratosphere. However, debate continues regarding dominant processes, and on whether the overall impact on the climate is one of warming once compensation for temperature-related feedbacks are taken into consideration in the upper troposphere and lower stratosphere.

Another major advance in the last 20 to 30 years is the appreciation that water vapor feedback also amplifies variability on seasonal, interannual, and decadal timescales. Estimates of the strength of interannual feedback vary substantially across models, and from differing observations. The reason for the spread in the latter is likely because of different methodologies, the use of different datasets such as different reanalyses or satellite products, different selected time periods, and the shortness of sampling. Differences in surface temperature patterns associated with variability and long-term climate change mean that measurements of feedback under interannual variability, for example, are not direct analogs of water vapor feedback under climate change. Nevertheless, they provide important tests for models and have a modest correlation with long-term climate change feedbacks in GCMs. Across a broad range of studies, models generally show skill in their ability to reproduce observed humidity change and radiative responses under variability from seasonal to interannual, and under the temperature increase in recent decades.

The sensitivity of feedback strength to base climate is also now much better understood. Paleo reconstructions and modeling studies indicate sensitivity of both water vapor and lapse rate feedback to global temperature and boundary forcing, such as that from ice sheets. These, combined with modeling studies with strong warming or cooling from large changes in CO<sub>2</sub>, suggest increasing water vapor feedback with global temperature, resulting from features such as a heightening tropopause, partially compensated for by increasingly negative lapse rate feedback. From a RH-based feedback paradigm, this implies little change in the Planck or lapse rate feedbacks. Sensitivity of feedbacks to different forcing agents such as solar, black carbon, sulphates, ozone, and volcanoes are better understood, with some but not all producing a feedback strength of comparable value to CO<sub>2</sub>. Under different forcings, as in many other aspects, a high degree of compensation between stronger and weaker water vapor and lapse rate feedback is apparent, again suggesting that the insensitivity to forcing is perhaps better framed in a RH-based approach where this offsetting is effectively removed. For large warming the partial-Simpsonian theory predicts total closure of the atmospheric water vapor window as continuum absorption overwhelms other radiative processes (Jeevanjee, 2018).

Traditionally defined lapse rate feedback is now much better understood. The overall paradigms of negative feedback in the tropics and subtropics from a lapse rate constrained at the saturated adiabatic level have been consistently

reproduced over generations of models and have also been consistent with theoretical understanding and observations of current climate and its interannual variability. An unchallenged demonstration of agreement between model and observations on upper tropospheric temperature *trends* continues to be elusive. Indications of systematic amplified warming in the upper troposphere in models compared to observations appear to be the result of several different factors. First, there are major difficulties in constructing universally accepted long-term observational satellite data sets. Second, comparisons can be confounded by natural variability, the incomplete inclusion of forcing such as that from volcanoes or anthropogenic aerosols in model studies or observations, and, third, from errors in surface temperature in model simulations propagating temperature differences aloft. Although these issues are not fully resolved, atmospheric models forced with observed SSTs show reasonable agreement with observations, and some but not all coupled GCMs show consistency with the somewhat uncertain observations.

The intimate and opposing relationship between water vapor and lapse rate feedbacks has been clarified through theoretical, observational, and modeling advances. Globally, the opposing nature results from differences in tropical and extratropical warming, implicating processes such as Southern Hemisphere sea ice cover and delayed Southern Ocean warming, which can differ across models. It is now well established that the spread in tropical combined water vapor plus lapse rate feedback results from relative humidity changes, rather than the magnitude of upper tropospheric warming. This places the RH-based decomposition of feedbacks on even surer footing, and in recent years increased emphasis has been given to this approach in the literature.

The role of feedbacks in contributing to the amplitude, timing, or progression of modes of variability such as ENSO, MJO, and the ITCZ are also better understood due to observational and modeling studies, but there is room for further research in this area to improve understanding of the role of feedbacks in other types of variability.

The importance of feedbacks, particularly lapse rate feedback, in the amplification of polar warming has been appreciated for at least two decades, but with much clarifying research in recent years. Reinforcing interactions between lapse rate feedback, surface albedo feedback, and other feedbacks and processes amplify polar warming, as confirmed by observation and modeling studies. Different studies, however, have found greater or lesser roles for individual feedbacks. Other processes, including equator to pole gradients of Planck cooling and CO<sub>2</sub> forcing, may also play important roles. Substantial differences also occur between the Arctic and the Antarctic, with the latter affected by delayed warming due to ocean heat uptake, and the effect of the elevated Antarctic plateau on lapse rate feedback and other processes. In the absence of an overlying theoretical framework and in the face of a large number of methodological approaches, the precise quantitative contribution of water vapor and lapse rate feedback to polar amplification remains somewhat elusive, although it is clear that lapse rate feedback plays a strong amplifying role.

Globally, many estimates have been made of the strength of water vapor, lapse rate, and the combined feedback. There is

strong consistency in the mean and ranges of feedbacks over the past four generations of GCMs, with values also consistent with estimates from observations, such as those from trends and from interannual variability scaled by various techniques to quantify long-term climate feedback. The evidence is now overwhelming that combined water vapor + lapse rate feedbacks provide the strongest positive feedback in the climate system, of a magnitude around that produced in climate models. Our estimate of overall strength of these combined feedbacks is  $1.25 \pm 0.15 \text{ W m}^{-2} \text{ K}^{-1}$ .

Although, as discussed in Sec. VII.B, issues remain to be clarified concerning water vapor and lapse rate feedbacks, it is extremely unlikely that these issues will result in major revisions in our confidence or their estimated combined feedback strength.

### B. A look to the future: Current research gaps

Despite this impressive progress, a range of key issues remain to be fully addressed. Further research is needed to do the following:

- (1) Improve estimates of water vapor and lapse rate feedbacks from interannual variability. Studies to date vary widely in their conclusions on water vapor feedback strength, in particular (Table I), with differences in approaches, periods, data, and analysis methods behind much of this spread. Refining observational and modeling estimates could help researchers test and verify physical processes in models controlling upper tropospheric temperature and water vapor changes, and clarify potential links with feedbacks under secular climate change, and it holds the hope of improving observation-based constraints of feedback strength.
- (2) Increase understanding of processes underlying the spread in relative humidity changes in the tropics under warming, including separately over land and oceans, as different responses in models drive much of the uncertainty in the combined water vapor–lapse rate feedback. Uncertainties include factors behind differing patterns of projected warming and uncertainties introduced by choices in convective parametrization and other microphysics choices. Comparing the observed and model-simulated patterns of relative humidity change will be important in this regard. This challenge links closely with the World Climate Research Program’s grand challenge on clouds, circulation, and climate sensitivity (Bony *et al.*, 2015).
- (3) Further develop, understand, and apply the RH-based approach for decomposing water vapor, lapse rate, and Planck feedbacks. Areas include an understanding of surface feedbacks and reasons for combined feedback spread (Po-Chedley *et al.*, 2018; Zelinka *et al.*, 2020; Zhang *et al.*, 2020).
- (4) Further explore the promising area of spectral-based feedbacks. These have the potential to produce a much greater fundamental understanding of changes in water vapor feedback strength with temperature, and indeed of a possible “peak” in overall climate sensitivity as temperatures continue to increase (Seeley and Jeevanjee, 2021).
- (5) Further assess the ability of climate models to simulate the bimodality of the water vapor distribution and determine whether the range in skill is of consequence in their representation of feedback processes under both climate variability and climate change.
- (6) Determine whether convection or cloud microphysics is playing a role in large-scale atmospheric circulation and therefore in controlling the humidity distribution. The successful AC approach for modeling water vapor distribution does not rule out the possibility of microphysical-induced changes in broadscale winds impacting moisture distribution, or therefore in water vapor feedback (Dessler and Minschwaner, 2007; Sherwood *et al.*, 2010b).
- (7) Better understand and model processes involved in the aggregation of tropical convection, its response to warming, and the impact on water vapor feedback of this change. If self-aggregation increases, this may weaken water vapor feedback due to the increased areas of tropical and subtropical radiative cooling and changes in high cloud shielding (Wing *et al.*, 2020). Multimodel comparisons to date have found that under SST warming the models were split roughly 50:50 on simulating increased or decreased self-aggregation. The use of a hierarchy of models in this project is a promising direction for understanding processes and sensitivities, but key questions remain regarding the reasons for model disagreement and the implications for water vapor feedback and climate sensitivity generally.
- (8) Better understanding of long-standing apparent disagreements between observed and modeled tropical lapse rate trends over recent decades. This includes better understanding of the differences in the observational datasets.
- (9) Improve understanding of stratospheric-tropospheric processes, including mechanisms for possible changes in lower stratospheric humidity under global warming. This requires improved observations of changes in stratospheric humidity, a better understanding of the effects of ozone and stratospheric water vapor feedback, and an understanding of how these processes are represented in models. Recent evidence is mixed. Kernel-based estimates from CMIP5 models diagnose a substantial positive feedback from stratospheric moisture increases, which, although substantially weaker than the tropospheric feedback, is nevertheless an important possible contributor to climate sensitivity, of the order of the strength of the surface albedo feedback in models (Banerjee *et al.*, 2019). However, contrary evidence has been found in a single model from a comparison of locked and unlocked stratospheric water vapor experiments, which suggested negligible additional surface warming (Huang, Wang, and Huang, 2020).
- (10) Test suggestions that there may be robust links between the magnitude of water vapor–lapse rate

feedbacks and cloud feedback across models (Huybers, 2010). Testing of such links and, where robust, an improved understanding of processes could shed light on both cloud feedbacks and water vapor–lapse rate feedbacks.

- (11) To explore beyond the linear feedback assumptions that are prevalent in much of the literature (Lahellec *et al.*, 2008; Knutti and Rugenstein, 2015). There is ample evidence of nonlinear evolution of feedbacks with warming and forcing, and understanding and quantifying these are important for increased confidence in future climate response (Knutti and Rugenstein, 2015). The issue will steadily become more important as global warming progresses later this century and beyond, and full use could be made of coordinated intercomparisons of long timescale, strongly forced scenarios (Rugenstein *et al.*, 2019).
- (12) Further clarify the role of feedbacks in high latitude amplification of warming. Although it is clear that lapse rate feedback is important, interactions are complex, with feedbacks operating at the TOA, within the atmospheric column, and at the surface. Some contributions, such as those from stratospheric water vapor, have received little consideration (Li and Newman, 2020). An overall unifying theory of the key processes would shed much light on polar amplification and the role of radiative feedbacks. As Russotto and Biasutti (2020) aptly pointed out, “A multi-GCM study perturbing all relevant feedbacks ... might help to resolve the disagreements over the causes of polar amplification obtained from limited GCM experiments and different diagnostic techniques.”

The focus of the research community in climate feedbacks over the past 10 to 15 years has moved to better understanding and constraining cloud feedback (Bony *et al.*, 2015; Sherwood *et al.*, 2020). This is due to an appreciation that differences in cloud feedbacks across models are large and responsible for much of the spread in the resulting climate sensitivity (Bony *et al.*, 2006, 2015). Nevertheless, significant issues remain unresolved in understanding and modeling water vapor and lapse rate feedbacks, and intermodel spread in the combined feedback is the second largest source of uncertainty in determining the value of the ECS (Dufresne and Bony, 2008); see Fig. 3. Given the magnitude of water vapor and lapse rate feedbacks and their fundamental role in projected climate change, it is imperative that they receive appropriate focus in the upcoming years.

#### LIST OF SYMBOLS AND ABBREVIATIONS

AC	Advection condensation
AIRS-MLS	Atmospheric Infrared Sounder– Microwave Limb Sounder
CERES	Clouds and the Earth’s Radiant Energy System
CMIP	Coupled Model Intercomparison Project
CRM	cloud resolving model

ECMWF	European Centre for Medium-Range Weather Forecasts
ECS	equilibrium climate sensitivity
ENSO	El Niño–Southern Oscillation
ERA	ECMWF reanalysis
GCM	global climate model
GHG	greenhouse gas
GPS	Global Positioning System
IPCC	Intergovernmental Panel on Climate Change
ITCZ	Intertropical Convergence Zone
JRA-25	Japanese 25-year Reanalysis
LGM	Last Glacial Maximum
LW	longwave (terrestrial) radiation
MJO	Madden-Julian oscillation
MERRA	Modern-Era Retrospective Analysis for Research and Applications
MSU/AMSU	microwave sounding unit/advanced microwave sounding unit
OLR	outgoing longwave radiation
PRP	partial radiation perturbation
RCM	radiative-convective model
SST	sea surface temperature
SW	shortwave (solar) radiation
TOA	top of atmosphere

#### ACKNOWLEDGMENTS

We thank Lily Gao for helpful searching, extraction, and management of papers, and assistance with Mendeley. Many thanks to Dr. David Jones, Dr. Sugata Narsey, and Dr. Scott Power for their careful review and helpful comments. We particularly acknowledge the thorough reviewing and constructive suggestions provided by three anonymous reviewers. R. C. was partially supported by funding from the Australian Government’s National Environmental Science Program. B. J. S. was supported by NASA Grant No. 80NSSC18K1032.

#### APPENDIX A: QUANTIFYING WATER VAPOR AND LAPSE RATE FEEDBACKS IN MODELS AND OBSERVATIONS

Major advances in quantifying feedbacks have been a key factor in the better understanding of feedbacks over the past three decades. These fall into several categories.

##### 1. TOA clear-sky radiation changes

The simplest method, and one long used, evaluates clear-sky changes under warming from the instantaneous zeroing of clouds prior to radiation calculations (Webb *et al.*, 2006). In the LW, this methodology provides a convolution of all temperature and LW water vapor responses (including the Planck response, water vapor, and lapse rate) and removes the sometimes large impact of cloud cover on these changes (Soden, Broccoli, and Hemler, 2004). In the SW it

is a convolution of SW water vapor impacts with surface albedo changes, again with the effect of clouds removed. Hence, these are not the radiation changes from the “true” feedbacks seen in the real world or by a GCM. The methodology can, however, be useful where limited fields are available from models or many models are being compared (Andrews, Gregory, and Webb, 2015). Most model simulations routinely archive the results of a cloud radiative effect calculation, whereby the radiation code is run once with all-sky conditions, then a second time with clouds removed, so the required analysis fields are widely available.

## 2. Partial radiative perturbation

A second, and much more accurate, approach, the PRP method, evaluates the radiative impact of feedbacks directly by performing instantaneous (perhaps daily) calculations within GCM radiation code, with water vapor and temperature changes swapped one by one between the climates under examination, e.g., the current climate and the future warmed climate (Wetherald and Manabe, 1988). Care must be taken because the field swapping introduces a radiation bias because of decorrelations between the variables (Colman and McAvaney, 1997; Schneider, Kirtman, and Lindzen, 1999; Klocke, Quaas, and Stevens, 2013), necessitating a second reverse swap from the current climate into the future, then a differencing of the results to remove this bias (Soden *et al.*, 2008). The PRP approach, despite having the advantage of high accuracy and a clear separation of feedback variables, has the downside of being extremely computationally and logistically intensive. There can also be significant interannual variability of the diagnosed strength of these feedbacks, with one study finding differences of 0.5–1.0 W m<sup>-2</sup> K<sup>-1</sup>, implying averaging periods of three and five years for accurate estimates of lapse rate and water vapor feedbacks, respectively (Klocke, Quaas, and Stevens, 2013). PRP has been used extensively for such studies as those regarding the responses to different forcings (Yoshimori and Broccoli, 2008), climate change under forcing scenarios (Colman, Fraser, and Rotstayn, 2001), and paleo experiments (Yoshimori, Yokohata, and Abe-Ouchi, 2009).

An extension beyond the PRP approach (the climate feedback-response analysis method) diagnoses all fluxes contributing to each of the traditional feedbacks (including water vapor and lapse rate), as represented by partial temperature change contributions at each point in latitude, longitude, and height including nonradiative processes such as dynamical changes and surface fluxes (Lu and Cai, 2009; Taylor *et al.*, 2013). Although this analysis differs from traditional feedback approaches, it has the advantage of providing well-defined fractional influences on temperature change from physical processes at each point in time and space, such as surface radiative contributions to amplified high latitude warming (Sejas and Cai, 2016).

## 3. Radiative kernels

A third approach that has become a standard methodology over the past decade is the use of radiative kernels (Soden and Held, 2006; Shell, Kiehl, and Shields, 2008; Soden *et al.*, 2008). This approach divides the total radiative response

$\lambda_x = (\partial R/\partial x)\partial x/\partial T_s$  into two terms: radiative transfer and climate response. The radiative transfer term is derived from one-sided PRP type calculations within a single model employing standardized perturbations on top of its base climate. Relevant to the evaluation of lapse rate and water vapor feedbacks are kernels derived from +1 K temperature increases with unchanged specific humidity, and with fixed relative humidity. These are then applied to other GCMs by multiplying the kernel by the temperature changes as a function of the height, latitude, and month found in that GCM (the climate response). Commonly kernels may be produced for both clear-sky and all-sky conditions, so as to study the impact of clouds on individual feedbacks. Details of the methodology were provided by Soden and Held (2006). This approach provides close approximations of the PRP methodology (Soden and Held, 2006) and permits a wide comparison of feedback strengths in GCMs, including those from multiple experiments such as perturbed parameter ensembles (Shell, Kiehl, and Shields, 2008; Sanderson, Shell, and Ingram, 2010). An important feature of radiative kernels is that they can also be used with observational or reanalysis data to provide estimates of radiative impacts from climate variability or change (Dessler, 2013; Colman and Hanson, 2013). The use of monthly means as field input, and the requirement for only a single forward calculation, make this an attractive alternative to PRP. A substantial number of kernels have been derived from different GCMs (Shell, Kiehl, and Shields, 2008; Soden *et al.*, 2008; Block and Mauritsen, 2013; Pendergrass, Conley, and Vitt, 2018; Smith *et al.*, 2018) and made widely available for research applications.

Owing to the state dependency of the kernels, if the climate moves far from the present (e.g., under much stronger CO<sub>2</sub> forcing, such as 4 × CO<sub>2</sub> or above), then the methodology leads to inaccuracies, necessitating recalculation of the kernels to a more appropriate, e.g., warmer, climate (Jonko *et al.*, 2012; Ceppi and Gregory, 2017).

An important approximation inherent in the methodology is that the kernels are calculated under the “climate” of one particular model and using a distinct radiation scheme from that of the GCM(s) being studied. Differing base model temperature, water vapor, and cloud climatologies between the kernel and the target GCM can result in different diagnosed radiative impact from temperature or water vapor changes to those seen in the original target GCM climate experiment (Soden *et al.*, 2008). A number of studies have found these effects to be relatively small, however (Soden *et al.*, 2008), and a recent study applying radiative kernels derived from six different GCMs found these effects to be unimportant overall in evaluating and comparing quantities such as global mean water vapor and lapse rate feedback (Zelinka *et al.*, 2020). It has been found that relatively high vertical resolution of the stratosphere may be needed to resolve temperature lapse rate or water vapor feedbacks in this region (Smith, Kramer, and Sima, 2020). Another issue when one uses kernels to estimate stratospheric changes in temperature and moisture is the need for the kernel to take into consideration rapid tropospheric temperature adjustments, as radiative affects are sensitive to these temperature changes (Maycock, Shine, and Joshi, 2011; Banerjee *et al.*, 2019).

#### 4. Cutting feedback loops

The three previous methods essentially represent postprocessing of GCM or observed results. A final approach has been to cut the feedback loop, i.e., isolate and suppress the radiative response from changes in water vapor and/or lapse rate in climate model experiments (Hall and Manabe, 1999, 2000a, 2000b; Schneider, Kirtman, and Lindzen, 1999; Langen, Graverson, and Mauritsen, 2012; Mauritsen *et al.*, 2013; Byrne and Zanna, 2020; Henry and Merlis, 2020). Comparing such decoupled experiments with standard model runs permits examination of the effect on associated physical processes and their response to the warming and cooling associated with the feedback. This has been shown to provide an extremely clean separation of feedbacks and to be in close agreement with PRP approaches. There needs, however, to be careful treatment of decorrelation issues between fields when calculating radiation, which affects both the unforced climate and the climate change in response to forcing (Mauritsen *et al.*, 2013). Using this approach Hall and Manabe (1999, 2000a, 2000b) directly demonstrated that water vapor

feedback amplifies not only climate change but also unforced natural variability in a coupled GCM. The method has also been useful for comparisons with observations in response to volcanic forcing (Soden *et al.*, 2002). This approach has also been used in a range of experiments examining the causes of high latitude amplification by systematically suppressing one or more feedback processes (Langen, Graverson, and Mauritsen, 2012; Henry and Merlis, 2020), the role of water vapor feedback in the seasonal shift in the ITCZ (Clark *et al.*, 2018), and the role of water vapor feedback in understanding the seasonal progression of the monsoon and its response to climate change (Byrne and Zanna, 2020).

#### APPENDIX B: EVALUATIONS OF WATER VAPOR AND LAPSE RATE FEEDBACKS

Table III shows a summary of estimates of water vapor and lapse rate feedbacks from the literature. Values are shown for water vapor (either LW alone or “net,” meaning LW+SW), lapse rate (LR), or combined water vapor and lapse rate (WV+LR), depending on availability from each source.

TABLE III. Summary of estimates of water vapor and lapse rate feedbacks from models and observations. SRES, Special Report on Emissions Scenarios (Nakicenovic *et al.*, 2000); RCP8.5, radiative concentration pathway scenario 8.5 (Van Vuuren *et al.*, 2011); LW, longwave component of the water vapor feedback only; net, LW + SW; LR, lapse rate feedback. The range of values shown is  $\pm 2\sigma$ .

Reference	Dataset(s)	Method	Value ( $\text{W m}^{-2} \text{K}^{-1}$ )
Cubasch and Cess (1990)	Cess <i>et al.</i> (1989) Raval and Ramanathan (1989).	Assessment from literature	1.2 (net)
Colman (2001)	RCMs and GCMs	Reported range in literature	$1.7 \pm 0.78$ (net) $-0.32 \pm 0.78$ (LR) $1.37 \pm 0.4$ (WV + LR)
Forster and Collins (2004)	Post-Mount Pinatubo cooling. NASA Water Vapor Project (NVAP), Microwave Limb Sounder (MLS)	Off-line radiation calculations on satellite moisture retrievals	1.6 (0.9–2.5) (net)
Soden and Held (2006)	CMIP2 models, climate projections	Kernels applied to CMIP2	$1.81 \pm 0.53$ (net) $-0.87 \pm 0.72$ (LR)
Soden and Held (2006)	CMIP3 models, climate projections	Kernels applied to CMIP3 SRES A1B	$1.80 \pm 0.36$ (net) $-0.84 \pm 0.52$ (LR)
Gordon <i>et al.</i> (2013)	AIRS sounder 2002–2009	Off-line radiative transfer model with observed water vapor distribution and CMIP3 model long-term: variability ratio	1.9–2.8 (net)
Dalton and Shell (2013)	CMIP3 Models over historical warming	Kernels	$1.79 \pm 0.26$ (LW)
Dalton and Shell (2013)	ERA-Interim (1989–2008)	Monthly variability scaled by model long-term:variability ratio	1.67 (0.48–1.91) (LW)
Koumoutsaris (2013)	CMIP3 models, climate projections	Kernels	$1.88 \pm 0.26$ (net) $-0.84 \pm 0.36$ (LR) $1.2 \pm 0.24$ (WV + LR)
Vial, Dufresne, and Bony (2013)	CMIP5 $4 \times \text{CO}_2$	Kernels (average of two used)	$1.65 \pm 0.28$ (net) $-0.60 \pm 0.40$ (LR) $1.05 \pm 0.11$ (WV + LR)
Boucher <i>et al.</i> (2013)	Multiple, including CMIP5 projections	Models and assessment of broad evidence	1.1 (0.92 to 1.3) (90% range)
Chung <i>et al.</i> (2014)	CMIP5 Historical experiments	Kernels applied to warming between 1979–1988 and 1989–1998.	$1.92 \pm 0.99$ (net)

(Table continued)

TABLE III. (Continued)

Reference	Dataset(s)	Method	Value ( $\text{W m}^{-2} \text{K}^{-1}$ )
Caldwell <i>et al.</i> (2016)	CMIP5 $4 \times \text{CO}_2$	Kernels	$1.70 \pm 0.36$ (net) $-0.55 \pm 0.50$ (LR)
Colman and Hanson (2017)	CMIP5 RCP 8.5	Kernels	$1.75 \pm 0.38$ (LW) $2.01 \pm 0.40$ (net) $-0.74 \pm 0.46$ (LR)
Colman and Hanson (2017)	CMIP5 $4 \times \text{CO}_2$	Kernels	$1.58 \pm 0.40$ (LW) $1.82 \pm 0.41$ (net) $-0.42 \pm 0.56$ (LR)
Liu <i>et al.</i> (2018)	AIRS-MLS	Interannual observed value scaled by model long-term:variability ratio	$1.85 \pm 0.32$ (net)
Zelinka <i>et al.</i> (2020)	CMIP5 $4 \times \text{CO}_2$	Kernels	$1.81 \pm 0.38$ (net) $-0.48 \pm 0.48$ (LR)
Zelinka <i>et al.</i> (2020)	CMIP6 $4 \times \text{CO}_2$	Kernels	$1.83 \pm 0.28$ (net) $-0.50 \pm 0.36$ (LR)
Sherwood <i>et al.</i> (2020)	Multiple, including CMIP5 and CMIP6	Assessment from the literature	$1.15 \pm 0.30$ (WV + LR)
Forster <i>et al.</i> (2021)	Multiple, including CMIP5 and CMIP6	Assessment from the literature	$1.80 \pm 0.52$ (net) $-0.5 \pm 0.4$ (LR) $1.30 \pm 0.2$ (WV + LR)

## REFERENCES

- Allan, R. P., 2004, "Simulation of the Earth's radiation budget by the European Centre for Medium-Range Weather Forecasts 40-year reanalysis (ERA40)," *J. Geophys. Res.* **109**, D18107.
- Allan, R. P., 2012, "The role of water vapour in Earth's energy flows," *Surv. Geophys.* **33**, 557–564.
- Allan, R. P., V. Ramaswamy, and A. Slingo, 2002, "Diagnostic analysis of atmospheric moisture and clear-sky radiative feedback in the Hadley Centre and Geophysical Fluid Dynamics Laboratory (GFDL) climate models," *J. Geophys. Res. Atmos.* **107**, ACL 4-1–ACL 4-7.
- Allan, R. P., M. A. Ringer, and A. Slingo, 2003, "Evaluation of moisture in the Hadley Centre climate model using simulations of HIRS water-vapour channel radiances," *Q. J. R. Meteorol. Soc.* **129**, 3371–3389.
- Allan, R. P., K. P. Shine, A. Slingo, and J. A. Pamment, 1999, "The dependence of clear-sky outgoing long-wave radiation on surface temperature and relative humidity," *Q. J. R. Meteorol. Soc.* **125**, 2103–2126.
- Allen, M. R., and W. J. Ingram, 2002, "Constraints on future changes in the hydrological cycle," *Nature (London)* **419**, 228–232.
- Andrews, T., and P. M. Forster, 2008, "CO<sub>2</sub> forcing induces semi-direct effects with consequences for climate feedback interpretations," *Geophys. Res. Lett.* **35**, L04802.
- Andrews, T., P. M. Forster, and J. M. Gregory, 2009, "A surface energy perspective on climate change," *J. Clim.* **22**, 2557–2570.
- Andrews, T., J. M. Gregory, and M. J. Webb, 2015, "The dependence of radiative forcing and feedback on evolving patterns of surface temperature change in climate models," *J. Clim.* **28**, 1630–1648.
- Andrews, T., and M. J. Webb, 2018, "The dependence of global cloud and lapse rate feedbacks on the spatial structure of tropical Pacific warming," *J. Clim.* **31**, 641–654.
- Armour, K. C., C. M. Bitz, and G. H. Roe, 2013, "Time-varying climate sensitivity from regional feedbacks," *J. Clim.* **26**, 4518–4534.
- Arrhenius, S., 1896, "XXXI. On the influence of carbonic acid in the air upon the temperature of the ground," *London Edinburgh Dublin Philos. Mag. J. Sci.* **41**, 237–276.
- Atwood, A. R., E. Wu, D. M. W. Frierson, D. S. Battisti, and J. P. Sachs, 2016, "Quantifying climate forcings and feedbacks over the last millennium in the CMIP5-PMIP3 models," *J. Clim.* **29**, 1161–1178.
- Banerjee, A., G. Chiodo, M. Previdi, M. Ponater, A. J. Conley, and L. M. Polvani, 2019, "Stratospheric water vapor: An important climate feedback," *Clim. Dyn.* **53**, 1697–1710.
- Baranov, Y. I., W. J. Lafferty, Q. Ma, and R. H. Tipping, 2008, "Water-vapor continuum absorption in the 800–1250 cm<sup>-1</sup> spectral region at temperatures from 311 to 363 K," *J. Quant. Spectrosc. Radiat. Transfer* **109**, 2291–2302.
- Bates, J. J., and D. L. Jackson, 1997, "A comparison of water vapor observations with AMIP1 simulations," *J. Geophys. Res. Atmos.* **102**, 21837–21852.
- Bates, J. J., and D. L. Jackson, 2001, "Trends in upper-tropospheric humidity," *Geophys. Res. Lett.* **28**, 1695–1698.
- Bates, J. J., D. L. Jackson, F.-M. Bréon, and Z. D. Bergen, 2001, "Variability of tropical upper tropospheric humidity 1979–1998," *J. Geophys. Res. Atmos.* **106**, 32271–32281.
- Berger, A., *et al.*, 1993, "Water vapour, CO<sub>2</sub> and insolation over the last glacial-interglacial cycles," *Phil. Trans. R. Soc. B* **341**, 253–261.
- Bitz, C. M., K. M. Shell, P. R. Gent, D. A. Bailey, G. Danabasoglu, K. C. Armour, M. M. Holland, and J. T. Kiehl, 2012, "Climate sensitivity of the community climate system model, version 4," *J. Clim.* **25**, 3053–3070.
- Blankenship, C. B., and T. T. Wilheit, 2001, "SSM/T-2 measurements of regional changes in three-dimensional water vapor fields during ENSO events," *J. Geophys. Res. Atmos.* **106**, 5239–5254.
- Block, K., and T. Mauritsen, 2013, "Forcing and feedback in the MPI-ESM-LR coupled model under abruptly quadrupled CO<sub>2</sub>," *J. Adv. Model. Earth Syst.* **5**, 676–691.
- Block, K., F. A. Schneider, J. Mülmenstädt, M. Salzmann, and J. Quaas, 2020, "Climate models disagree on the sign of total radiative feedback in the Arctic," *Tellus A* **72**, 1–14.
- Bode, H. W., 1945, *Network Analysis and Feedback Amplifier Design* (D. Van Nostrand, New York).

- Boé, J., A. Hall, and X. Qu, 2009, "September sea-ice cover in the Arctic Ocean projected to vanish by 2100," *Nat. Geosci.* **2**, 341–343.
- Boer, G. J., K. Hamilton, and W. Zhu, 2005, "Climate sensitivity and climate change under strong forcing," *Clim. Dyn.* **24**, 685–700.
- Bony, S., and K. A. Emanuel, 2005, "On the role of moist processes in tropical intraseasonal variability: Cloud-radiation and moisture-convection feedbacks," *J. Atmos. Sci.* **62**, 2770–2789.
- Bony, S., A. Semie, R. J. Kramer, B. Soden, A. M. Tompkins, and K. A. Emanuel, 2020, "Observed modulation of the tropical radiation budget by deep convective organization and lower-tropospheric stability," *Am. Geophys. Union Adv.* **1**, e2019AV000155.
- Bony, S., *et al.*, 2006, "How well do we understand and evaluate climate change feedback processes?," *J. Clim.* **19**, 3445–3482.
- Bony, S., *et al.*, 2015, "Clouds, circulation and climate sensitivity," *Nat. Geosci.* **8**, 261–268.
- Boucher, O., G. Myhre, and A. Myhre, 2004, "Direct human influence of irrigation on atmospheric water vapour and climate," *Clim. Dyn.* **22**, 597–603.
- Boucher, O., *et al.*, 2013, "Clouds and aerosols," in *Climate Change 2013: The Physical Science Basis. Contribution of Working Group I to the Fifth Assessment Report of the Intergovernmental Panel on Climate Change*, edited by T. F. Stocker, D. Qin, G.-K. Plattner, M. Tignor, S. K. Allen, J. Boschung, A. Nauels, Y. Xia, V. Bex, and P. M. Midgley (Cambridge University Press Cambridge, England), pp. 571–658.
- Bretherton, C. S., M. E. Peters, and L. E. Back, 2004, "Relationships between water vapor path and precipitation over the tropical oceans," *J. Clim.* **17**, 1517–1528.
- Brewer, A. W., 1949, "Evidence for a world circulation provided by the measurements of helium and water vapour distribution in the stratosphere," *Q. J. R. Meteorol. Soc.* **75**, 351–363.
- Brogniez, H., G. Clain, and R. Roca, 2015, "Validation of upper-tropospheric humidity from SAPHIR on board megha-tropiques using tropical soundings," *J. Appl. Meteorol. Climatol.* **54**, 896–908.
- Brogniez, H., and R. T. Pierrehumbert, 2006, "Using microwave observations to assess large-scale control of free tropospheric water vapor in the mid-latitudes," *Geophys. Res. Lett.* **33**, L14801.
- Brown, P. T., W. Li, J. H. Jiang, and H. Su, 2016, "Unforced surface air temperature variability and its contrasting relationship with the anomalous TOA energy flux at local and global spatial scales," *J. Clim.* **29**, 925–940.
- Brunt, D., 1932, "Notes on radiation in the atmosphere. I," *Q. J. R. Meteorol. Soc.* **58**, 389–420.
- Butler, A. H., D. W. J. Thompson, and R. Heikes, 2010, "The steady-state atmospheric circulation response to climate change-like thermal forcings in a simple general circulation model," *J. Clim.* **23**, 3474–3496.
- Byrne, M. P., and P. A. O’Gorman, 2013, "Link between land-ocean warming contrast and surface relative humidities in simulations with coupled climate models," *Geophys. Res. Lett.* **40**, 5223–5227.
- Byrne, M. P., and P. A. O’Gorman, 2016, "Understanding decreases in land relative humidity with global warming: Conceptual model and GCM simulations," *J. Clim.* **29**, 9045–9061.
- Byrne, M. P., and L. Zanna, 2020, "Radiative effects of clouds and water vapor on an axisymmetric monsoon," *J. Clim.* **33**, 8789–8811.
- Caballero, R., and M. Huber, 2013, "State-dependent climate sensitivity in past warm climates and its implications for future climate projections," *Proc. Natl. Acad. Sci. U.S.A.* **110**, 14162–14167.
- Caldwell, P. M., M. D. Zelinka, K. E. Taylor, and K. Marvel, 2016, "Quantifying the sources of intermodel spread in equilibrium climate sensitivity," *J. Clim.* **29**, 513–524.
- Ceppi, P., F. Brient, M. D. Zelinka, and D. L. Hartmann, 2017, "Cloud feedback mechanisms and their representation in global climate models," *Wiley Interdiscip. Rev. Clim. Change* **8**, e465.
- Ceppi, P., and J. M. Gregory, 2017, "Relationship of tropospheric stability to climate sensitivity and Earth’s observed radiation budget," *Proc. Natl. Acad. Sci. U.S.A.* **114**, 13126–13131.
- Ceppi, P., and J. M. Gregory, 2019, "A refined model for the Earth’s global energy balance," *Clim. Dyn.* **53**, 4781–4797.
- Cess, R. D., 1975, "Global climate change: An investigation of atmospheric feedback mechanisms," *Tellus* **27**, 193–198.
- Cess, R. D., 2005, "Water vapor feedback in climate models," *Science* **310**, 795–796.
- Cess, R. D., *et al.*, 1989, "Interpretation of cloud-climate feedback as produced by 14 atmospheric general circulation models," *Science* **245**, 513–516.
- Chamberlin, T. C., 1899, "An attempt to frame a working hypothesis of the cause of glacial periods on an atmospheric basis," *J. Geol.* **7**, 751–787.
- Chambers, L. H., B. Lin, and D. F. Young, 2002, "Examination of new CERES data for evidence of tropical iris feedback," *J. Clim.* **15**, 3719–3726.
- Charney, J. G., *et al.*, 1979, *Carbon Dioxide And Climate: A Scientific Assessment* (National Academies Press, Washington, DC).
- Chung, E., B. Soden, B. J. Sohn, and L. Shi, 2014, "Upper-tropospheric moistening in response to anthropogenic warming," *Proc. Natl. Acad. Sci. U.S.A.* **111**, 11636–11641.
- Chung, E.-S., D. Yeomans, and B. J. Soden, 2010, "An assessment of climate feedback processes using satellite observations of clear-sky OLR," *Geophys. Res. Lett.* **37**, L02702.
- Clark, S. K., Y. Ming, I. M. Held, and P. J. Philipps, 2018, "The role of the water vapor feedback in the ITCZ response to hemispherically asymmetric forcings," *J. Clim.* **31**, 3659–3678.
- Clough, S. A., F. X. Kneizys, and R. W. Davies, 1989, "Line shape and the water vapor continuum," *Atmos. Res.* **23**, 229–241.
- Collins, M., B. B. Booth, G. R. Harris, J. M. Murphy, D. M. H. Sexton, and M. J. Webb, 2006, "Towards quantifying uncertainty in transient climate change," *Clim. Dyn.* **27**, 127–147.
- Collins, M., *et al.*, 2013, "Long-term climate change: Projections, commitments and irreversibility," in *Climate Change 2013: The Physical Science Basis. Contribution of Working Group I to the Fifth Assessment Report of the Intergovernmental Panel on Climate Change*, edited by T. F. Stocker, D. Qin, G.-K. Plattner, M. Tignor, S. K. Allen, J. Boschung, A. Nauels, Y. Xia, V. Bex, and P. M. Midgley (Cambridge University Press Cambridge, England), pp. 1029–1076.
- Colman, R., 2001, "On the vertical extent of atmospheric feedbacks," *Clim. Dyn.* **17**, 391–405.
- Colman, R., 2003a "A comparison of climate feedbacks in general circulation models," *Clim. Dyn.* **20**, 865–873.
- Colman, R., 2003b "Seasonal contributions to climate feedbacks," *Clim. Dyn.* **20**, 825–841.
- Colman, R., 2004, "On the structure of water vapour feedbacks in climate models," *Geophys. Res. Lett.* **31**, L21109.
- Colman, R., 2015, "Climate radiative feedbacks and adjustments at the Earth’s surface," *J. Geophys. Res. Atmos.* **120**, 3173–3182.
- Colman, R., J. R. Brown, C. Franklin, L. Hanson, H. Ye, and M. D. Zelinka, 2019, "Evaluating cloud feedbacks and rapid responses in the ACCESS model," *J. Geophys. Res. Atmos.* **124**, 2018JD029189.

- Colman, R., J. Fraser, and L. Rotstayn, 2001, "Climate feedbacks in a general circulation model incorporating prognostic clouds," *Clim. Dyn.* **18**, 103–122.
- Colman, R., and L. Hanson, 2013, "On atmospheric radiative feedbacks associated with climate variability and change," *Clim. Dyn.* **40**, 475–492.
- Colman, R., and L. Hanson, 2017, "On the relative strength of radiative feedbacks under climate variability and change," *Clim. Dyn.* **49**, 2115–2129.
- Colman, R., and B. J. McAvaney, 1997, "A study of general circulation model climate feedbacks determined from perturbed sea surface temperature experiments," *J. Geophys. Res. Atmos.* **102**, 19383–19402.
- Colman, R., and B. J. McAvaney, 2009, "Climate feedbacks under a very broad range of forcing," *Geophys. Res. Lett.* **36**, L01702.
- Colman, R., and B. J. McAvaney, 2011, "On tropospheric adjustment to forcing and climate feedbacks," *Clim. Dyn.* **36**, 1649–1658.
- Colman, R., and S. B. Power, 2018, "What can decadal variability tell us about climate feedbacks and sensitivity?," *Clim. Dyn.* **51**, 3815–3828.
- Colman, R., and S. B. Power, 2010, "Atmospheric radiative feedbacks associated with transient climate change and climate variability," *Clim. Dyn.* **34**, 919–933.
- Cronin, T. W., 2020, "How well do we understand the Planck feedback?," in *Proceedings of the AGU Fall Meeting 2020*, <https://agu.confex.com/agu/fm20/meetingapp.cgi/Paper/756253>.
- Cronin, T. W., and M. F. Jansen, 2016, "Analytic radiative-advective equilibrium as a model for high-latitude climate," *Geophys. Res. Lett.* **43**, 449–457.
- Crook, J. A., P. M. Forster, and N. Stuber, 2011, "Spatial patterns of modeled climate feedback and contributions to temperature response and polar amplification," *J. Clim.* **24**, 3575–3592.
- Crucifix, M., 2006, "Does the last glacial maximum constrain climate sensitivity?," *Geophys. Res. Lett.* **33**, L18701.
- Cubasch, U., and R. D. Cess, 1990, "Processes and modelling," in *Climate Change: The IPCC Scientific Assessment*, edited by J. T. Houghton, G. J. Jenkins, and J. J. Ephraums (Cambridge University Press, Cambridge, England), pp. 69–72.
- Curry, J. A., J. L. Schramm, M. C. Serreze, and E. E. Ebert, 1995, "Water vapor feedback over the Arctic Ocean," *J. Geophys. Res.* **100**, 14223.
- Dacie, S., L. Kluft, H. Schmidt, B. Stevens, S. A. Buehler, P. J. Nowack, S. Dietmüller, N. L. Abraham, and T. Birner, 2019, "A 1D RCE study of factors affecting the tropical tropopause layer and surface climate," *J. Clim.* **32**, 6769–6782.
- Dai, A., J. Wang, P. W. Thorne, D. E. Parker, L. Haimberger, and X. L. Wang, 2011, "A new approach to homogenize daily radiosonde humidity data," *J. Clim.* **24**, 965–991.
- Dalton, M. M., and K. M. Shell, 2013, "Comparison of short-term and long-term radiative feedbacks and variability in twentieth-century global climate model simulations," *J. Clim.* **26**, 10051–10070.
- DeAngelis, A. M., X. Qu, M. D. Zelinka, and A. Hall, 2015, "An observational radiative constraint on hydrologic cycle intensification," *Nature (London)* **528**, 249–253.
- Dee, D. P., *et al.*, 2011, "The ERA-interim reanalysis: Configuration and performance of the data assimilation system," *Q. J. R. Meteorol. Soc.* **137**, 553–597.
- Dekker, E., R. Bintanja, and C. Severijns, 2019, "Nudging the Arctic Ocean to quantify sea ice feedbacks," *J. Clim.* **32**, 2381–2395.
- Del Genio, A. D., 2002, "The dust settles on water vapor feedback," *Science* **296**, 665–666.
- Del Genio, A. D., and W. Kovari, 2002, "Climatic properties of tropical precipitating convection under varying environmental conditions," *J. Clim.* **15**, 2597–2615.
- Dessler, A. E., 2013, "Observations of climate feedbacks over 2000–10 and comparisons to climate models," *J. Clim.* **26**, 333–342.
- Dessler, A. E., 2020, "Potential problems measuring climate sensitivity from the historical record," *J. Clim.* **33**, 2237–2248.
- Dessler, A. E., and S. M. Davis, 2010, "Trends in tropospheric humidity from reanalysis systems," *J. Geophys. Res.* **115**, D19127.
- Dessler, A. E., E. J. Hints, E. M. Weinstock, J. G. Anderson, and K. R. Chan, 1995, "Mechanisms controlling water vapor in the lower stratosphere: A tale of two stratospheres," *J. Geophys. Res. Atmos.* **100**, 23167–23172.
- Dessler, A. E., T. Mauritsen, and B. Stevens, 2018, "The influence of internal variability on Earth's energy balance framework and implications for estimating climate sensitivity," *Atmos. Chem. Phys.* **18**, 5147–5155.
- Dessler, A. E., and K. Minschwaner, 2007, "An analysis of the regulation of tropical tropospheric water vapor," *J. Geophys. Res. Atmos.* **112**, D10120.
- Dessler, A. E., M. R. Schoeberl, T. Wang, S. M. Davis, and K. H. Rosenlof, 2013, "Stratospheric water vapor feedback," *Proc. Natl. Acad. Sci. U.S.A.* **110**, 18087–18091.
- Dessler, A. E., and S. C. Sherwood, 2000, "Simulations of tropical upper tropospheric humidity," *J. Geophys. Res. Atmos.* **105**, 20155–20163.
- Dessler, A. E., and S. Wong, 2009, "Estimates of the water vapor climate feedback during el Niño–Southern Oscillation," *J. Clim.* **22**, 6404–6412.
- Dessler, A. E., Z. Zhang, and P. Yang, 2008, "Water-vapor climate feedback inferred from climate fluctuations, 2003–2008," *Geophys. Res. Lett.* **35**, L20704.
- Dickinson, R. E., V. Meleshko, D. Randall, E. Sarachik, P. Silva-Dias, and A. Slingo, 1995, "Climate processes," in *Climate Change 1995: The Science of Climate Change. Contribution of Working Group I to the Second Assessment Report of the Intergovernmental Panel on Climate Change*, edited by J. T. Houghton, L. G. Meiro Filho, B. A. Callander, N. Harris, A. Kattenburg, and K. Maskell (Cambridge University Press, Cambridge, England).
- Döscher, R., T. Vihma, and E. Maksimovich, 2014, "Recent advances in understanding the Arctic climate system state and change from a sea ice perspective: A review," *Atmos. Chem. Phys.* **14**, 13571–13600.
- Dufresne, J.-L., and S. Bony, 2008, "An assessment of the primary sources of spread of global warming estimates from coupled atmosphere/ocean models," *J. Clim.* **21**, 5135–5144.
- Durre, I., C. N. Williams, X. Yin, and R. S. Vose, 2009, "Radiosonde-based trends in precipitable water over the Northern Hemisphere: An update," *J. Geophys. Res. Atmos.* **114**, D05112.
- Emanuel, K. A., and R. T. Pierrehumbert, 1996, "Microphysical and dynamical control of tropospheric water vapor," in *Clouds, Chemistry and Climate*, edited by P. J. Crutzen and V. Ramanathan, NATO Advanced Study Institutes, Ser. I, Vol. 35 (Springer, Berlin), pp. 17–28.
- Emanuel, K. A., and M. Živković-Rothman, 1999, "Development and evaluation of a convection scheme for use in climate models," *J. Atmos. Sci.* **56**, 1766–1782.
- Eyring, V., S. Bony, G. A. Meehl, C. A. Senior, B. Stevens, R. J. Stouffer, and K. E. Taylor, 2016, "Overview of the Coupled Model Intercomparison Project phase 6 (CMIP6) experimental design and organization," *Geosci. Model Dev.* **9**, 1937–1958.
- Fasullo, J. T., 2010, "Robust land-ocean contrasts in energy and water cycle feedbacks," *J. Clim.* **23**, 4677–4693.

- Feldl, N., B. T. Anderson, and S. Bordoni, 2017, "Atmospheric eddies mediate lapse rate feedback and arctic amplification," *J. Clim.* **30**, 9213–9224.
- Feldl, N., S. Bordoni, and T. M. Merlis, 2017, "Coupled high-latitude climate feedbacks and their impact on atmospheric heat transport," *J. Clim.* **30**, 189–201.
- Feldl, N., and G. H. Roe, 2013, "The nonlinear and nonlocal nature of climate feedbacks," *J. Clim.* **26**, 8289–8304.
- Ferraro, A. J., F. H. Lambert, M. Collins, and G. M. Miles, 2015, "Physical mechanisms of tropical climate feedbacks investigated using temperature and moisture trends," *J. Clim.* **28**, 8968–8987.
- Flannaghan, T. J., S. Fueglistaler, I. M. Held, S. Po-Chedley, B. Wyman, and M. Zhao, 2014, "Tropical temperature trends in atmospheric general circulation model simulations and the impact of uncertainties in observed SSTs," *J. Geophys. Res. Atmos.* **119**, 13327–13337.
- Flato, G., *et al.*, 2013, "Evaluation of climate models," in *Climate Change 2013: The Physical Science Basis. Contribution of Working Group I to the Fifth Assessment Report of the Intergovernmental Panel on Climate Change*, edited by T. F. Stocker, D. Qin, G.-K. Plattner, M. Tignor, S. K. Allen, J. Boschung, A. Nauels, Y. Xia, V. Bex, and P. M. Midgley (Cambridge University Press, Cambridge, England), pp. 741–866.
- Fleming, J. R., 1998, "Introduction: Apprehending climate change," in *Historical Perspectives on Climate Change* (Oxford University Press, New York).
- Folkens, I., K. K. Kelly, and E. M. Weinstock, 2002, "A simple explanation for the increase in relative humidity between 11 and 14 km in the tropics," *J. Geophys. Res. Atmos.* **107**, ACL 26-1–ACL 26-7.
- Folkens, I., and R. V. Martin, 2005, "The vertical structure of tropical convection and its impact on the budgets of water vapor and ozone," *J. Atmos. Sci.* **62**, 1560–1573.
- Forster, P. M. de F., *et al.*, 2007, "Changes in atmospheric constituents and in radiative forcing," in *Climate Change 2007: The Physical Science Basis. Contribution of Working Group I to the Fourth Assessment Report of the Intergovernmental Panel on Climate Change*, edited by S. Solomon *et al.* (Cambridge University Press, Cambridge, England).
- Forster, P. M. de F., and M. Collins, 2004, "Quantifying the water vapour feedback associated with post-Pinatubo global cooling," *Clim. Dyn.* **23**, 207–214.
- Forster, P. M. de F., and K. P. Shine, 1999, "Stratospheric water vapour changes as a possible contributor to observed stratospheric cooling," *Geophys. Res. Lett.* **26**, 3309–3312.
- Forster, P. M. de F., *et al.*, 2021, "The Earth's energy budget, climate feedbacks, and climate sensitivity," in *Climate Change 2021: The Physical Science Basis. Contribution of Working Group I to the Sixth Assessment Report of the Intergovernmental Panel on Climate Change*, edited by V. Masson-Delmotte *et al.* (Cambridge University Press, Cambridge, England), Chap. 7.
- Fourier, J. B. J., 1827, "On the temperatures of the terrestrial sphere and interplanetary space," *Mem. Acad. R. Sci. Inst. Fr.* **7**, 570–604.
- Frierson, D. M. W., 2006, "Robust increases in midlatitude static stability in simulations of global warming," *Geophys. Res. Lett.* **33**, L24816.
- Fu, Q., M. Baker, and D. L. Hartmann, 2002, "Tropical cirrus and water vapor: An effective Earth infrared iris feedback?," *Atmos. Chem. Phys.* **2**, 31–37.
- Fu, Q., S. Manabe, and C. M. Johanson, 2011, "On the warming in the tropical upper troposphere: Models versus observations," *Geophys. Res. Lett.* **38**, L15704.
- Fueglistaler, S., C. Radley, and I. M. Held, 2015, "The distribution of precipitation and the spread in tropical upper tropospheric temperature trends in CMIP5/AMIP simulations," *Geophys. Res. Lett.* **42**, 6000–6007.
- Fujiwara, M., *et al.*, 2017, "Introduction to the SPARC Reanalysis Intercomparison Project (S-RIP) and overview of the reanalysis systems," *Atmos. Chem. Phys.* **17**, 1417–1452.
- Gaffen, D. J., R. D. Rosen, D. A. Salstein, and J. S. Boyle, 1997, "Evaluation of tropospheric water vapor simulations from the Atmospheric Model Intercomparison Project," *J. Clim.* **10**, 1648–1661.
- Galewsky, J., A. Sobel, and I. Held, 2005, "Diagnosis of subtropical humidity dynamics using tracers of last saturation," *J. Atmos. Sci.* **62**, 3353–3367.
- Gates, W. L., J. F. B. Mitchell, G. J. Boer, U. Cubasch, and V. P. Meleshko, 1992, "Climate modelling, climate prediction and model validation," in *Climate Change 1992: The Supplementary Report to the Intergovernmental Panel on Climate Change Scientific Assessment*, edited by J. T. Houghton, B. A. Callander, and S. K. Varney (Cambridge University Press, Cambridge, England).
- Gettelman, A., 2012, "The evolution of climate sensitivity and climate feedbacks in the community atmosphere model," *J. Clim.* **25**, 1453–1469.
- Gettelman, A., and Q. Fu, 2008, "Observed and simulated upper-tropospheric water vapor feedback," *J. Clim.* **21**, 3282–3289.
- Gettelman, A., J. R. Holton, and A. R. Douglass, 2000, "Simulations of water vapor in the lower stratosphere and upper troposphere," *J. Geophys. Res. Atmos.* **105**, 9003–9023.
- Gettelman, A., *et al.*, 2009, "The tropical tropopause layer 1960–2100," *Atmos. Chem. Phys.* **9**, 1621–1637.
- Gettelman, A., *et al.*, 2010, "Multimodel assessment of the upper troposphere and lower stratosphere: Tropics and global trends," *J. Geophys. Res.* **115**, D00M08.
- Ghatak, D., and J. Miller, 2013, "Implications for Arctic amplification of changes in the strength of the water vapor feedback," *J. Geophys. Res. Atmos.* **118**, 7569–7578.
- Goody, R. M., and G. D. Robinson, 1951, "Radiation in the troposphere and lower stratosphere," *Q. J. R. Meteorol. Soc.* **77**, 151–187.
- Gordon, N. D., A. K. Jonko, P. M. Forster, and K. M. Shell, 2013, "An observationally based constraint on the water-vapor feedback," *J. Geophys. Res. Atmos.* **118**, 12435–12443.
- Graversen, R. G., and M. Wang, 2009, "Polar amplification in a coupled climate model with locked albedo," *Clim. Dyn.* **33**, 629–643.
- Graversen, R. G., P. L. Langen, and T. Mauritsen, 2014a, "Polar amplification in CCSM4: Contributions from the lapse rate and surface albedo feedbacks," *J. Clim.* **27**, 4433–4450.
- Graversen, R. G., P. Langen, and T. Mauritsen, 2014b, "The lapse-rate feedback leads to polar temperature amplification," *Geophys. Res. Abstr.* **16**, 14551, <http://meetingorganizer.copernicus.org/EGU2014/EGU2014-14551.pdf>.
- Gregory, J., and M. Webb, 2008, "Tropospheric adjustment induces a cloud component in CO<sub>2</sub> forcing," *J. Clim.* **21**, 58–71.
- Gregory, J. M., T. Andrews, and P. Good, 2015, "The inconstancy of the transient climate response parameter under increasing CO<sub>2</sub>," *Phil. Trans. R. Soc. A* **373**, 20140417.
- Grose, M. R., J. Gregory, R. Colman, and T. Andrews, 2018, "What climate sensitivity index is most useful for projections?," *Geophys. Res. Lett.* **45**, 1559–1566.
- Guichard, F., and F. Couvreur, 2017, "A short review of numerical cloud-resolving models," *Tellus A* **69**, 1373578.
- Hahn, L. C., K. C. Armour, D. S. Battisti, A. Donohoe, A. G. Pauling, and C. M. Bitz, 2020, "Antarctic elevation drives hemispheric asymmetry in polar lapse rate climatology and feedback," *Geophys. Res. Lett.* **47**, 1–10.

- Hall, A., 2004, "The role of surface albedo feedback in climate," *J. Clim.* **17**, 1550–1568.
- Hall, A., and S. Manabe, 1999, "The role of water vapor feedback in unperturbed climate variability and global warming," *J. Clim.* **12**, 2327–2346.
- Hall, A., and S. Manabe, 2000a, "Suppression of ENSO in a coupled model without water vapor feedback," *Clim. Dyn.* **16**, 393–403.
- Hall, A., and S. Manabe, 2000b, "Effect of water vapor feedback on internal and anthropogenic variations of the global hydrologic cycle," *J. Geophys. Res. Atmos.* **105**, 6935–6944.
- Hallegatte, S., A. Lahellec, and J.-Y. Grandpeix, 2006, "An elicitation of the dynamic nature of water vapor feedback in climate change using a 1D model," *J. Atmos. Sci.* **63**, 1878–1894.
- Hansen, J., A. Lacis, D. Rind, G. Russell, P. Stone, I. Fung, R. Ruedy, and J. Lerner, 1984, "Climate sensitivity: Analysis of feedback mechanisms," in *Climate Processes and Climate Sensitivity*, edited by J. E. Hansen and T. Takahashi, AGU Geophysical Monograph 29, Maurice Ewing Vol. 5 (American Geophysical Union, Washington, DC), pp. 130–163.
- Hansen, J., M. Sato, P. Kharecha, D. Beerling, R. Berner, V. Masson-Delmotte, M. Pagani, M. Raymo, D. L. Royer, and J. C. Zachos, 2008, "Target atmospheric CO<sub>2</sub>: Where should humanity aim?," *Open Atmos. Sci. J.* **2**, 217–231.
- Hartmann, D. L., and K. Larson, 2002, "An important constraint on tropical cloud–climate feedback," *Geophys. Res. Lett.* **29**, 12–14.
- Hartmann, D. L., and M. L. Michelsen, 2002, "No evidence for iris," *Bull. Am. Meteorol. Soc.* **83**, 249–254.
- Hartmann, D. L., *et al.*, 2013, "Observations: Atmosphere and surface," in *Climate Change 2013: The Physical Science Basis. Contribution of Working Group I to the Fifth Assessment Report of the Intergovernmental Panel on Climate Change*, edited by T. F. Stocker, D. Qin, G.-K. Plattner, M. Tignor, S. K. Allen, J. Boschung, A. Nauels, Y. Xia, V. Bex, and P. M. Midgley (Cambridge University Press, Cambridge, England), pp. 159–254.
- Hasumi, H., and S. Emori, 2004, Eds., "K-1 coupled GCM (MIROC) description," K-1 Technical Report No. 1, [https://ccsr.aori.u-tokyo.ac.jp/~hasumi/miroc\\_description.pdf](https://ccsr.aori.u-tokyo.ac.jp/~hasumi/miroc_description.pdf).
- He, H., R. J. Kramer, and B. Soden, 2021, "Constraining the intermodel spread in cloud and water vapor feedback," <https://doi.org/10.1002/essoar.10506101.1>.
- Hegerl, G. C., F. W. Zwiers, P. Braconnot, N. P. Gillett, Y. Luo, J. A. Marengo Orsini, N. Nicholls, J. E. Penner, and P. A. Stott, 2007, "Understanding and attributing climate change," in *Climate Change 2007: The Physical Science Basis. Contribution of Working Group I to the Fourth Assessment Report of the Intergovernmental Panel on Climate Change*, edited by S. Solomon *et al.* (Cambridge University Press, Cambridge, England), pp. 663–746.
- Heglin, M. I., *et al.*, 2014, "Vertical structure of stratospheric water vapour trends derived from merged satellite data," *Nat. Geosci.* **7**, 768–776.
- Heinze, C., *et al.*, 2019, "ESD reviews: Climate feedbacks in the Earth system and prospects for their evaluation," *Earth Syst. Dyn.* **10**, 379–452.
- Held, I. M., and K. M. Shell, 2012, "Using relative humidity as a state variable in climate feedback analysis," *J. Clim.* **25**, 2578–2582.
- Held, I. M., and B. J. Soden, 2000, "Water vapor feedback and global warming," *Annu. Rev. Energy Environ.* **25**, 441–475.
- Held, I. M., and B. J. Soden, 2006, "Robust responses of the hydrological cycle to global warming," *J. Clim.* **19**, 5686–5699.
- Hendon, H. H., and M. L. Salby, 1994, "The life cycle of the Madden-Julian oscillation," *J. Atmos. Sci.* **51**, 2225–2237.
- Henry, M., and T. M. Merlis, 2019, "The role of the nonlinearity of the Stefan-Boltzmann law on the structure of radiatively forced temperature change," *J. Clim.* **32**, 335–348.
- Henry, M., and T. M. Merlis, 2020, "Forcing dependence of atmospheric lapse rate changes dominates residual polar warming in solar radiation management climate scenarios," *Geophys. Res. Lett.* **47**, e2020GL087929.
- Ho, S.-P., L. Peng, C. Mears, and R. A. Anthes, 2018, "Comparison of global observations and trends of total precipitable water derived from microwave radiometers and COSMIC radio occultation from 2006 to 2013," *Atmos. Chem. Phys.* **18**, 259–274.
- Holland, M. M., and C. M. Bitz, 2003, "Polar amplification of climate change in coupled models," *Clim. Dyn.* **21**, 221–232.
- Holloway, C. E., and J. D. Neelin, 2009, "Moisture vertical structure, column water vapor, and tropical deep convection," *J. Atmos. Sci.* **66**, 1665–1683.
- Hu, H., 1996, "Water vapor and temperature lapse rate feedbacks in the mid-latitude seasonal cycle," *Geophys. Res. Lett.* **23**, 1761–1764.
- Hu, X., *et al.*, 2017, "Inter-model warming projection spread: Inherited traits from control climate diversity," *Sci. Rep.* **7**, 1–8.
- Huang, Y., V. Ramaswamy, and B. Soden, 2007, "An investigation of the sensitivity of the clear-sky outgoing longwave radiation to atmospheric temperature and water vapor," *J. Geophys. Res. Atmos.* **112**, D05104.
- Huang, Y., Y. Wang, and H. Huang, 2020, "Stratospheric water vapor feedback disclosed by a locking experiment," *Geophys. Res. Lett.* **47**, e2020GL087987, [https://agupubs.onlinelibrary.wiley.com/doi/full/10.1029/2020GL087987?casa\\_token=-7ibF5OWLhkAAAAA%3AsKhXmSKZjebbkQF43B4wiHIVPK2ypumfyW-uLridIakJDzfAjZ9JWm1B6Ui4i0ILHCPobKNPX1D1Ay4](https://agupubs.onlinelibrary.wiley.com/doi/full/10.1029/2020GL087987?casa_token=-7ibF5OWLhkAAAAA%3AsKhXmSKZjebbkQF43B4wiHIVPK2ypumfyW-uLridIakJDzfAjZ9JWm1B6Ui4i0ILHCPobKNPX1D1Ay4).
- Huang, Y., M. Zhang, Y. Xia, Y. Hu, and S.-W. Son, 2016, "Is there a stratospheric radiative feedback in global warming simulations?," *Clim. Dyn.* **46**, 177–186.
- Hurley, J. V., and J. Galewsky, 2010, "A last saturation analysis of ENSO humidity variability in the subtropical Pacific," *J. Clim.* **23**, 918–931.
- Hurst, D. F., S. J. Oltmans, H. Vömel, K. H. Rosenlof, S. M. Davis, E. A. Ray, E. G. Hall, and A. F. Jordan, 2011, "Stratospheric water vapor trends over Boulder, Colorado: Analysis of the 30 year Boulder record," *J. Geophys. Res.* **116**, D02306.
- Huybers, P., 2010, "Compensation between model feedbacks and curtailment of climate sensitivity," *J. Clim.* **23**, 3009–3018.
- Hwang, J., Y.-S. Choi, W. Kim, H. Su, and J. H. Jiang, 2018, "Observational estimation of radiative feedback to surface air temperature over northern high latitudes," *Clim. Dyn.* **50**, 615–628.
- Hwang, Y.-T., D. M. W. Frierson, and J. E. Kay, 2011, "Coupling between Arctic feedbacks and changes in poleward energy transport," *Geophys. Res. Lett.* **38**, L17704.
- Inamdar, A. K., and V. Ramanathan, 1998, "Tropical and global scale interactions among water vapor, atmospheric greenhouse effect, and surface temperature," *J. Geophys. Res. Atmos.* **103**, 32177–32194.
- Inamdar, A. K., V. Ramanathan, and N. G. Loeb, 2004, "Satellite observations of the water vapor greenhouse effect and column longwave cooling rates: Relative roles of the continuum and vibration-rotation to pure rotation bands," *J. Geophys. Res. Atmos.* **109**, D06104.
- Ingram, W., 2010, "A very simple model for the water vapour feedback on climate change," *Q. J. R. Meteorol. Soc.* **136**, 30–40.
- Ingram, W., 2013a, "A new way of quantifying GCM water vapour feedback," *Clim. Dyn.* **40**, 913–924.

- Ingram, W., 2013b “Some implications of a new approach to the water vapour feedback,” *Clim. Dyn.* **40**, 925–933.
- Ingram, W. J., 2002, “On the robustness of the water vapor feedback: GCM vertical resolution and formulation,” *J. Clim.* **15**, 917–921.
- Ingram, W. J., 2012, “Water vapor feedback in a small ensemble of GCMs: Two approaches,” *J. Geophys. Res. Atmos.* **117**, 1–10.
- InterAcademy Council, 2010, “Climate change assessments: Review of the processes and procedures of the IPCC,” report, [https://archive.ipcc.ch/pdf/IAC\\_report/IAC%20Report.pdf](https://archive.ipcc.ch/pdf/IAC_report/IAC%20Report.pdf).
- Intergovernmental Panel on Climate Change, 1999, *Aviation and the Global Atmosphere* (Cambridge University Press, Cambridge, England).
- Intergovernmental Panel on Climate Change, 2013, *Climate Change 2013: The Physical Science Basis* (Cambridge University Press, Cambridge, England).
- Intergovernmental Panel on Climate Change, 2014, *Climate Change 2014: Impacts, Adaptation and Vulnerability* (Cambridge University Press, Cambridge, England).
- Intergovernmental Panel on Climate Change, 2019, “Special report on the ocean and cryosphere in a changing climate,” IPCC report, edited by H.-O. Pörtner *et al.*, <https://www.ipcc.ch/srocc/>.
- Intergovernmental Panel on Climate Change, 2021, “*Climate Change 2021: The Physical Science Basis. Contribution of Working Group I to the Sixth Assessment Report of the Intergovernmental Panel on Climate Change*,” edited by V. Masson-Delmotte *et al.* (Cambridge University Press, Cambridge, England).
- Jackson, D. L., and B. J. Soden, 2007, “Detection and correction of diurnal sampling bias in HIRS/2 brightness temperatures,” *J. Atmos. Oceanic Technol.* **24**, 1425–1438.
- Jeevanjee, N., 2018, “The physics of climate change: Simple models in climate science,” arXiv:1802.02695.
- Jeevanjee, N., N. Lutsko, and D. Koll, 2021, “Simpson’s law and the spectral cancellation of climate feedbacks,” *Earth Space Sci. Open Arch.*, <https://doi.org/10.1002/essoar.10506744.1>.
- Jensen, E. J., *et al.*, 2005, “Ice supersaturations exceeding 100% at the cold tropical tropopause: Implications for cirrus formation and dehydration,” *Atmos. Chem. Phys.* **5**, 851–862.
- Jiang, J. H., H. Su, L. Wu, C. Zhai, and Schiro K. A., 2021. Improvements in cloud and water vapor simulations over the tropical oceans in CMIP6 compared to CMIP5,” *Earth Space Sci.* **8**, e2020EA001520.
- Jiang, J. H., *et al.*, 2012, “Evaluation of cloud and water vapor simulations in CMIP5 climate models using NASA ‘A-train’ satellite observations,” *J. Geophys. Res. Atmos.* **117**, D14105.
- Jin, S., X. L. Chang, and S. L. Wang, 2007, “Seasonal variability of GPS-derived zenith tropospheric delay (1994–2006) and climate implications,” *J. Geophys. Res.* **112**, D09110.
- John, V. O., G. Holl, R. P. Allan, S. A. Buehler, D. E. Parker, and B. J. Soden, 2011, “Clear-sky biases in satellite infrared estimates of upper tropospheric humidity and its trends,” *J. Geophys. Res.* **116**, D14108.
- John, V. O., and B. J. Soden, 2006, “Does convectively-detained cloud ice enhance water vapor feedback?,” *Geophys. Res. Lett.* **33**, L20701.
- John, V. O., and B. J. Soden, 2007, “Temperature and humidity biases in global climate models and their impact on climate feedbacks,” *Geophys. Res. Lett.* **34**, L18704.
- Jonko, A. K., K. M. Shell, B. M. Sanderson, and G. Danabasoglu, 2012, “Climate feedbacks in CCSM3 under changing CO<sub>2</sub> forcing. Part I: Adapting the linear radiative kernel technique to feedback calculations for a broad range of forcings,” *J. Clim.* **25**, 5260–5272.
- Jonko, A. K., K. M. Shell, B. M. Sanderson, and G. Danabasoglu, 2013, “Climate feedbacks in CCSM3 under changing CO<sub>2</sub> forcing. Part II: Variation of climate feedbacks and sensitivity with forcing,” *J. Clim.* **26**, 2784–2795.
- Joshi, Manoj M., and K. P. Shine, 2003, “A GCM study of volcanic eruptions as a cause of increased stratospheric water vapor,” *J. Clim.* **16**, 3525–3534.
- Juckes, M. N., 2000, “The static stability of the midlatitude troposphere: The relevance of moisture,” *J. Atmos. Sci.* **57**, 3050–3057.
- Keith, D. W., 2000, “Stratosphere-troposphere exchange: Inferences from the isotopic composition of water vapor,” *J. Geophys. Res. Atmos.* **105**, 15167–15173.
- Kiehl, J. T., J. J. Hack, and J. W. Hurrell, 1998, “The energy budget of the NCAR community climate model: CCM3,” *J. Clim.* **11**, 1151–1178.
- Kiehl, J. T., and K. E. Trenberth, 1997, “Earth’s annual global mean energy budget,” *Bull. Am. Meteorol. Soc.* **78**, 197–208.
- Kim, D., S. M. Kang, Y. Shin, and N. Feldl, 2018, “Sensitivity of polar amplification to varying insolation conditions,” *J. Clim.* **31**, 4933–4947.
- Kim, Y., Y.-S. Choi, B.-M. Kim, and H. Kim, 2016, “Influence of altered low cloud parameterizations for seasonal variation of Arctic cloud amount on climate feedbacks,” *Clim. Dyn.* **47**, 1661–1672.
- Kirtman, B., *et al.*, 2013, “Near-term climate change: Projections and predictability,” in *Climate Change 2013: The Physical Science Basis. Contribution of Working Group I to the Fifth Assessment Report of the Intergovernmental Panel on Climate Change*, edited by T. F. Stocker, D. Qin, G.-K. Plattner, M. Tignor, S. K. Allen, J. Boschung, A. Nauels, Y. Xia, V. Bex, and P. M. Midgley (Cambridge University Press, Cambridge, England).
- Klocke, D., R. Pincus, and J. Quaas, 2011, “On constraining estimates of climate sensitivity with present-day observations through model weighting,” *J. Clim.* **24**, 6092–6099.
- Klocke, D., J. Quaas, and B. Stevens, 2013, “Assessment of different metrics for physical climate feedbacks,” *Clim. Dyn.* **41**, 1173–1185.
- Kluft, K., S. Dacie, M. Brath, S. A. Buehler, and B. Stevens, 2021, “Temperature-dependent clear-sky feedbacks in radiative-convective equilibrium,” Max Planck Institute for Meteorology Reports on Earth System Science.
- Kluft, L., S. Dacie, S. A. Buehler, H. Schmidt, and B. Stevens, 2019, “Re-examining the first climate models: Climate sensitivity of a modern radiative-convective equilibrium model,” *J. Clim.* **32**, 8111–8125.
- Knutti, R., and M. A. A. Rugenstein, 2015, “Feedbacks, climate sensitivity and the limits of linear models,” *Phil. Trans. R. Soc. A* **373**, 20150146.
- Koll, D. D. B., and T. W. Cronin, 2018, “Earth’s outgoing longwave radiation linear due to H<sub>2</sub>O greenhouse effect,” *Proc. Natl. Acad. Sci. U.S.A.* **115**, 10293–10298.
- Koumoutsaris, S., 2013, “What can we learn about climate feedbacks from short-term climate variations?,” *Tellus A* **65**, 18887.
- Kramer, R. J., B. J. Soden, and A. G. Pendergrass, 2019, “Evaluating climate model simulations of the radiative forcing and radiative response at Earth’s surface,” *J. Clim.* **32**, 4089–4102.
- Kuang, Z., and D. L. Hartmann, 2007, “Testing the fixed anvil temperature hypothesis in a cloud-resolving model,” *J. Clim.* **20**, 2051–2057.
- Lacis, A. A., J. E. Hansen, G. L. Russell, V. Oinas, and J. Jonas, 2013, “The role of long-lived greenhouse gases as principal LW control knob that governs the global surface temperature for past and future climate change,” *Tellus B* **65**, 19734.
- Lahellec, A., S. Hallegatte, J.-Y. Grandpeix, P. Dumas, and S. Blanco, 2008, “Feedback characteristics of nonlinear dynamical systems,” *Europhys. Lett.* **81**, 60001.

- Lainé, A., M. Yoshimori, and A. Abe-Ouchi, 2016, “Surface Arctic amplification factors in CMIP5 models: Land and oceanic surfaces and seasonality,” *J. Clim.* **29**, 3297–3316.
- Lambert, F. H., G. R. Harris, M. Collins, J. M. Murphy, D. M. H. Sexton, and B. B. Booth, 2013, “Interactions between perturbations to different Earth system components simulated by a fully-coupled climate model,” *Clim. Dyn.* **41**, 3055–3072.
- Lambert, F. H., and P. C. Taylor, 2014, “Regional variation of the tropical water vapor and lapse rate feedbacks,” *Geophys. Res. Lett.* **41**, 7634–7641.
- Langen, P. L., R. G. Graverson, and T. Mauritsen, 2012, “Separation of contributions from radiative feedbacks to polar amplification on an aquaplanet,” *J. Clim.* **25**, 3010–3024.
- Lariviere, J. P., A. C. Ravelo, A. Crimmins, P. S. Dekens, H. L. Ford, M. Lyle, and M. W. Wara, 2012, “Late Miocene decoupling of oceanic warmth and atmospheric carbon dioxide forcing,” *Nature (London)* **486**, 97–100.
- Larson, K., and D. L. Hartmann, 2003, “Interactions among cloud, water vapor, radiation, and large-scale circulation in the tropical climate. Part II: Sensitivity to spatial gradients of sea surface temperature,” *J. Clim.* **16**, 1425–1440.
- Lau, K. M., and H. T. Wu, 2003, “Warm rain processes over tropical oceans and climate implications,” *Geophys. Res. Lett.* **30**, CLM 7-1–CLM 7-5.
- Lechevallier, L., S. Vasilchenko, R. Grilli, D. Mondelain, D. Romanini, and A. Campargue, 2018, “The water vapour self-continuum absorption in the infrared atmospheric windows: New laser measurements near 3.3 and 2.0  $\mu\text{m}$ ,” *Atmos. Meas. Tech.* **11**, 2159–2171.
- Li, F., and P. Newman, 2020, “Stratospheric water vapor feedback and its climate impacts in the coupled atmosphere-ocean Goddard Earth observing system chemistry-climate model,” *Clim. Dyn.* **55**, 1585–1595.
- Liakka, J., and M. Lofverstrom, 2018, “Arctic warming induced by the Laurentide Ice Sheet topography,” *Clim. Past* **14**, 887–900.
- Lin, B., B. A. Wielicki, L. H. Chambers, Y. Hu, and K.-M. Xu, 2002, “The iris hypothesis: A negative or positive cloud feedback?,” *J. Clim.* **15**, 3–7.
- Lin, B., T. Wong, B. A. Wielicki, and Y. Hu, 2004, “Examination of the decadal tropical mean ERBS nonscanner radiation data for the iris hypothesis,” *J. Clim.* **17**, 1239–1246.
- Lindberg, K., 2003, “Supporting evidence for a positive water vapor/infrared radiative feedback on large scale SST perturbations from a recent parameterization of surface long wave irradiance,” *Meteorol. Atmos. Phys.* **84**, 285–292.
- Lindzen, R. S., 1990, “Some coolness concerning global warming,” *Bull. Am. Meteorol. Soc.* **71**, 288–299.
- Lindzen, R. S., 1994, “On the scientific basis for global warming scenarios,” *Environ. Pollut.* **83**, 125–134.
- Lindzen, R. S., M.-D. Chou, and A. Y. Hou, 2001, “Does the Earth have an adaptive infrared iris?,” *Bull. Am. Meteorol. Soc.* **82**, 417–432.
- Liu, R., H. Su, K.-N. Liou, J. H. Jiang, Y. Gu, S. C. Liu, and C.-J. Shiu, 2018, “An assessment of tropospheric water vapor feedback using radiative kernels,” *J. Geophys. Res. Atmos.* **123**, 1499–1509.
- Lu, J., and M. Cai, 2009, “A new framework for isolating individual feedback processes in coupled general circulation climate models. Part I: Formulation,” *Clim. Dyn.* **32**, 873–885.
- Luo, Z., and W. B. Rossow, 2004, “Characterizing tropical cirrus life cycle, evolution, and interaction with upper-tropospheric water vapor using Lagrangian trajectory analysis of satellite observations,” *J. Clim.* **17**, 4541–4563.
- Madden, R. A., and P. R. Julian, 1994, “Observations of the 40–50-day tropical oscillation—A review,” *Mon. Weather Rev.* **122**, 814–837.
- Manabe, S., R. J. Stouffer, M. J. Spelman, and K. Bryan, 1991, “Transient responses of a coupled ocean-atmosphere model to gradual changes of atmospheric CO<sub>2</sub>. Part I. Annual mean response,” *J. Clim.* **4**, 785–818.
- Manabe, S., and R. F. Strickler, 1964, “Thermal equilibrium of the atmosphere with a convective adjustment,” *J. Atmos. Sci.* **21**, 361–385.
- Manabe, S., and R. T. Wetherald, 1967, “Thermal equilibrium of the atmosphere with a given distribution of relative humidity,” *J. Atmos. Sci.* **24**, 241–259.
- Manabe, S., and R. T. Wetherald, 1975, “The effects of doubling the CO<sub>2</sub> concentration on the climate of a general circulation model,” *J. Atmos. Sci.* **32**, 3–15.
- Marsden, D., and F. P. J. Valero, 2004, “Observation of water vapor greenhouse absorption over the Gulf of Mexico using aircraft and satellite data,” *J. Atmos. Sci.* **61**, 745–753.
- Masson-Delmotte, V., *et al.*, 2006, “Past and future polar amplification of climate change: Climate model intercomparisons and ice-core constraints,” *Clim. Dyn.* **26**, 513–529.
- Masson-Delmotte, V., *et al.*, 2018, Eds., “Global warming of 1.5°C. An IPCC special report on the impacts of global warming of 1.5°C above pre-industrial levels and related global greenhouse gas emission pathways, in the context of strengthening the global response to the threat of climate change,” Intergovernmental Panel on Climate Change report.
- Masson-Delmotte, V. M., *et al.*, 2013, “Information from paleoclimate archives,” in *Climate Change 2013: The Physical Science Basis. Contribution of Working Group I to the Fifth Assessment Report of the Intergovernmental Panel on Climate Change*, edited by T. F. Stocker, D. Qin, G.-K. Plattner, M. Tignor, S. K. Allen, J. Boschung, A. Nauels, Y. Xia, V. Bex, and P. M. Midgley (Cambridge University Press, Cambridge, England), pp. 383–464.
- Mauritsen, T., R. G. Graverson, D. Klocke, P. L. Langen, B. Stevens, and L. Tomassini, 2013, “Climate feedback efficiency and synergy,” *Clim. Dyn.* **41**, 2539–2554.
- Mauritsen, T., *et al.*, 2012, “Tuning the climate of a global model,” *J. Adv. Model. Earth Syst.* **4**, M00A01.
- Maycock, A. C., and K. P. Shine, 2012, “Stratospheric water vapor and climate: Sensitivity to the representation in radiation codes,” *J. Geophys. Res. Atmos.* **117**, D13102.
- Maycock, A. C., K. P. Shine, and M. M. Joshi, 2011, “The temperature response to stratospheric water vapour changes,” *Q. J. R. Meteorol. Soc.* **137**, 1070–1082.
- McCarthy, M. P., P. W. Thorne, and H. A. Titchner, 2009, “An analysis of tropospheric humidity trends from radiosondes,” *J. Clim.* **22**, 5820–5838.
- McCarthy, M. P., and R. Toumi, 2004, “Observed interannual variability of tropical troposphere relative humidity,” *J. Clim.* **17**, 3181–3191.
- McKittrick, R., and J. Christy, 2018, “A test of the tropical 200- to 300-hPa warming rate in climate models,” *Earth Space Sci.* **5**, 529–536.
- Meehl, G. A., C. Covey, T. Delworth, M. Latif, B. McAvaney, J. F. B. Mitchell, R. J. Stouffer, and K. E. Taylor, 2007, “The WCRP CMIP3 multimodel dataset: A new era in climate change research,” *Bull. Am. Meteorol. Soc.* **88**, pp. 1383–1394.
- Meraner, K., T. Mauritsen, and A. Voigt, 2013, “Robust increase in equilibrium climate sensitivity under global warming,” *Geophys. Res. Lett.* **40**, 5944–5948.

- Miloshevich, L. M., H. Vömel, D. N. Whiteman, and T. Leblanc, 2009, "Accuracy assessment and correction of Vaisala RS92 radiosonde water vapor measurements," *J. Geophys. Res.* **114**, D11305.
- Minder, J. R., T. W. Letcher, and C. Liu, 2018, "The character and causes of elevation-dependent warming in high-resolution simulations of Rocky Mountain climate change," *J. Clim.* **31**, 2093–2113.
- Minschwaner, K., and A. E. Dessler, 2004, "Water vapor feedback in the tropical upper troposphere: Model results and observations," *J. Clim.* **17**, 1272–1282.
- Minschwaner, K., A. E. Dessler, and P. Sawaengphokhai, 2006, "Multimodel analysis of the water vapor feedback in the tropical upper troposphere," *J. Clim.* **19**, 5455–5464.
- Mitchell, D. M., Y. T. E. Lo, W. J. M. Seviour, L. Haimberger, and L. M. Polvani, 2020, "The vertical profile of recent tropical temperature trends: Persistent model biases in the context of internal variability," *Environ. Res. Lett.* **15**, 1040b4.
- Mitchell, D. M., P. W. Thorne, P. A. Stott, and L. J. Gray, 2013, "Revisiting the controversial issue of tropical tropospheric temperature trends," *Geophys. Res. Lett.* **40**, 2801–2806.
- Mitchell, J. F. B., and W. J. Ingram, 1992, "Carbon dioxide and climate: Mechanisms of changes in cloud," *J. Clim.* **5**, 5–21.
- Mokhov, I. I., M. G. Akperov, and M. A. Dembitskaya, 2016, "Lapse-rate feedback assessment from reanalysis data," [https://www.wcrp-climate.org/WGNE/BlueBook/2016/individual-articles/02\\_Mokhov\\_Igor\\_Lapse\\_rate.pdf](https://www.wcrp-climate.org/WGNE/BlueBook/2016/individual-articles/02_Mokhov_Igor_Lapse_rate.pdf).
- Möller, F., 1961, "Atmospheric water vapor measurements at 6–7 microns from a satellite," *Planet. Space Sci.* **5**, 202–206.
- Muller, C. J., and I. M. Held, 2012, "Detailed investigation of the self-aggregation of convection in cloud-resolving simulations," *J. Atmos. Sci.* **69**, 2551–2565.
- Müller, R., A. Kunz, D. F. Hurst, C. Rolf, M. Krämer, and M. Riese, 2016, "The need for accurate long-term measurements of water vapor in the upper troposphere and lower stratosphere with global coverage," *Earth's Future* **4**, 25–32.
- Murphy, J. M., D. M. H. Sexton, D. N. Barnett, G. S. Jones, M. J. Webb, M. Collins, and D. A. Stainforth, 2004, "Quantification of modelling uncertainties in a large ensemble of climate change simulations," *Nature (London)* **430**, 768–772.
- Nakajima, S., Y.-Y. Hayashi, and Y. Abe, 1992, "A study on the runaway greenhouse effect with a one-dimensional radiative-convective equilibrium model," *J. Atmos. Sci.* **49**, 2256–2266.
- Nakicenovic, N., *et al.*, 2000, *Special Report on Emissions Scenarios (SRES): A Special Report of Working Group III of the Intergovernmental Panel on Climate Change* (Cambridge University Press, Cambridge, England).
- Neelin, J. D., and I. M. Held, 1987, "Modeling tropical convergence based on the moist static energy budget," *Mon. Weather Rev.* **115**, 3–12.
- Nowack, P. J., N. L. Abraham, P. Braesicke, and J. A. Pyle, 2018, "The impact of stratospheric ozone feedbacks on climate sensitivity estimates," *J. Geophys. Res. Atmos.* **123**, 4630–4641.
- O’Gorman, P. A., and C. J. Muller, 2010, "How closely do changes in surface and column water vapor follow Clausius-Clapeyron scaling in climate change simulations?," *Environ. Res. Lett.* **5**, 025207.
- O’Gorman, P. A., and M. S. Singh, 2013, "Vertical structure of warming consistent with an upward shift in the middle and upper troposphere," *Geophys. Res. Lett.* **40**, 1838–1842.
- Onogi, K., *et al.*, 2007, "The JRA-25 reanalysis," *J. Meteorol. Soc. Jpn.* **85**, 369–432.
- Oueslati, B., B. Pohl, V. Moron, S. Rome, and S. Janicot, 2017, "Characterization of heat waves in the Sahel and associated physical mechanisms," *J. Clim.* **30**, 3095–3115.
- Palazzi, E., L. Filippi, and J. von Hardenberg, 2017, "Insights into elevation-dependent warming in the Tibetan Plateau-Himalayas from CMIP5 model simulations," *Clim. Dyn.* **48**, 3991–4008.
- Parker, D. E., and D. I. Cox, 1995, "Towards a consistent global climatological rawinsonde data-base," *Int. J. Climatol.* **15**, 473–496.
- Payne, A. E., M. F. Jansen, and T. W. Cronin, 2015, "Conceptual model analysis of the influence of temperature feedbacks on polar amplification," *Geophys. Res. Lett.* **42**, 9561–9570.
- Pendergrass, A. G., A. Conley, and F. M. Vitt, 2018, "Surface and top-of-atmosphere radiative feedback kernels for CESM-CAM5," *Earth Syst. Sci. Data* **10**, 317–324.
- Pendergrass, A. G., and D. L. Hartmann, 2014, "The atmospheric energy constraint on global-mean precipitation change," *J. Clim.* **27**, 757–768.
- Pepin, N., *et al.*, 2015, "Elevation-dependent warming in mountain regions of the world," *Nat. Clim. Change* **5**, 424–430.
- Peters, M. E., and C. S. Bretherton, 2005, "A simplified model of the walker circulation with an interactive ocean mixed layer and cloud-radiative feedbacks," *J. Clim.* **18**, 4216–4234.
- Peterson, H. G., and W. R. Boos, 2020, "Feedbacks and eddy diffusivity in an energy balance model of tropical rainfall shifts," *npj Clim. Atmos. Sci.* **3**, 11.
- Philipona, R., B. Dürr, C. Marty, A. Ohmura, and M. Wild, 2004, "Radiative forcing—measured at Earth’s surface—corroborate the increasing greenhouse effect," *Geophys. Res. Lett.* **31**, L03202.
- Philipona, R., B. Dürr, A. Ohmura, and C. Ruckstuhl, 2005, "Anthropogenic greenhouse forcing and strong water vapor feedback increase temperature in Europe," *Geophys. Res. Lett.* **32**, L19809.
- Pierrehumbert, R. T., 1995, "Thermostats, radiator fins, and the local runaway greenhouse," *J. Atmos. Sci.* **52**, 1784–1806.
- Pierrehumbert, R. T., 1998, "Lateral mixing as a source of subtropical water vapor," *Geophys. Res. Lett.* **25**, 151–154.
- Pierrehumbert, R. T., 1999, "Subtropical water vapor as a mediator of rapid global climate change," in *Mechanisms of Global Climate Change at Millennial Time Scales*, Geophysics Monograph Series Vol. 112, edited by P. U. Clark, R. S. Webb, and L. D. Keigwin (American Geophysical Union, Washington, DC), pp. 339–361.
- Pierrehumbert, R. T., 2010, *Principles of Planetary Climate* (Cambridge University Press, Cambridge, England).
- Pierrehumbert, R. T., H. Brogniez, and R. Roca, 2007, "On the relative humidity of the atmosphere," in *The Global Circulation of the Atmosphere*, edited by T. Schneider and A. H. Sobel (Princeton University Press, Princeton, NJ), pp. 143–185, <http://citeseerx.ist.psu.edu/viewdoc/download?doi=10.1.1.76.6479&rep=rep1&type=pdf>.
- Pierrehumbert, R. T., and R. Roca, 1998, "Evidence for control of Atlantic subtropical humidity by large scale advection," *Geophys. Res. Lett.* **25**, 4537–4540.
- Pincus, R., P. M. Forster, and B. Stevens, 2016, "The Radiative Forcing Model Intercomparison Project (RFMIP): Experimental protocol for CMIP6," *Geosci. Model Dev.* **9**, 3447–3460.
- Pithan, F., and T. Mauritsen, 2014, "Arctic amplification dominated by temperature feedbacks in contemporary climate models," *Nat. Geosci.* **7**, 181–184.
- Po-Chedley, S., K. C. Armour, C. M. Bitz, M. D. Zelinka, B. D. Santer, and Q. Fu, 2018, "Sources of intermodel spread in the lapse rate and water vapor feedbacks," *J. Clim.* **31**, 3187–3206.

- Po-Chedley, S., and Q. Fu, 2012, "Discrepancies in tropical upper tropospheric warming between atmospheric circulation models and satellites," *Environ. Res. Lett.* **7**, 044018.
- Po-Chedley, S., T. J. Thorsen, and Q. Fu, 2015, "Removing diurnal cycle contamination in satellite-derived tropospheric temperatures: Understanding tropical tropospheric trend discrepancies," *J. Clim.* **28**, 2274–2290.
- Po-Chedley, S., M. D. Zelinka, N. Jeevanjee, T. J. Thorsen, and B. D. Santer, 2019, "Climatology explains intermodel spread in tropical upper tropospheric cloud and relative humidity response to greenhouse warming," *Geophys. Res. Lett.* **46**, 13399–13409.
- Prata, F., 2008, "The climatological record of clear-sky longwave radiation at the Earth's surface: Evidence for water vapour feedback?," *Int. J. Remote Sens.* **29**, 5247–5263.
- Previdi, M., 2010, "Radiative feedbacks on global precipitation," *Environ. Res. Lett.* **5**, 025211.
- Previdi, M., and B. G. Liepert, 2012, "The vertical distribution of climate forcings and feedbacks from the surface to top of atmosphere," *Clim. Dyn.* **39**, 941–951.
- Rädel, G., K. P. Shine, and I. V. Ptashnik, 2015, "Global radiative and climate effect of the water vapour continuum at visible and near-infrared wavelengths," *Q. J. R. Meteorol. Soc.* **141**, 727–738.
- Ramanathan, V., 1977, "Interactions between ice-albedo, lapse-rate and cloud-top feedbacks: An analysis of the nonlinear response of a GCM climate model," *J. Atmos. Sci.* **34**, 1885–1897.
- Ramanathan, V., 2014, "Climate change and protection of the habitat: Empirical evidence for the greenhouse effect and global warming," in *Complexity and Analogy in Science: Theoretical, Methodological and Epistemological Aspects*, edited by W. Arber, J. Mittelstaß, and M. Sánchez Sorondo (ACTA Publications, Chicago), pp. 230–241, <http://www.academiasdelasociencias.va/content/dam/accademia/pdf/acta22/acta22-ramanathan.pdf>.
- Ramanathan, V., and J. A. Coakley, 1978, "Climate modeling through radiative-convective models," *Rev. Geophys.* **16**, 465–489.
- Randall, D. A., *et al.*, 2007, "Evaluation of climate models," in *Climate Change 2007: The Physical Science Basis. Contribution of Working Group I to the Fourth Assessment Report of the Intergovernmental Panel on Climate Change*, edited by S. Solomon *et al.* (Cambridge University Press, Cambridge, England), pp. 801–866.
- Rangwala, I., 2013, "Amplified water vapour feedback at high altitudes during winter," *Int. J. Climatol.* **33**, 897–903.
- Rangwala, I., J. R. Miller, G. L. Russell, and M. Xu, 2010, "Using a global climate model to evaluate the influences of water vapor, snow cover and atmospheric aerosol on warming in the Tibetan Plateau during the twenty-first century," *Clim. Dyn.* **34**, 859–872.
- Rangwala, I., J. R. Miller, and M. Xu, 2009, "Warming in the Tibetan Plateau: Possible influences of the changes in surface water vapor," *Geophys. Res. Lett.* **36**, L06703.
- Rangwala, I., E. Sinsky, and J. R. Miller, 2013, "Amplified warming projections for high altitude regions of the Northern Hemisphere mid-latitudes from CMIP5 models," *Environ. Res. Lett.* **8**, 024040.
- Rapp, A., C. Kummerow, W. Berg, and B. Griffith, 2005, "An evaluation of the proposed mechanism of the adaptive infrared iris hypothesis using TRMM VIRS and PR measurements," *J. Clim.* **18**, 4185–4194.
- Raval, A., and V. Ramanathan, 1989, "Observational determination of the greenhouse effect," *Nature (London)* **342**, 758–761.
- Rennó, N. O., K. A. Emanuel, and P. H. Stone, 1994, "Radiative-convective model with an explicit hydrologic cycle: 1. Formulation and sensitivity to model parameters," *J. Geophys. Res. Atmos.* **99**, 14429.
- Rieger, V. S., S. Dietmüller, and M. Ponater, 2017, "Can feedback analysis be used to uncover the physical origin of climate sensitivity and efficacy differences?," *Clim. Dyn.* **49**, 2831–2844.
- Rienecker, M. M., *et al.*, 2011, "MERRA: NASA's modern-era retrospective analysis for research and applications," *J. Clim.* **24**, 3624–3648.
- Rind, D., E.-W. Chiou, W. Chu, J. Larsen, S. Oltmans, J. Lerner, M. P. McCormick, and L. McMaster, 1991, "Positive water vapour feedback in climate models confirmed by satellite data," *Nature (London)* **349**, 500–503.
- Rind, D., and A. Lacis, 1993, "The role of the stratosphere in climate change," *Surv. Geophys.* **14**, 133–165.
- Robock, A., B. Kravitz, and O. Boucher, 2011, "Standardizing experiments in geoengineering," *EOS Trans. Am. Geophys. Union* **92**, 197.
- Robock, A., and J. Mao, 1995, "The volcanic signal in surface temperature observations," *J. Clim.* **8**, 1086–1103.
- Romps, D. M., 2014, "An analytical model for tropical relative humidity," *J. Clim.* **27**, 7432–7449.
- Rose, B. E. J., and M. C. Rencurrel, 2016, "The vertical structure of tropospheric water vapor: Comparing radiative and ocean-driven climate changes," *J. Clim.* **29**, 4251–4268.
- Rosenlof, K. H., 2003, "How water enters the stratosphere," *Science* **302**, 1691–1692.
- Rosenlof, K. H., A. F. Tuck, K. K. Kelly, J. M. Russell, and M. P. McCormick, 1997, "Hemispheric asymmetries in water vapor and inferences about transport in the lower stratosphere," *J. Geophys. Res. Atmos.* **102**, 13213–13234.
- Rugenstein, M., *et al.*, 2019, "LongRunMIP: Motivation and design for a large collection of millennial-length AOGCM simulations," *Bull. Am. Meteorol. Soc.* **100**, 2551–2570.
- Rugenstein, M., *et al.*, 2020, "Equilibrium climate sensitivity estimated by equilibrating climate models," *Geophys. Res. Lett.* **47**, e2019GL083898.
- Russell, G. L., A. A. Lacis, D. H. Rind, C. Colose, and R. F. Opstbaum, 2013, "Fast atmosphere-ocean model runs with large changes in CO<sub>2</sub>," *Geophys. Res. Lett.* **40**, 5787–5792.
- Russotto, R. D., and M. Biasutti, 2020, "Polar amplification as an inherent response of a circulating atmosphere: Results from the TRACMIP aquaplanets," *Geophys. Res. Lett.* **47**, e2019GL086771.
- Ryoo, J., T. Igusa, and D. W. Waugh, 2009, "PDFs of tropical tropospheric humidity measurements and theory," *J. Clim.* **22**, 3357–3373.
- Salathé, E. P., and D. L. Hartmann, 1997, "A trajectory analysis of tropical upper-tropospheric moisture and convection," *J. Clim.* **10**, 2533–2547.
- Salathé, E. P., and D. L. Hartmann, 2000, "Subsidence and upper-tropospheric drying along trajectories in a general circulation model," *J. Clim.* **13**, 257–263.
- Salzmann, M., 2017, "The polar amplification asymmetry: Role of Antarctic surface height," *Earth Syst. Dyn.* **8**, 323–336.
- Sanderson, B. M., K. M. Shell, and W. Ingram, 2010, "Climate feedbacks determined using radiative kernels in a multi-thousand member ensemble of AOGCMs," *Clim. Dyn.* **35**, 1219–1236.
- Santer, B. D., R. Sausen, T. M. L. Wigley, J. S. Boyle, K. AchutaRao, C. Doutriaux, and G. Schmidt, 2003, "Behavior of tropopause height and atmospheric temperature in models, reanalyses, and observations: Decadal changes," *J. Geophys. Res.* **108**, 4002.
- Santer, B. D., M. F. Wehner, T. M. L. Wigley, R. Sausen, G. A. Meehl, K. E. Taylor, and W. Brüggemann, 2003, "Contributions of anthropogenic and natural forcing to recent tropopause height changes," *Science* **301**, 479–483.

- Santer, B. D., *et al.*, 2005, "Amplification of surface temperature trends and variability in the tropical atmosphere," *Science* **309**, 1551–1556.
- Santer, B. D., *et al.*, 2007, "Identification of human-induced changes in atmospheric moisture content," *Proc. Natl. Acad. Sci. U.S.A.* **104**, 15248–15253.
- Santer, B. D., *et al.*, 2013, "Human and natural influences on the changing thermal structure of the atmosphere," *Proc. Natl. Acad. Sci. U.S.A.* **110**, 17235–17240.
- Santer, B. D., *et al.*, 2014, "Volcanic contribution to decadal changes in tropospheric temperature," *Nat. Geosci.* **7**, 185–189.
- Santer, B. D., *et al.*, 2017, "Causes of differences in model and satellite tropospheric warming rates," *Nat. Geosci.* **10**, 478–485.
- Santer, B. D., *et al.*, 2018, "Human influence on the seasonal cycle of tropospheric temperature," *Science* **361**, eaas8806.
- Schlesinger, M. E., 1988, "Quantitative analysis of feedbacks in climate model simulations of CO<sub>2</sub>-induced warming," in *Physically-Based Modelling and Simulation of Climate and Climatic Change*, Nato Science Series C Vol. 243, edited by M. E. Schlesinger (Springer Netherlands, Dordrecht), pp. 653–735.
- Schlesinger, M. E., C. Entwistle, and B. Li, 2012, "Temperature-profile/lapse-rate feedback: A misunderstood feedback of the climate system," *Atmos. Clim. Sci.* **02**, 474–478.
- Schneider, E. K., B. P. Kirtman, and R. S. Lindzen, 1999, "Tropospheric water vapor and climate sensitivity," *J. Atmos. Sci.* **56**, 1649–1658.
- Seeley, J. T., and N. Jeevanjee, 2021, "H<sub>2</sub>O windows and CO<sub>2</sub> radiator fins: A clear-sky explanation for the peak in equilibrium climate sensitivity," *Geophys. Res. Lett.* **48**, e2020GL089609.
- Seidel, D. J., *et al.*, 2009, "Reference upper-air observations for climate: Rationale, progress, and plans," *Bull. Am. Meteorol. Soc.* **90**, 361–369.
- Seidel, S. D., and D. Yang, 2020a, "The incredible lightness of water vapor," *J. Clim.* **33**, 2841–2851.
- Seidel, S. D., and D. Yang, 2020b, "The lightness of water vapor helps to stabilize tropical climate," *Sci. Adv.* **6**, eaba1951.
- Sejas, S. A., and M. Cai, 2016, "Isolating the temperature feedback loop and its effects on surface temperature," *J. Atmos. Sci.* **73**, 3287–3303.
- Shell, K. M., 2013, "Consistent differences in climate feedbacks between atmosphere-ocean GCMs and atmospheric GCMs with slab-ocean models," *J. Clim.* **26**, 4264–4281.
- Shell, K. M., J. T. Kiehl, and C. A. Shields, 2008, "Using the radiative kernel technique to calculate climate feedbacks in NCAR's community atmospheric model," *J. Clim.* **21**, 2269–2282.
- Sherwood, S. C., 1996a "Maintenance of the free-tropospheric tropical water vapor distribution. Part I: Clear regime budget," *J. Clim.* **9**, 2903–2918.
- Sherwood, S. C., 1996b "Maintenance of the free-tropospheric tropical water vapor distribution. Part II: Simulation by large-scale advection," *J. Clim.* **9**, 2919–2934.
- Sherwood, S. C., 1999, "On moistening of the tropical troposphere by cirrus clouds," *J. Geophys. Res. Atmos.* **104**, 11949–11960.
- Sherwood, S. C., 2006, "The general circulation and robust relative humidity," *J. Clim.* **19**, 6278–6290.
- Sherwood, S. C., S. Bony, O. Boucher, C. Bretherton, P. M. Forster, J. M. Gregory, and B. Stevens, 2015, "Adjustments in the forcing-feedback framework for understanding climate change," *Bull. Am. Meteorol. Soc.* **96**, 217–228.
- Sherwood, S. C., and A. E. Dessler, 2000, "On the control of stratospheric humidity," *Geophys. Res. Lett.* **27**, 2513–2516.
- Sherwood, S. C., W. Ingram, Y. Tsushima, M. Satoh, M. Roberts, P. L. Vidale, and P. A. O'Gorman, 2010a, "Relative humidity changes in a warmer climate," *J. Geophys. Res.* **115**, D09104.
- Sherwood, S. C., and C. L. Meyer, 2006, "The general circulation and robust relative humidity," *J. Clim.* **19**, 6278–6290.
- Sherwood, S. C., R. Roca, T. M. Weckwerth, and N. G. Andronova, 2010b, "Tropospheric water vapor, convection, and climate," *Rev. Geophys.* **48**, RG2001.
- Sherwood, S. C., *et al.*, 2020, "An assessment of Earth's climate sensitivity using multiple lines of evidence," *Rev. Geophys.* **58**, e2019RG000678.
- Shi, L., and J. J. Bates, 2011, "Three decades of intersatellite-calibrated high-resolution infrared radiation sounder upper tropospheric water vapor," *J. Geophys. Res.* **116**, D04108.
- Shine, K. P., I. V. Ptashnik, and G. Rädcl, 2012, "The water vapour continuum: Brief history and recent developments," *Surv. Geophys.* **33**, 535–555.
- Shine, K. P., and A. Sinha, 1991, "Sensitivity of the Earth's climate to height-dependent changes in the water vapour mixing ratio," *Nature (London)* **354**, 382–384.
- Simpson, S. G. C., 1929, "Some studies in terrestrial radiation," *Mem. R. Meteorol. Soc.* **2**, 69–95.
- Slingo, A., J. A. Pamment, R. P. Allan, and P. S. Wilson, 2000, "Water vapor feedbacks in the ECMWF reanalyses and Hadley Centre climate model," *J. Clim.* **13**, 3080–3098.
- Slingo, A., J. A. Pamment, and M. J. Webb, 1998, "A 15-year simulation of the clear-sky greenhouse effect using the ECMWF reanalyses: Fluxes and comparisons with ERBE," *J. Clim.* **11**, 690–708.
- Slingo, A., and M. J. Webb, 1997, "The spectral signature of global warming," *Q. J. R. Meteorol. Soc.* **123**, 293–307.
- Smalley, K. M., A. E. Dessler, S. Bekki, M. Deushi, M. Marchand, O. Morgenstern, D. A. Plummer, K. Shibata, Y. Yamashita, and G. Zeng, 2017, "Contribution of different processes to changes in tropical lower-stratospheric water vapor in chemistry-climate models," *Atmos. Chem. Phys.* **17**, 8031–8044.
- Smith, C. J., R. J. Kramer, and A. Sima, 2020, "The HadGEM3-GA7.1 radiative kernel: The importance of a well-resolved stratosphere," *Earth Syst. Sci. Data* **12**, 2157–2168.
- Smith, C. J., *et al.*, 2018, "Understanding rapid adjustments to diverse forcing agents," *Geophys. Res. Lett.* **45**, 12023–12031.
- Sobel, A. H., J. Nilsson, and L. M. Polvani, 2001, "The weak temperature gradient approximation and balanced tropical moisture waves," *J. Atmos. Sci.* **58**, 3650–3665.
- Soden, B. J., 1997, "Variations in the tropical greenhouse effect during El Niño," *J. Clim.* **10**, 1050–1055.
- Soden, B. J., 2000, "The sensitivity of the tropical hydrological cycle to ENSO," *J. Clim.* **13**, 538–549.
- Soden, B. J., 2004, "The impact of tropical convection and cirrus on upper tropospheric humidity: A Lagrangian analysis of satellite measurements," *Geophys. Res. Lett.* **31**, L20104.
- Soden, B. J., and F. P. Bretherton, 1996, "Interpretation of TOVS water vapor radiances in terms of layer-average relative humidities: Method and climatology for the upper, middle, and lower troposphere," *J. Geophys. Res. Atmos.* **101**, 9333–9343.
- Soden, B. J., A. J. Broccoli, and R. S. Hemler, 2004, "On the use of cloud forcing to estimate cloud feedback," *J. Clim.* **17**, 3661–3665.
- Soden, B. J., and R. Fu, 1995, "A satellite analysis of deep convection, upper-tropospheric humidity, and the greenhouse effect," *J. Clim.* **8**, 2333–2351.
- Soden, B. J., and I. M. Held, 2006, "An assessment of climate feedbacks in coupled ocean-atmosphere models," *J. Clim.* **19**, 3354–3360.

- Soden, B. J., I. M. Held, R. Colman, K. M. Shell, J. T. Kiehl, and C. A. Shields, 2008, "Quantifying climate feedbacks using radiative kernels," *J. Clim.* **21**, 3504–3520.
- Soden, B. J., D. L. Jackson, V. Ramaswamy, M. D. Schwarzkopf, and X. Huang, 2005, "The radiative signature of upper tropospheric moistening," *Science* **310**, 841–844.
- Soden, B. J., and S. R. Schroeder, 2000, "Decadal variations in tropical water vapor: A comparison of observations and a model simulation," *J. Clim.* **13**, 3337–3341.
- Soden, B. J., R. T. Wetherald, G. L. Stenchikov, and A. Robock, 2002, "Global cooling after the eruption of Mount Pinatubo: A test of climate feedback by water vapor," *Science* **296**, 727–730.
- Soden, B. J., *et al.*, 2000, "An intercomparison of radiation codes for retrieving upper-tropospheric humidity in the 6.3-mm band: A report from the first GVaP workshop," *Bull. Am. Meteorol. Soc.* **81**, 797–808.
- Solomon, S., K. H. Rosenlof, R. W. Portmann, J. S. Daniel, S. M. Davis, T. J. Sanford, and G.-K. Plattner, 2010, "Contributions of stratospheric water vapor to decadal changes in the rate of global warming," *Science* **327**, 1219–1224.
- Spencer, R. W., and W. D. Braswell, 1997, "How dry is the tropical free troposphere? Implications for global warming theory," *Bull. Am. Meteorol. Soc.* **78**, 1097–1106.
- Spencer, R. W., and J. R. Christy, 1990, "Precise monitoring of global temperature trends from satellites," *Science* **247**, 1558–1562.
- Stainforth, D. A., *et al.*, 2005, "Uncertainty in predictions of the climate response to rising levels of greenhouse gases," *Nature (London)* **433**, 403–406.
- Stevens, B., and S. Bony, 2013, "Water in the atmosphere," *Phys. Today* **66**, No. 6, 29–34.
- Stocker, T. F., *et al.*, 2001, "Physical climate processes and feedbacks," in *Climate Change 2001: The Scientific Basis. Contribution of Working Group I to the Third Assessment Report of the Intergovernmental Panel on Climate Change*, edited by J. T. Houghton, Y. Ding, D. J. Griggs, M. Noguer, P. J. van der Linden, X. Dai, K. Maskell, and C. A. Johnson (Cambridge University Press, Cambridge, England), pp. 417–470, <https://www.ipcc.ch/site/assets/uploads/2018/03/TAR-07.pdf>.
- Stone, P. H., 1978, "Baroclinic adjustment," *J. Atmos. Sci.* **35**, 561–571.
- Stone, P. H., and J. H. Carlson, 1979, "Atmospheric lapse rate regimes and their parameterization," *J. Atmos. Sci.* **36**, 415–423.
- Stuber, N., M. Ponater, and R. Sausen, 2001, "Is the climate sensitivity to ozone perturbations enhanced by stratospheric water vapor feedback?," *Geophys. Res. Lett.* **28**, 2887–2890.
- Stuecker, M. F., *et al.*, 2018, "Polar amplification dominated by local forcing and feedbacks," *Nat. Clim. Change* **8**, 1076–1081.
- Su, H., W. G. Read, J. H. Jiang, J. W. Waters, D. L. Wu, and E. J. Fetzer, 2006, "Enhanced positive water vapor feedback associated with tropical deep convection: New evidence from Aura MLS," *Geophys. Res. Lett.* **33**, L05709.
- Su, H., *et al.*, 2008, "Variations of tropical upper tropospheric clouds with sea surface temperature and implications for radiative effects," *J. Geophys. Res.* **113**, D10211.
- Sun, D.-Z., and R. S. Lindzen, 1993, "Distribution of tropical tropospheric water vapor," *J. Atmos. Sci.* **50**, 1643–1660.
- Takahashi, H., H. Su, and J. H. Jiang, 2016, "Water vapor changes under global warming and the linkage to present-day interannual variabilities in CMIP5 models," *Clim. Dyn.* **47**, 3673–3691.
- Takahashi, K., 2009, "The global hydrological cycle and atmospheric shortwave absorption in climate models under CO<sub>2</sub> forcing," *J. Clim.* **22**, 5667–5675.
- Tan, I., and T. Storelvmo, 2019, "Evidence of strong contributions from mixed-phase clouds to Arctic climate change," *Geophys. Res. Lett.* **46**, 2894–2902.
- Taylor, K. E., R. J. Stouffer, and G. A. Meehl, 2012, "An overview of CMIP5 and the experiment design," *Bull. Am. Meteorol. Soc.* **93**, 485–498.
- Taylor, P. C., M. Cai, A. Hu, J. Meehl, W. Washington, and G. J. Zhang, 2013, "A decomposition of feedback contributions to polar warming amplification," *J. Clim.* **26**, 7023–7043.
- Taylor, P. C., R. G. Ellingson, and M. Cai, 2011, "Geographical distribution of climate feedbacks in the NCAR CCSM3.0," *J. Clim.* **24**, 2737–2753.
- Thorne, P. W., J. R. Lanzante, T. C. Peterson, D. J. Seidel, and K. P. Shine, 2011, "Tropospheric temperature trends: History of an ongoing controversy," *Wiley Interdiscip. Rev. Clim. Change* **2**, 66–88.
- Thorne, P. W., and R. S. Vose, 2010, "Reanalyses suitable for characterizing long-term trends," *Bull. Am. Meteorol. Soc.* **91**, 353–362.
- Tian, B., E. J. Fetzer, B. H. Kahn, J. Teixeira, E. Manning, and T. Hearty, 2013, "Evaluating CMIP5 models using AIRS tropospheric air temperature and specific humidity climatology," *J. Geophys. Res. Atmos.* **118**, 114–134.
- Tian, E. W., H. Su, B. Tian, and J. H. Jiang, 2019, "Interannual variations of water vapor in the tropical upper troposphere and the lower and middle stratosphere and their connections to ENSO and QBO," *Atmos. Chem. Phys.* **19**, 9913–9926.
- Tierney, J. E., *et al.*, 2020, "Past climates inform our future," *Science* **370**, eaay3701.
- Tipping, R. H., and Q. Ma, 1995, "Theory of the water vapor continuum and validations," *Atmos. Res.* **36**, 69–94.
- Tobin, I., S. Bony, C. E. Holloway, J.-Y. Grandpeix, G. Sèze, D. Coppin, S. J. Woolnough, and R. Roca, 2013, "Does convective aggregation need to be represented in cumulus parameterizations?," *J. Adv. Model. Earth Syst.* **5**, 692–703.
- Tobin, I., S. Bony, and R. Roca, 2012, "Observational evidence for relationships between the degree of aggregation of deep convection, water vapor, surface fluxes, and radiation," *J. Clim.* **25**, 6885–6904.
- Tompkins, A. M., and G. C. Craig, 1999, "Sensitivity of tropical convection to sea surface temperature in the absence of large-scale flow," *J. Clim.* **12**, 462–476.
- Tompkins, A. M., and K. A. Emanuel, 2000, "The vertical resolution sensitivity of simulated equilibrium temperature and water-vapour profiles," *Q. J. R. Meteorol. Soc.* **126**, 1219–1238.
- Trenberth, K. E., J. Fasullo, and L. Smith, 2005, "Trends and variability in column-integrated atmospheric water vapor," *Clim. Dyn.* **24**, 741–758.
- Trenberth, K. E., Y. Zhang, J. T. Fasullo, and S. Taguchi, 2015, "Climate variability and relationships between top-of-atmosphere radiation and temperatures on Earth," *J. Geophys. Res. Atmos.* **120**, 3642–3659.
- Tsushima, Y., A. Abe-Ouchi, and S. Manabe, 2005, "Radiative damping of annual variation in global mean surface temperature: Comparison between observed and simulated feedback," *Clim. Dyn.* **24**, 591–597.
- Tsushima, Y., M. A. Ringer, G. M. Martin, J. W. Rostron, and D. M. H. Sexton, 2020, "Investigating physical constraints on climate feedbacks using a perturbed parameter ensemble," *Clim. Dyn.* **55**, 1159–1185.
- Tyndall, J., 1861, "XXIII. On the absorption and radiation of heat by gases and vapours, and on the physical connexion of radiation,

- absorption, and conduction—The Bakerian lecture,” *London Edinburgh Dublin Philos. Mag. J. Sci.* **22**, 169–194.
- Tyndall, J., 1872, *Contributions to Molecular Physics in the Domain of Radiant Heat* (Longmans, Green, and Co., London).
- Uppala, S. M., *et al.*, 2005, “The ERA-40 re-analysis,” *Q. J. R. Meteorol. Soc.* **131**, 2961–3012.
- Van Vuuren, D. P., *et al.*, 2011, “The representative concentration pathways: An overview,” *Clim. Change* **109**, 5.
- Vergados, P., A. J. Mannucci, C. O. Ao, and E. J. Fetzer, 2016, “Using GPS radio occultations to infer the water vapor feedback,” *Geophys. Res. Lett.* **43**, 11841–11851.
- Vial, J., J. L. Dufresne, and S. Bony, 2013, “On the interpretation of inter-model spread in CMIP5 climate sensitivity estimates,” *Clim. Dyn.* **41**, 3339–3362.
- Voltaire, A., *et al.*, 2019, “Evaluation of CMIP6 DECK experiments with CNRM-CM6-1,” *J. Adv. Model. Earth Syst.* **11**, 2177–2213.
- Wang, J., A. Dai, and C. Mears, 2016, “Global water vapor trend from 1988 to 2011 and its diurnal asymmetry based on GPS, radiosonde, and microwave satellite measurements,” *J. Clim.* **29**, 5205–5222.
- Wang, J., J. Wang, P. Wang, M. Sparrow, J. Yang, and H. Chen, 2007, “A near-global, 2-hourly data set of atmospheric precipitable water from ground-based GPS measurements,” *J. Geophys. Res. Atmos.* **112**, D11107.
- Wang, J., and L. Zhang, 2008, “Systematic errors in global radiosonde precipitable water data from comparisons with ground-based GPS measurements,” *J. Clim.* **21**, 2218–2238.
- Wang, X., H. Liu, and G. R. Foltz, 2017, “Persistent influence of tropical North Atlantic wintertime sea surface temperature on the subsequent Atlantic hurricane season,” *Geophys. Res. Lett.* **44**, 7927–7935.
- Wang, Y., and Y. Huang, 2020, “Stratospheric radiative feedback limited by the tropospheric influence in global warming,” *Clim. Dyn.* **55**, 2343–2350.
- Watanabe, M., Y. Kamae, H. Shiogama, A. M. DeAngelis, and K. Suzuki, 2018, “Low clouds link equilibrium climate sensitivity to hydrological sensitivity,” *Nat. Clim. Change* **8**, 901–906.
- Webb, M. J., *et al.*, 2006, “On the contribution of local feedback mechanisms to the range of climate sensitivity in two GCM ensembles,” *Clim. Dyn.* **27**, 17–38.
- Wei, N., *et al.*, 2017, “Observational evidence for desert amplification using multiple satellite datasets,” *Sci. Rep.* **7**, 1–15.
- Wentz, F. J., L. Ricciardulli, K. Hilburn, and C. Mears, 2007, “How much more rain will global warming bring?,” *Science* **317**, 233–235.
- Wentz, F. J., and M. Schabel, 2000, “Precise climate monitoring using complementary satellite data sets,” *Nature (London)* **403**, 414–416.
- Wetherald, R. T., and S. Manabe, 1988, “Cloud feedback processes in a general circulation model,” *J. Atmos. Sci.* **45**, 1397–1416.
- Wielicki, B. A., B. R. Barkstrom, E. F. Harrison, R. B. Lee, G. L. Smith, and J. E. Cooper, 1996, “Clouds and the Earth’s radiant energy system (CERES): An Earth observing system experiment,” *Bull. Am. Meteorol. Soc.* **77**, 853–868.
- Willett, K. M., R. J. H. Dunn, P. W. Thorne, S. Bell, M. de Podesta, D. E. Parker, P. D. Jones, and C. N. Williams, Jr., 2014, “HadISDH land surface multi-variable humidity and temperature record for climate monitoring,” *Clim. Past* **10**, 1983–2006.
- Willett, K. M., P. D. Jones, N. P. Gillett, and P. W. Thorne, 2008, “Recent changes in surface humidity: Development of the Had-CRUH dataset,” *J. Clim.* **21**, 5364–5383.
- Wing, A. A., K. A. Reed, M. Satoh, B. Stevens, S. Bony, and T. Ohno, 2018, “Radiative-convective equilibrium model intercomparison project,” *Geosci. Model Devel.* **11**, 793–813.
- Wing, A. A., *et al.*, 2020, “Clouds and convective self-aggregation in a multimodel ensemble of radiative-convective equilibrium simulations,” *J. Adv. Model. Earth Syst.* **12**, e2020MS002138.
- Winton, M., 2006, “Amplified Arctic climate change: What does surface albedo feedback have to do with it?,” *Geophys. Res. Lett.* **33**, L03701.
- Wu, Q., D. J. Karoly, and G. R. North, 2008, “Role of water vapor feedback on the amplitude of season cycle in the global mean surface air temperature,” *Geophys. Res. Lett.* **35**, L08711.
- Xavier, P. K., V. O. John, S. A. Buehler, R. S. Ajayamohan, and S. Sijikumar, 2010, “Variability of Indian summer monsoon in a new upper tropospheric humidity data set,” *Geophys. Res. Lett.* **37**, L05705.
- Xiang, B., B. Wang, A. Lauer, J.-Y. Lee, and Q. Ding, 2014, “Upper tropospheric warming intensifies sea surface warming,” *Clim. Dyn.* **43**, 259–270.
- Xu, K.-M., and K. A. Emanuel, 1989, “Is the tropical atmosphere conditionally unstable?,” *Mon. Weather Rev.* **117**, 1471–1479.
- Yokohata, T., S. Emori, T. Nozawa, Y. Tsushima, T. Ogura, and M. Kimoto, 2005, “Climate response to volcanic forcing: Validation of climate sensitivity of a coupled atmosphere-ocean general circulation model,” *Geophys. Res. Lett.* **32**, L21710.
- Yoshimori, M., and A. J. Broccoli, 2008, “Equilibrium response of an atmosphere-mixed layer ocean model to different radiative forcing agents: Global and zonal mean response,” *J. Clim.* **21**, 4399–4423.
- Yoshimori, M., and A. J. Broccoli, 2009, “On the link between Hadley circulation changes and radiative feedback processes,” *Geophys. Res. Lett.* **36**, L20703.
- Yoshimori, M., J. C. Hargreaves, J. D. Annan, T. Yokohata, and A. Abe-Ouchi, 2011, “Dependency of feedbacks on forcing and climate state in physics parameter ensembles,” *J. Clim.* **24**, 6440–6455.
- Yoshimori, M., T. Yokohata, and A. Abe-Ouchi, 2009, “A comparison of climate feedback strength between CO<sub>2</sub> doubling and LGM experiments,” *J. Clim.* **22**, 3374–3395.
- Zelinka, M. D., and D. L. Hartmann, 2012, “Climate feedbacks and their implications for poleward energy flux changes in a warming climate,” *J. Clim.* **25**, 608–624.
- Zelinka, M. D., T. A. Myers, D. T. McCoy, S. Po-Chedley, P. M. Caldwell, P. Ceppi, S. A. Klein, and K. E. Taylor, 2020, “Causes of higher climate sensitivity in CMIP6 models,” *Geophys. Res. Lett.* **47**, 2847–2866.
- Zhang, B., R. J. Kramer, and B. J. Soden, 2019, “Radiative feedbacks associated with the Madden-Julian oscillation,” *J. Clim.* **32**, 7055–7065.
- Zhang, C., B. E. Mapes, and B. J. Soden, 2003, “Bimodality in tropical water vapour,” *Q. J. R. Meteorol. Soc.* **129**, 2847–2866.
- Zhang, J., *et al.*, 2020, “Surface warming patterns dominate the uncertainty in global water vapor plus lapse rate feedback,” *Acta Oceanol. Sin.* **39**, 81–89.
- Zhang, M. H., J. Ma, J. Che, Z. Zhou, and G. Gao, 1994, “Diagnostic study of climate feedback processes in atmospheric general circulation models,” *J. Geophys. Res.* **99**, 5525.
- Zhang, R., H. Wang, Q. Fu, A. G. Pendergrass, M. Wang, Y. Yang, P.-L. Ma, and P. J. Rasch, 2018, “Local radiative feedbacks over the arctic based on observed short-term climate variations,” *Geophys. Res. Lett.* **45**, 5761–5770.

- Zhang, T., M. P. Hoerling, J. Perlwitz, D.-Z. Sun, and D. Murray, 2011, "Physics of U.S. surface temperature response to ENSO," *J. Clim.* **24**, 4874–4887.
- Zhang, Y., N. Jeevanjee, and S. Fueglistaler, 2020, Linearity of outgoing longwave radiation: From an atmospheric column to global climate models," *Geophys. Res. Lett.* **47**, e2020GL089235.
- Zhou, L., 2016, "Desert amplification in a warming climate," *Sci. Rep.* **6**, 1–13.
- Zhou, L., H. Chen, W. Hua, Y. Dai, and N. Wei, 2016, "Mechanisms for stronger warming over drier ecoregions observed since 1979," *Clim. Dyn.* **47**, 2955–2974.